Radiation Characteristics of Asymmetrically Slotted Spheroidal Prolate Antennas

by

Ming Zhang

A thesis

presented to the University of Manitoba

in fulfillment of the

thesis requirement for the degree of

Master of Science

in

Electrical and Computer Engineering

Winnipeg, Manitoba,Canada, 1994

ISBN 0-612-16386-5

Name _____

Dissertation Abstracts International is arranged by broad, general subject categories. Please select the one subject which most nearly describes the content of your dissertation. Enter the corresponding four-digit code in the spaces provided.

Electrics and Electrical Engineering
SUBJECT TERM

0	5	4	4

SUBJECT CODE

U·M·I

Subject Categories

THE HUMANITIES AND SOCIAL SCIENCES

COMMUNICATIONS AND THE ARTS
Architecture 0729
Art History 0377
Cinema 0900
Dance 0378
Fine Arts 0357
Information Science 0723
Journalism 0391
Library Science 0399
Mass Communications 0708
Music 0413
Speech Communication 0459
Theater 0465

EDUCATION
General 0515
Administration 0514
Adult and Continuing 0516
Agricultural 0517
Art 0273
Bilingual and Multicultural 0282
Business 0688
Community College 0275
Curriculum and Instruction 0727
Early Childhood 0518
Elementary 0524
Finance 0277
Guidance and Counseling 0519
Health 0680
Higher 0745
History of 0520
Home Economics 0278
Industrial 0521
Language and Literature 0279
Mathematics 0280
Music 0522
Philosophy of 0998
Physical 0523
Psychology 0525
Reading 0535
Religious 0527
Sciences 0714
Secondary 0533
Social Sciences 0534
Sociology of 0340
Special 0529
Teacher Training 0530
Technology 0710
Tests and Measurements 0288
Vocational 0747

LANGUAGE, LITERATURE AND LINGUISTICS
Language
- General 0679
- Ancient 0289
- Linguistics 0290
- Modern 0291

Literature
- General 0401
- Classical 0294
- Comparative 0295
- Medieval 0297
- Modern 0298
- African 0316
- American 0591
- Asian 0305
- Canadian (English) 0352
- Canadian (French) 0355
- English 0593
- Germanic 0311
- Latin American 0312
- Middle Eastern 0315
- Romance 0313
- Slavic and East European 0314

PHILOSOPHY, RELIGION AND THEOLOGY
Philosophy 0422
Religion
- General 0318
- Biblical Studies 0321
- Clergy 0319
- History of 0320
- Philosophy of 0322

Theology 0469

SOCIAL SCIENCES
American Studies 0323
Anthropology
- Archaeology 0324
- Cultural 0326
- Physical 0327

Business Administration
- General 0310
- Accounting 0272
- Banking 0770
- Management 0454
- Marketing 0338

Canadian Studies 0385
Economics
- General 0501
- Agricultural 0503
- Commerce-Business 0505
- Finance 0508
- History 0509
- Labor 0510
- Theory 0511

Folklore 0358
Geography 0366
Gerontology 0351
History
- General 0578
- Ancient 0579
- Medieval 0581
- Modern 0582
- Black 0328
- African 0331
- Asia, Australia and Oceania 0332
- Canadian 0334
- European 0335
- Latin American 0336
- Middle Eastern 0333
- United States 0337

History of Science 0585
Law 0398
Political Science
- General 0615
- International Law and Relations 0616
- Public Administration 0617

Recreation 0814
Social Work 0452
Sociology
- General 0626
- Criminology and Penology 0627
- Demography 0938
- Ethnic and Racial Studies 0631
- Individual and Family Studies 0628
- Industrial and Labor Relations 0629
- Public and Social Welfare 0630
- Social Structure and Development 0700
- Theory and Methods 0344

Transportation 0709
Urban and Regional Planning 0999
Women's Studies 0453

THE SCIENCES AND ENGINEERING

BIOLOGICAL SCIENCES
Agriculture
- General 0473
- Agronomy 0285
- Animal Culture and Nutrition 0475
- Animal Pathology 0476
- Food Science and Technology 0359
- Forestry and Wildlife 0478
- Plant Culture 0479
- Plant Pathology 0480
- Plant Physiology 0817
- Range Management 0777
- Wood Technology 0746

Biology
- General 0306
- Anatomy 0287
- Biostatistics 0308
- Botany 0309
- Cell 0379
- Ecology 0329
- Entomology 0353
- Genetics 0369
- Limnology 0793
- Microbiology 0410
- Molecular 0307
- Neuroscience 0317
- Oceanography 0416
- Physiology 0433
- Radiation 0821
- Veterinary Science 0778
- Zoology 0472

Biophysics
- General 0786
- Medical 0760

EARTH SCIENCES
Biogeochemistry 0425
Geochemistry 0996
Geodesy 0370
Geology 0372
Geophysics 0373
Hydrology 0388
Mineralogy 0411
Paleobotany 0345
Paleoecology 0426
Paleontology 0418
Paleozoology 0985
Palynology 0427
Physical Geography 0368
Physical Oceanography 0415

HEALTH AND ENVIRONMENTAL SCIENCES
Environmental Sciences 0768
Health Sciences
- General 0566
- Audiology 0300
- Chemotherapy 0992
- Dentistry 0567
- Education 0350
- Hospital Management 0769
- Human Development 0758
- Immunology 0982
- Medicine and Surgery 0564
- Mental Health 0347
- Nursing 0569
- Nutrition 0570
- Obstetrics and Gynecology 0380
- Occupational Health and Therapy 0354
- Ophthalmology 0381
- Pathology 0571
- Pharmacology 0419
- Pharmacy 0572
- Physical Therapy 0382
- Public Health 0573
- Radiology 0574
- Recreation 0575
- Speech Pathology 0460
- Toxicology 0383

Home Economics 0386

PHYSICAL SCIENCES
Pure Sciences
Chemistry
- General 0485
- Agricultural 0749
- Analytical 0486
- Biochemistry 0487
- Inorganic 0488
- Nuclear 0738
- Organic 0490
- Pharmaceutical 0491
- Physical 0494
- Polymer 0495
- Radiation 0754

Mathematics 0405
Physics
- General 0605
- Acoustics 0986
- Astronomy and Astrophysics 0606
- Atmospheric Science 0608
- Atomic 0748
- Electronics and Electricity 0607
- Elementary Particles and High Energy 0798
- Fluid and Plasma 0759
- Molecular 0609
- Nuclear 0610
- Optics 0752
- Radiation 0756
- Solid State 0611

Statistics 0463

Applied Sciences
Applied Mechanics 0346
Computer Science 0984
Engineering
- General 0537
- Aerospace 0538
- Agricultural 0539
- Automotive 0540
- Biomedical 0541
- Chemical 0542
- Civil 0543
- Electronics and Electrical 0544
- Heat and Thermodynamics 0348
- Hydraulic 0545
- Industrial 0546
- Marine 0547
- Materials Science 0794
- Mechanical 0548
- Metallurgy 0743
- Mining 0551
- Nuclear 0552
- Packaging 0549
- Petroleum 0765
- Sanitary and Municipal 0554
- System Science 0790

Geotechnology 0428
Operations Research 0796
Plastics Technology 0795
Textile Technology 0994

PSYCHOLOGY
General 0621
Behavioral 0384
Clinical 0622
Developmental 0620
Experimental 0623
Industrial 0624
Personality 0625
Physiological 0989
Psychobiology 0349
Psychometrics 0632
Social 0451

RADIATION CHARACTERISTICS OF ASYMMETRICALLY SLOTTED SPHEROIDAL PROLATE ANTENNAS

BY

MING ZHANG

A Thesis submitted to the Faculty of Graduate Studies of the University of Manitoba in partial fulfillment of the requirements of the degree of

MASTER OF SCIENCE

I hereby declare that I am the sole author of this thesis.

I authorize the University of the Manitoba to lend this thesis to other institutions or individuals for the purpose of scholarly research.

I further authorize the University of Manitoba to reproduce this thesis by photocopying or by other means, in total or in part, at the request of other institutions or individuals for the purpose of scholarly research.

ABSTRACT

The radiation properties for asymmetrical slot antennas on conducting uncoated and coated prolate spheroids are investigated. The method used is based on the separation of variables technique in the spheroidal coordinates. Analytic series expansions in terms of prolate spheroidal vector functions are employed to formulate the electromagnetic fields. The unknown expansion coefficients are determined by a system of equations derived using appropriate boundary conditions. For uncoated asymmetrical slot antennas, numerical results for near electric field, radiation patterns and aperture conductance are obtained. The accuracy of the solution is attested by both examining the behavior of the solution over the boundary region and comparing with published data for slotted spheres. The effect of the slot length and the shape of the spheroid on the magnitude of the radiated field is also presented. For coated slot antennas, the solution is applied to obtain the radiation characteristics of both symmetrically and asymmetrically excited narrow slots. Numerical results for the radiation patterns and radiated power are presented. Similarly, comparison with the corresponding published data for coated spheres are also used to confirm the accuracy of the solution. Furthermore, the effect of coating thickness and other physical parameters on the radiation power is investigated to show the resonance effects on the slotted spheroidal antennas.

ACKNOWLEDGEMENTS

First of all I would like to express my sincere gratitude to Dr. A. Sebak, my supervisor, for his advice, continuous encouragement and helpful discussion throughout the course of this research, especially for providing the opportunity of pursing my first degree in electrical engineering.

I would like to thank Mr. K. Y. Sze, Zaifu Zhang, M. Ouda and all my colleagues for all the discussion and support they provided in numerous ways in carrying out this research.

Special thanks to my wife, daughter and my parents for their patience, constant encouragements and understanding.

Finally, I would like to acknowledge the financial assistance of the Natural Science and Engineering Research Council of Canada, which made this research possible.

TABLE OF CONTENTS

Page

LIST OF FIGURES

LIST OF PRINCIPAL SYMBOLS

j	$\sqrt{-1}$
ξ, η and ϕ	Spheroidal Coordinates
h_η , h_ϕ and h_ξ	Scalar Factors of Spheroidal Coordinate System
k	Wave Number
λ	Wave Length
F	Semifocal Distance
a and b	Semimajor and Semiminor Axes of Conducting Spheroid
c and d	Semimajor and Semiminor Axes of Outer Surface of Coating Layer
h	$=Fk$ Parameter of Spheroidal Coordinate System
ϵ_o	Permittivity of Free Space
ϵ_r	Relative Permittivity of Dielectric Material
μ_o	Permeability of Free Space
μ_r	Relative Permeability of Dielectric Material
Z_r	Refractive Index of Dielectric Material
Z_o	Intrinsic Impedance of Free Space
$\Psi_{\substack{e \\ o}m,n}$	Scalar Wave Function
$\lambda_{m,n}$	Eignvalue of Spheroidal Scalar Wave Function

$S_{m,n}$	Spheroidal Angular Function
$R_{m,n}^{(j)}$	Spheroidal Radial Function of the j kind
$d_r^{m,n}$	Expansion Coefficients of Spheroidal Angular Function
$a_r^{m,n}$	Expansion Coefficients of Spheroidal Radial Function
$\vec{M}_{e\,o}^{q\,(j)}{}_{m,n}$ and $\vec{N}_{e\,o}^{q\,(j)}{}_{m,n}$	Spheroidal Prolate Vector Wave Functions
L	Slot Length of Excitation Source
η_o and $\Delta\eta$	Angular Location and Width of Slot
E_{η}^{ex}	Excitation Electric Field
$E_{\eta,m}^{ex}$	Expansion Coefficients of Excitation Electric Field
$\vec{E}^R$ and $\vec{H}^R$	Radiated Electric and Magnetic Field
$\vec{E}^t$ and $\vec{H}^t$	Transmitted Electric and Magnetic Field
α, β ,γ and δ	Expansion Coefficients of Radiated and Transmitted Fields
$I_{p,m,n}$	Integration Constant
p	Radial Component of Poynting Vector
P_o	Total Radiated Power without Dielectric Coating
P	Total Radiated Power with Dielectric Coating
G_a	Aperture Conductance
$k_o a$	Spheroid Electric Size

$A^{(j)}_{m,N,n}$, $B^{(j)}_{m,N,n}$,

Known Matrix Element

$C^{(j)}_{m,N,n}$ and $D^{(j)}_{m,N,n}$

CHAPTER 1

INTRODUCTION

Radiation from a slot antenna mounted on a perfectly conducting object, with or without coating, is a well–known problem in electromagnetic field theory. Analytic solutions to the problem have long been of considerable interest to scientists and engineers, not only for engineering applications in devices but also because the solutions are starting points for verification of newly developed numerical and approximate techniques. There has been a fairly large amount of work done so far concerning circumferential or axial slot(s) on circular and elliptic cylinders,and rotationally symmetric or asymmetric slot(s) on spheres [1]–[7]. However, by comparison, very few theoretical studies have been carried out on slotted spheroidal objects. This is mainly due to the complex nature and nonorthogonality of spheroidal vector wave functions. Moreover, numerical computations of these functions are very difficult compared to those functions in circular and spherical geometries.

The study of radiation from slotted spheroidal antennas has many practical applications. For example, with respect to the spheroidal geometry itself, it provides a better model for the fuselage of an aircraft or space shuttle than a cylinder or sphere. One practical concern, involving a space shuttle, is the effect of the heat–shielding tiles or the ionized coating on the antenna of the space vehicle. Theoretically, one approach to study this problem is to assume that the heat–shielding tiles or ionized coating may be represented approximately by a confocal equivalent dielectric coating.

The research into the applications of wavefunctions in the spheroidal coordinate system goes as far back as 1880 [8]. However, it was in 1941 when Stratton [9] first gave an analytic

solution for the radiation from a perfectly conducting spheroid, fed by a rotationally symmetric circumferential narrow central slot (or a narrow gap). His work aimed to set up a model of practical dipole antennas by using spheroids with larger axial ratios, and gave explicit expressions for conductance and susceptance. Another more realistic model of a prolate spheroidal dipole was studied by Flammer [10] who assumed a finite width gap. Wait has presented a review of the spheroidal antenna excited by a rotationally symmetric circumferential narrow slot [11]. Based on the theory of spheroidal wave functions by Flammer[8], Sinha and MacPhie [12] improved the computation scheme for the eignvalues of prolate spheroidal wave functions and radial functions. Furthermore, they discussed the admittance characteristics of an antenna system consisting of two prolate slotted spheroids, excited by rotationally symmetric circumferential narrow slots in parallel configuration [13]. In their work, each spheroidal dipole is equivalently replaced by a solid spheroidal conductor of the same size without a gap, encircled by a filamentary ring. Employing the translation addition theorems for vector spheroidal wave functions by Sinha and MacPhie [14], Ciric and Cooray [15] have further investigated two spheroidal dipole antennas in an arbitrary configuration. More recently, the effect of the ultraspherical gap field distribution on the admittance of thin prolate spheroidal dipole antennas has been investigated by Do–Nhat and MacPhie [16]. In their analysis, the geometry considered is still a perfectly conducting spheroid with a finite width gap, but the gap field is of ultraspherical form. Numerical results were presented for the input admittance and current distribution and compared with those of solid circular cylinder dipole antennas.

For complex and general geometrical configuration, namely, spheroidal antennas coated with electrical or magnetic materials, only a few investigations have been carried out.

One difficulty of treating this class of problem is that for the spheroidal coordinate system, both the angular and radial functions depend on the properties of the medium. There is no orthogonality of spheroidal wave functions that can be applied when employing the boundary–matching technique. This situation does not pertain a spherical geometry or an uncoated spheroid. Weeks [17] and Yeh [18] have respectively investigated a spheroidal antenna, which is excited by a narrow gap and coated with a single coating. Some numerical results for far–field patterns have been presented with different design parameters. When dealing with the boundary value problem, Weeks uses Lengendre functions to replace the spheroidal functions. In Yeh's approach, the basic idea is to represent the angular function in the coating region as an expansion of the natural angular functions of the uncoated region. In evaluating the relative advantage between these two approaches, it has been noted [11] that Yeh's approach is highly convergent in comparison with that of Weeks.

From the above review, it is not difficult to conclude that nearly all analyses were concentrated on a basic geometric configuration in which the excitation is through a narrow or finite gap, centrally fed by a field source. Obviously, in this rotationally symmetric configuration, the field quantities are independent of the variable ϕ (except the array system). Thus, if the applied field on the gap has only an η –component, then the excited magnetic field has only a ϕ –component and at the same time $E_\phi = 0$. With these simplifications, this three–dimensional problem can be reduced to one of two dimensions. Moreover, the solutions of field components can be obtained directly from Maxwell's equations by the simple variable separation technique. However, if the circumferential slot extends only part way on the spheroid at a given angle, then it will lead to a non–rotationally symmetric geometric configuration. Discussions or formulations treating the radiation problem have not been un-

dertaken for such an antenna configuration. The work presented in this thesis is mainly concerned with this type of spheroidal antennas. The thesis also presents a study of the effect of different design parameters on the radiation characteristics of the antennas under consideration.

The basic geometry to be considered is a perfectly conducting prolate spheroid, with or without coating, which is excited by a circumferential narrow slot with an arbitrary length and location (azimuthal angle). The study is carried out using the analytical technique. To be precise, the solutions of vector wave equations are first expanded in terms of spheroidal vector wave functions analogous to those developed for the case of a sphere [9]. The unknown expansion coefficients for the radiated fields are determined by enforcing the boundary matching technique.

For the sake of completeness and to facilitate the explanation of notation to be used in this thesis, Chapter 2 will be a brief introduction to the theory of prolate spheroidal wave functions. The first part of Chapter 2 will be composed of a description of the geometry of a prolate spheroidal system. Next, the scalar wave functions Ψ, which is the solution of the scalar Hemholtz equation, will be given. The angular and radial functions associated with Ψ, as well as the asymptotic forms of the radial functions will be described briefly and explicitly. Finally, the derivation of different vector wave functions from this scalar wave function will be presented.

In Chapter 3, the case of an asymmetrically slotted spheroidal antenna is considered. The spheroid is taken to be perfectly conducting, and situated in free space. The circumferential narrow slot on the spheroid is of an arbitrary length and location, and is excited by a sinusoidal field distribution. The solution is obtained by using the expansion–of–vector

wave function technique stated above. The unknown radiated field is expressed in terms of a set of appropriate spheroidal vector functions which are chosen based on the radiation condition at infinity and the ϕ – dependence of the excitation function. When considering the boundary matching problem, a technique analogous to that used by Shoji and Giichi [19] is employed to set up simultaneous linear equations for the unknown expansion coefficients. Numerical results for the radiation patterns and conductance are obtained. To check validity and accuracy, data obtained when the axial ratio approaches one is compared with the published data for a slotted sphere.

Chapter 4 presents a general solution for a coated spheroidal antenna excited by a asymmetric slot. The basic geometry is taken to be the same as that discussed in chapter 3, except with an electric or magnetic coating. The method used is similar to that used in chapter 3, but the transmitted electric and magnetic fields in the coating region must be considered. After evaluating the expansion coefficients of the transmitted and radiated fields by the boundary value technique, the far–zone field and radiated power are obtained. The solution is then applied to two cases of perfectly conducting spheroidal coated antennas. In the first application, the excitation is through a rotationally symmetric narrow slot with a Dirac's function gap field. In the second case, the application is shown for a rotationally asymmetrical slot fed with a sinusoidal electric field function. The properties of both cases are studied. Numerical results are obtained for the far–zone radiated field and radiation patterns for certain parameters. Of considerable practical importance is the effect of the coating thickness and other physical parameters on the radiated power. In a fashion similar to that of Shafai [4], who studied resonance effects in slotted spherical antennas coated with homogeneous materials, the resonance effect in slotted spheriodal cases is discussed. In addition, to check

the validity and accuracy of the solution, numerical results for both cases are compared well with the known results of corresponding spherical cases when the major and minor axes are approximately equal.

Finally, in Chapter 5, conclusions are summarized and some recommendations for future research are presented.

CHAPTER 2

PROLATE SPHEROIDAL GEOMETRY AND SPHEROIDAL WAVE FUNCTIONS

2.1 Introduction

In this chapter, a brief introduction to the theory of the prolate spheroidal coordinate system and scalar and vector wave functions will be presented. It can be noted that, although there is no uniformity in notation, the coordinate system and notations used in this thesis are mainly according to the comprehensive text by Flammer [8]. A description of the prolate spheroidal coordinates is given in section 2.1. The definition of the vector wave equations for $\vec{E}$ and $\vec{H}$ fields of an electromagnetic wave are given in section2.2. Theoretically, the solution to the vector wave equation is formed from the solution to the scalar wave equation in terms of the procedure set forth by Stratton [9]. Therefore, in section 2.3, there is a review of the solution of scalar wave equation and the prolate spheroidal eignvalue, as well as the angular and radial functions associated with the eignvalues. Finally, in section 2.4, different vector wave functions are obtained from the scalar wave function by the application of vector differential operators.

2.2 Prolate spheroidal coordinate system

As illustrated in Fig. 2.1, the prolate coordinate system is formed by rotating two–dimensional ellipses and hyperbolas about the major axis of the ellipses. Customarily, the z–axis is taken as the axis of revolution. Let the semi interfocal distance of the confocal ellipses be denoted by F. The prolate spheroidal coordinates (ξ, η, ϕ) are related to the Cartesian sys

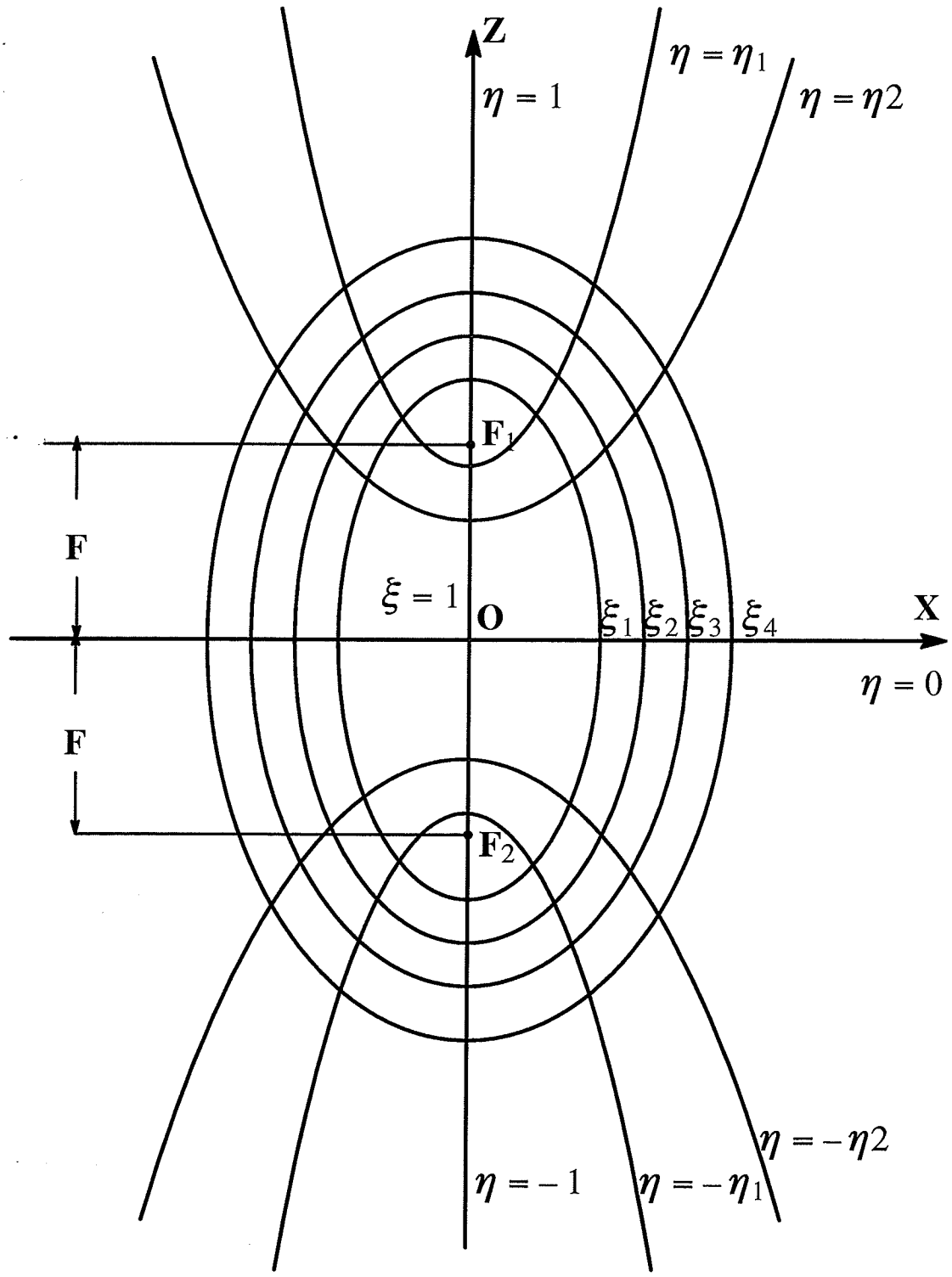

Fig. 2.1 Prolate Spheroidal Geometry

tem (x, y, z) by the transformations

$$x = F[(1-\eta^2)(\xi^2-1)]^{1/2}\cos\phi \tag{2.1}$$

$$y = F[(1-\eta^2)(\xi^2-1)]^{1/2}\sin\phi \tag{2.2}$$

$$z = F\eta\xi \tag{2.3}$$

with $1 \leq \xi < \infty$, $-1 \leq \eta \leq 1$ and $0 \leq \phi < 2\pi$.

As indicated in Fig. 2.1, ξ is a radial coordinate, η is an angular one, and ϕ is a circumferential one. It is readily noted that the size and the shape of the ellipses are specified by the two quantities, the semi–interfocal distance F and the eccentricity e, which is related to the radial coordinate ξ by

$$e = 1/\xi \tag{2.4}$$

It is also worth noting that in the limiting case when the semifocal distance F becomes zero, the prolate spheroidal system reduces to the spherical coordinate system. For F finite, the surface ξ =constant becomes spherical as ξ approaches infinity; thus

$$F\xi \rightarrow r \text{ and } \eta \rightarrow \cos\theta \text{ , as } \xi \rightarrow \infty$$

where r and θ are the usual spherical coordinates.

2.3 Vector wave equation

The theory of electromagnetic radiation is developed by starting with the well–known Maxwell's equations. In general, a time–harmonic electromagnetic field (time factor $e^{j\omega t}$,

ω being the angular frequency) satisfies Maxwell's equations [9]

$$\nabla \times \vec{E} = -j\,\omega\,\mu\vec{H} \tag{2.5}$$

$$\nabla \times \vec{H} = j\,\omega\,(\,\epsilon - j\frac{\sigma}{\omega})\vec{E} = j\,\omega\,\epsilon'\vec{E} \tag{2.6}$$

Where

$$\epsilon' = \epsilon - j\sigma/\omega \tag{2.7}$$

is the complex permittivity.

In (2.5) and (2.6), $\vec{E}$ and $\vec{H}$ are the phasor electromagnetic fields, μ and ϵ represent the permeability and permittivity of the medium, respectively, and σ is the conductivity of the medium. If the wave number of free space is denoted by k_o, then,

$$k_o = 2\pi\ /\lambda_o \tag{2.8}$$

$$= \omega\ (\mu_o\ \epsilon_o)^{1/2} \tag{2.9}$$

where λ_o is the wavelength in free space, and μ_o and ϵ_o the permeability and permittivity of free space, respectively.

Inserting (2.8) and (2.9) into (2.5) and (2.6) for ω gives

$$\nabla \times \vec{E} = -j\,\frac{\mu}{(\mu_o\ \epsilon_o)^{1/2}} k_o\vec{H} \tag{2.10}$$

$$\nabla \times \vec{H} = j\frac{\epsilon'}{(\mu_o\ \epsilon_o)^{1/2}} k_o\vec{E} \tag{2.11}$$

Taking the cross product of both sides of (2.10) yields

$$\nabla\nabla\cdot\vec{E}-\nabla^2\vec{E}=(\frac{\mu}{\mu_o})(\frac{\epsilon'}{\epsilon_o})k_o{}^2\vec{E} \tag{2.12}$$

$$=\mu_r\epsilon_r k_o{}^2\vec{E} \tag{2.13}$$

where $\mu_r=\frac{\mu}{\mu_o}$ and $\epsilon_r=\frac{\epsilon'}{\epsilon_o}$ are the relative permeability and permittivity of the medium, respectively. Assuming a charge free space ($\varrho=o\rightarrow\nabla\cdot\vec{E}=0$) , equation (2.13) becomes

$$\nabla^2\vec{E}+(\mu_r\epsilon_r)k_o{}^2\vec{E}=0 \tag{2.14}$$

In the same fashion, taking the cross product of both sides of (2.11), we have

$$\nabla^2\vec{H}+(\mu_r\epsilon_r)k_o{}^2\vec{H}=0 \tag{2.15}$$

By setting $$k=Z_r\ k_o=(\epsilon'/\epsilon_o)^{1/2}(\mu/\mu_o)^{1/2}\ k_o \tag{2.16}$$

where Z_r is the complex refractive index of the medium and k_o is the wave number of free space, the vector wave equations for $\vec{E}$ and $\vec{H}$ fields can be written

$$\nabla^2\vec{E}+k^2\vec{E}=0 \tag{2.17}$$

$$\nabla^2\vec{H}+k^2\vec{H}=0 \tag{2.18}$$

These are known as vector Helmhotz equations. For many problems in electromagnetic wave theory, solutions of the vector wave equation are required. One of the methods of obtaining solutions to the vector wave equation is by the application of vector operators to the scalar wave function. Hence it is necessary to consider the solution of the scalar wave equation.

2.4 Scalar wave function

As mentioned above, the solutions of the vector wave equations (2.17) and (2.18) are formed from solutions of the following scalar wave equation

$$(\nabla^2 + k^2)\Psi = 0 \tag{2.19}$$

In the prolate spheroidal coordinates, (2.19) has the explicit form

$$\left[\frac{\partial}{\partial\xi}(\xi^2-1)\frac{\partial}{\partial\xi}+\frac{\partial}{\partial\eta}(1-\eta^2)\frac{\partial}{\partial\eta}+\frac{\xi^2-\eta^2}{(\xi^2-1)(1-\eta^2)}\frac{\partial^2}{\partial\phi^2}+h^2(\xi^2-\eta^2)\right]\Psi = 0 \tag{2.20}$$

where $h = kF$. In regions where h depends not on the coordinates, but rather on the properties of the medium, the above equation is separable. Thus, following the notation of Flammer [8], the basic solution can be written in the form

$$\Psi_{m\,n} = S_{m\,n}(h,\eta)R_{m\,n}(h,\xi)\begin{matrix}\cos\\ \sin\end{matrix} m\phi \tag{2.21}$$

where $R_{m\,n}$ and $S_{m\,n}$ satisfy

$$\frac{d}{d\xi}[(\xi^2-1)\frac{d}{d\xi}R_{m\,n}] - (\lambda_{m\,n} - h^2\xi^2 + \frac{m^2}{\xi^2-1})R_{m\,n} = 0 \tag{2.22}$$

$$\frac{d}{d\eta}[(1-\eta^2)\frac{d}{d\eta}S_{m\,n}] + (\lambda_{m\,n} - h^2\eta^2 - \frac{m^2}{1-\eta^2})S_{m\,n} = 0 \tag{2.23}$$

Here, m and n may be taken as integers, since the solutions are to be periodic in both $\theta = \cos^{-1}\eta$ and ϕ. Also, it should be noted that $\lambda_{m,n}(h)$, a function of $h = kF$, is a separa-

tion constant, and only takes those desired values of $\lambda_{m,n}(h)$ for which the differential equation (2.23) gives finite solution at $\eta = \pm 1$.

2.4.1 Angular functions

In accordance with Flammer [8], the prolate angular functions are the associated eignfunctions $S_{mn}(h,\eta)$ corresponding to eignvalues $\lambda_{m,n}(h)$. Generally speaking, there are two kinds of angular functions $S^{(1)}_{mn}(h,\eta)$ and $S^{(2)}_{mn}(h,\eta)$. However, only $S^{(1)}_{mn}(h,\eta)$ is used frequently in physical problems due to its regular behavior over the entire domain $|\eta| \leq 1$. Hence, we simplify the notation by stating that $S_{mn}(h,\eta)$ means the angular function of the first kind. The prolate angular function can be expressed in an infinite series of the associated Legendre functions of the first kind as

$$S_{m,n}(h,\eta) = \sum_{r=0,1,2\ldots}^{\infty}{}' d_r^{m,n}(h) P^m_{m+r}(\eta) \tag{2.24}$$

where the prime over the summation indicates that the $\sum'$ is over only even values of r when $(n-m)$ is even and over only odd values of r when $(n-m)$ is odd. The expansion coefficients $d_r^{m,n}(h)$ originating in the calculated eignvalues are given by the following second –order difference equation.

$$\frac{(2m+r+1)(2m+r+2)}{(2m+2r+3)(2m+2r+5)}h^2 d_{r+2}^{m,n}(h) +$$

$$+ [(m+r)(m+r+1) - \lambda_{m,n} + \frac{2(m+r)(m+r+1) - 2m^2 - 1}{(2m+2r-1)(2m+2r+3)}h^2] d_r^{m,n}(h) +$$

$$+ \frac{(r+1)(r+2)}{(2m+2r-3)(2m+2r-1)}h^2 d_{r-2}^{m,n}(h) = 0 \qquad (2.25)$$

There are two non–trivial independent solutions to equation (2.25). However, of these two solutions, only the one in which $d_r^{m,n}/d_{r-2}^{m,n} \to -h^2/4r^2 \to 0$ leads to a convergent series as r increases [8].

It is also worth noting that from the general theory of Sturm–Liouville differential equations, the angular functions $S_{m\,n}(h,\eta)$ form an orthogonal set on the entire domain $|\eta| \leq 1$, that is

$$\int_{-1}^{+1} S_{m,n}(h,\eta) S_{m,n'}(h,\eta) d\eta = \begin{cases} N_{m,n} & \text{if } n = n' \\ 0 & \text{if } n \neq n' \end{cases} \qquad (2.27)$$

where $N_{m,n}$ is easily shown with the help of the normalization factor of the associated Legendre function. To be explicit,

$$N_{m,n} = 2 \sum_{r=0,1,2,\ldots}^{\infty}{}' \frac{(r+2m)!}{(2r+2m+1)r!} (d_r^{m,n}(h))^2 \qquad (2.28)$$

2.4.2 Radial functions

The radial functions are the solutions of the differential equation (2.22). Obviously, the eignvalues related to (2.22) should be those to which the angular functions $S_{m\,n}(h,\eta)$ belong. In a familiar fashion, the two independent solutions of equation (2.22) $R^{(1)}_{m\,n}(h,\xi)$ and $R^{(2)}_{m\,n}(h,\xi)$ can be expanded as the sum of an infinite series in the form [20]:

$$R^{(1)}_{m,\,n}(h,\xi) = \left(\frac{\xi^2-1}{\xi^2}\right)^{1/2} \sum_{r=0,1,2,\,..\,..}^{\infty\,\prime} a_r^{m,\,n}(h) j_{m+r}(h\xi) \tag{2.29}$$

$$R^{(2)}_{m,\,n}(h,\xi) = \left(\frac{\xi^2-1}{\xi^2}\right)^{1/2} \sum_{r=0,1,2,\,..\,..}^{\infty\,\prime} a_r^{m,\,n}(h) n_{m+r}(h\xi) \tag{2.30}$$

where $j_{m,\,n}(h\xi)$ and $n_{m,\,n}(h\xi)$ are spherical Bessel and Neumann functions, respectively. $a_r^{m,\,n}(h)$ are convergent coefficients such that $a_r^{m,\,n}/a_{r-2}^{m,\,n} \to -h^2/4r^2 \to 0$ as $r \to \infty$. More details about the expansion coefficients $a_r^{m,\,n}(h)$ are to be found in the dissertation by Sinha [20]. The radial functions of the third and fourth types are obtained from

$$R^{(3)}_{m,\,n}(h,\xi) = R^{(1)}_{m,\,n}(h,\xi) + jR^{(2)}_{m,\,n}(h,\xi) \tag{2.31}$$

$$R^{(4)}_{m,\,n}(h,\xi) = R^{(1)}_{m,\,n}(h,\xi) - jR^{(2)}_{m,\,n}(h,\xi) \tag{2.32}$$

The asymptotic behavior of $R^{(1)}_{m\,n}(h,\xi)$, $R^{(2)}_{m\,n}(h,\xi)$, $R^{(3)}_{m\,n}(h,\xi)$ and $R^{(4)}_{m\,n}(h,\xi)$ is readily obtained by the asymptotic behavior of the spherical Bessel and Neumann functions as $h\xi \to \infty$, and that is

$$R^{(1)}_{m,n}(h,\xi) \rightarrow \frac{1}{h\xi}\cos[h\xi - (n+1)\pi/2] \tag{2.33}$$

$$R^{(2)}_{m,n}(h,\xi) \rightarrow \frac{1}{h\xi}\sin[h\xi - (n+1)\pi/2] \tag{2.34}$$

$$R^{(3)}_{m,n}(h,\xi) \rightarrow \frac{1}{h\xi}e^{j\,[h\xi-(n+1)\pi/2]} \tag{2.35}$$

$$R^{(4)}_{m,n}(h,\xi) \rightarrow \frac{1}{h\xi}e^{-j\,[h\xi-(n+1)\pi/2]} \tag{2.36}$$

From the asymptotic behavior of $R^{(3)}_{m\,n}(h,\xi)$ and $R^{(4)}_{m\,n}(h,\xi)$, it is obvious that they have the properties of diverging "ingoing" and "outgoing" spherical waves at infinity. Finally, the wronskian relationships for the radial functions may be found from (2.22) in the usual manner. Thus, for example,

$$R^{(1)}_{m,n}\frac{dR^{(2)}_{m,n}}{d\xi} - R^{(2)}_{m,n}\frac{dR^{(1)}_{m,n}}{d\xi} = \frac{1}{h(\xi^2-1)} \tag{2.37}$$

These relationships will give an important indication of the accuracy of calculating the radial functions and their differentials.

2.5 Spheroidal vector wave functions

By the application of vector differential operators to the spheroidal scalar wave function given in (2.21), the spheroidal vector wave functions $\vec{M}_{m,n}$ and $\vec{N}_{m,n}$ can be obtained:

$$\vec{M}_{m,n} = \nabla\Psi_{m,n} \times \hat{q} \tag{2.38}$$

and

$$\vec{N}_{m,n} = k^{-1}(\nabla \times \vec{M}_{m,n}) \tag{2.39}$$

It is easily shown that the function $\vec{M}_{m,n}$ and $\vec{N}_{m,n}$ are related by

$$\vec{M}_{m,n} = k^{-1}(\nabla \times \vec{N}_{m,n}) \tag{2.40}$$

Where the unit vector $\hat{q}$ is an arbitrary constant vector, which in fact may be $\hat{x}$, $\hat{y}$, $\hat{z}$ or the position vector $\hat{r}$. However, in this research, it is natural to choose $\hat{q}$ to be the position vector $\hat{r}$. The immediate advantage of this choice is that the far–zone field expressions, being similar to the spherical case, will be obtained and may be used to check our derivation. Moreover, to test our computation scheme, the numerical data when the ratio of major axis to minor axis approaches one, is expected to agree with that of the corresponding spherical case. Thus, setting $\hat{q} = \hat{r}$ in expressions (2.38), we rewrite the expressions (2.41) and (2.42) in the following more explicit forms

$$\vec{M}^{r(j)}_{\substack{e \\ o}\, m\, n} = \nabla\Psi^{(j)}_{\substack{e \\ o}\, m\, n} \times \hat{r} \tag{2.41}$$

and

$$\vec{N}^{r(j)}_{\substack{e \\ o}\, m\, n} = k^{-1}\nabla \times \vec{M}^{r(j)}_{\substack{e \\ o}\, m\, n} \tag{2.42}$$

where the superscript j may take the value 1, 2, 3 or 4, indicating one of the four types of spheroidal radial functions. The suffixes e and o refer to even and odd ϕ – dependence, respectively. Explicit expressions for these prolate spheroidal vector wave functions are available in [8] or [20], but are also listed in Appendix **A** for the sake of convenience.

From (2.33) to (2.36), it can be shown that by neglecting the terms of orders higher than $1/r$, the asymptotic forms of $\vec{M}^{r(4)}_{m,n}$ and $\vec{N}^{r(4)}_{m,n}$ in the case of the prolate spheroidal sys-

tem, as $h\xi \to \infty, F\xi \to r$ and $\eta \to \cos\theta$, become as follows:

$$M_{e\ o\ m\,n,\eta}^{r\,(4)} \to (j)^{n+1} m \frac{S_{m\,n}(h,\cos\theta)}{\sin\theta} \frac{1}{kr} e^{-j\,kr} \begin{matrix}\sin\\(-1)\cos\end{matrix} m\phi \ , \tag{2.43}$$

$$M_{e\ o\ m\,n,\phi}^{r\,(4)} \to (j)^{n+1} m \frac{dS_{m\,n}(h,\cos\theta)}{d\cos\theta} \sin\theta \frac{1}{kr} e^{-j\,kr} \begin{matrix}\cos\\\sin\end{matrix} m\phi \ , \tag{2.44}$$

$$N_{e\ o\ m\,n,\eta}^{r\,(4)} \to (j)^{n} \frac{dS_{m\,n}(h,\cos\theta)}{d(\cos\theta)} \sin\theta \frac{1}{kr} e^{-j\,kr} \begin{matrix}\cos\\\sin\end{matrix} m\phi \ , \tag{2.45}$$

$$N_{e\ o\ m\,n,\phi}^{r\,(4)} \to -(j)^{n}\ m \frac{S_{m\,n}(h,\cos\theta)}{\sin\theta} \frac{1}{kr} e^{-j\,kr} \begin{matrix}\cos\\(-1)\sin\end{matrix} m\phi \ , \tag{2.46}$$

$$M_{e\ o\ m\,n,\xi}^{r\,(4)} \to 0 \qquad \text{and} \tag{2.47}$$

$$N_{e\ o\ m\,n,\xi}^{r\,(4)} \to 0 \ . \tag{2.48}$$

It is evident that the radial components of $\vec{M}_{m,\,n}^{r(4)}$ and $\vec{N}_{m,\,n}^{r(4)}$ for large values of $h\xi$ tend to zero. The radiated field wave represented by $\vec{M}_{m,\,n}^{r(4)}$ and $\vec{N}_{m,\,n}^{r(4)}$ becomes a purely transverse wave at a large distance from the spheroid.

2.6 Numerical computation of spheroidal wave function

In this investigation, we will employe the scheme developed by Sinha and MacPhie [20] to generate the eignvalues $\lambda_{m,\,n}$ and the expansion coefficients $d_r^{\,m\,n}(h)$ of the angular and radial functions. It is also worth noting that the series representations of $R_{m\,n}^{(1)}(h,\xi)$ given

in (2.29) have very good convergence, whereas the one of $R^{(2)}_{m\,n}(h,\xi)$ is an asymptotic series which is not absolutely convergent for any finite value of $h\xi$ [21]. An integral technique developed by Sinha and MacPhie [22] overcomes this difficulty to a certain extent. Their calculated results for $R^{(2)}_{m\,n}(h,\xi)$ for the values of $h \leq 9$ are of high precision. But if the value of h is larger than 9, the accuracy of the results becomes low [20].

CHAPTER 3

RADIATION CHARACTERISTICS OF A SLOT ANTENNA ON A CONDUCTING PROLATE SPHEROID

3.1 Introduction

In this chapter, the solution to the problem of radiation by an asymmetrically fed slot antenna mounted on a spheroidal object is presented. In this analysis, the slot field distribution is assumed to be known and of a sinusoidal form. The basic geometry to be considered is a narrow slot with an arbitrary length and location. The radiated fields are expanded in terms of prolate spheroidal vector wave functions. The unknown expansion coefficients are determined by a system of equations derived from the boundary conditions. Radiation patterns and aperture conductance are computed for the slotted spheroidal antenna. To check the validity of the solution, these results, when the axial ratio approaches one, are compared with those of the corresponding sphere. In addition, calculated aperture conductance results are presented to show the effect of the slot length and the shape of the spheroid on the radiated field.

3.2 Formulation of the Problem

3.2.1. Geometry of the problem

Consider a perfectly conducting prolate spheroid with a narrow slot, as illustrated in Fig. 3.1. The semimajor and semiminor axes are denoted by a and b, and semifocal distance by F. It is convenient that the spheroidal coordinates (ξ, η, ϕ) are to be used for expressing spheroidal antenna behavior. The slot of length $2L$ and angular width $2\Delta\eta$ is located at $\eta = \eta_0$ on the spheroidal surface defined by $\xi = \xi_0$.

3.2.2. Excitation Field

For a centrically driven slot located on the spheroid, as shown in Fig. 3.1, following Mushiake [23], the tangential electric field distribution is assumed to be a common sinusoidal form:

$$E_\eta^{ex} = \begin{cases} \dfrac{V_o}{2h_\eta(\Delta\eta)} \sin[k_o(L - b'|\phi\ |)] \ , \ |b'\phi\ | \le L \ \ , \eta_0 - \Delta\eta \le \eta \ \le \eta_0 + \Delta\eta \\ 0 \qquad\qquad\qquad\qquad \text{otherwise} \end{cases} \tag{3.1}$$

where $h_\eta = F\sqrt{\dfrac{\xi_0^2 - \eta^2}{1-\eta^2}}$, $b' = b\sqrt{1 - \dfrac{F^2\xi_o^2\eta_o^2}{a^2}}$. V_0 is the voltage across the center of the slot, and k_o is the wave number of free space. The time dependence factor $e^{j\omega t}$ is assumed and suppressed throughout. To develop a solution in the spheroidal coordinate system, it is convenient to express E_η^{ex} as follows.

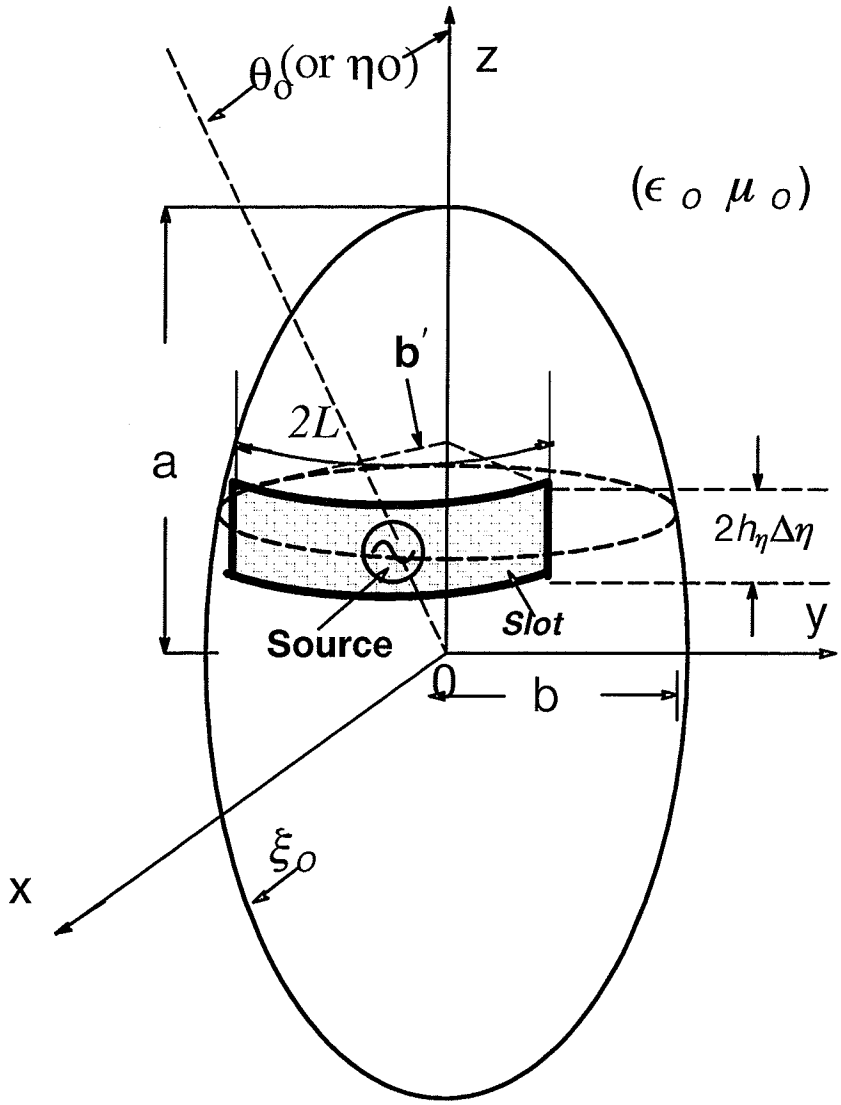

Fig. 3.1 Geometry of the slotted spheroid

$$E_{\eta}^{ex}(\phi) = \sum_{m=0}^{\infty} E_{\eta\, m}^{ex} \cos m\phi. \qquad (3.2)$$

where the expansion coefficients $E_{\eta\, m}^{ex}$ are given by

$$E_{\eta\, m}^{ex} = \frac{V_o}{(1+\delta_m)\pi\ h_\eta(\Delta\eta)} \times \int_0^{L/b'} \sin[k_o(L - b'\phi)] \cos m\phi d\phi \qquad (3.3)$$

$$= \frac{V_0}{\pi\ h_\eta(\Delta\eta)} E_m \qquad (m=0,\ 1,\ 2\ .....)$$

with

$$E_m = \begin{cases} \dfrac{1}{k_o b'}(1 - \cos(k_o L\ )) & m = 0 \\ \dfrac{2k_o b'}{\pi\ [(k_o b)^2 - m^2]}[\cos(m\dfrac{L}{b'}) - cos(k_o L)] & m \neq 0\ or\ \neq k_o b' \\ \dfrac{L}{b'}\sin(k_o L) & m = k_o b' \end{cases} \qquad (3.4)$$

3.2.3 Radiated Field

The radiated fields must be expanded in terms of the fourth kind of $\vec{M}_{m,\,n}^{r(4)}$ and $\vec{N}_{m,\,n}^{r(4)}$ vectors. The reason for choosing this is that, at large distance from the spheroid, the radiated field approaches a spherical diverging wave emanating from the center of the spheroid, see section2.5. In addition, the components of the radiated field must have the same ϕ –dependence as the corresponding components of the excitation field. Thus, the radiated electric field is set up in the following form:

$$\vec{E}^{R} = \sum_{m=0}^{\infty} \sum_{n=m}^{\infty} [\alpha_{m\,n} \vec{M}_{o\ m\,n}^{r\,(4)} + \beta_{m\,n} \vec{N}_{e\ m\,n}^{r\,(4)}] \qquad (3.5)$$

where α_{mn} and β_{mn} are unknown expansion coefficients. From (3.5) and the asymptotic forms for $\vec{M}^{r(4)}_{\substack{o \\ mn}}$ and $\vec{N}^{r(4)}_{\substack{e \\ mn}}$ as $\xi \to \infty$, as given in (2.43) through (2.46), the far –zone radiated electric field for the slotted antenna is obtained as

$$E_\eta{}^R = \frac{e^{-jk_o r}}{k_o r} \sum_{m=0}^{\infty} \sum_{n=m}^{\infty} j^n \left(-\frac{m\ jS_{mn}(h,\cos\theta\ )}{\sin\theta}\alpha_{mn} + \sin\theta \frac{dS_{mn}(h,\cos\theta\ )}{d(\cos\theta)}\beta_{mn}\right)\cos(m\phi) \tag{3.6a}$$

and

$$E_\phi{}^R = \frac{e^{-jk_o r}}{k_o r} \sum_{m=0}^{\infty} \sum_{n=m}^{\infty} j^n \left(\sin\theta\ j\frac{dS_{mn}(h,\cos\theta\ )}{d(\cos\theta)}\alpha_{mn} - \frac{m\ S_{mn}(h,\cos\theta\ )}{\sin\theta}\beta_{mn}\right)\sin(m\phi)\ . \tag{3.6b}$$

It can be noted that the forms in (3.6) are similar to those of the corresponding spherical case [9] in the far–zone region, except for the angular function $S_{mn}(h,\cos\theta)$.

3.3 Formulation of boundary condition

The unknown expansion coefficients in (3.5) can be determined by using the boundary conditions that the tangential components of the electric field must be zero at the spheroidal surface $\xi = \xi_0$ except across the slot. Thus, the boundary conditions on the surface are:

$$E_\eta{}^R = \begin{cases} E_\eta{}^{ex} & \text{at the slot, } i.e.\quad \xi = \xi_0\ ,\ \eta_0 - \Delta\eta < \eta < \eta_0 + \Delta\eta \text{ and } |b'\ \phi| \le L \\ 0 & \text{otherwise} \end{cases} \tag{3.7a}$$

and

$$E_\phi{}^R = 0 \tag{3.7b}$$

Substituting for E^{ex} and E^{R} from (3.3) and (3.7), respectively, multiplying the results with $\cos m\phi$ $(m = 0, 1, 2 \ldots .)$ for (3.7a) and $\sin m\phi$ $(m = 1, 2 \ldots .)$ for (3.7b), and applying the orthogonality properties of triangular functions, (3.7a) and (3.7b) reduce to

$$\sum_{n=0}^{\infty} -\alpha_{m,\,m+n} m\xi_0 \frac{S_{m,\,m+n}(h,\eta) R^{(4)}_{m,\,m+n}(\xi_0, h)}{(\xi_0^2-\eta^2)^{1/2}(1-\eta^2)^{1/2}} + \sum_{n=0}^{\infty} \beta_{m,\,m+n} \frac{(1-\eta^2)^{1/2}}{h(\xi_0^2-\eta^2)^{1/2}} \left\{ \frac{dS_{m,\,m+n}(h,\eta)}{d\eta} \times \right.$$

$$\times \frac{\partial}{\partial\xi}\left[\frac{\xi_o(\xi_o^2-1)}{\xi_o^2-\eta^2} R^{(4)}_{m,\,m+n}(h,\xi_o)\right] - \eta S_{m,\,m+n}(h,\eta) \frac{\partial}{\partial\xi}\left[\frac{(\xi_o^2-1)}{(\xi_o^2-\eta^2)} \frac{dR^{(4)}_{m,\,m+n}(h,\xi_o)}{d\xi}\right] + \qquad (3.8a)$$

$$\left. + \frac{m^2\eta}{(1-\eta^2)(\xi_0^2-1)} S_{m,\,m+n}(h,\eta) R^{(4)}_{m,\,m+n}(h,\xi_0) \right\} = -\frac{V_0 k_0}{2h(\Delta\eta)} E_m \sqrt{\frac{(1-\eta^2)}{(\xi_0^2-\eta^2)}}$$

and

$$\sum_{n=0}^{\infty} \frac{(1-\eta^2)^{1/2}(\xi_0^2-1)^{1/2}}{(\xi_0^2-\eta^2)} \left\{ \alpha_{m,\,m+n} \left[\xi_0 R^{(4)}_{m,\,m+n}(h,\xi_0) \frac{dS_{m,\,m+n}(h,\eta)}{d\eta} - \eta\ S_{m,\,m+n}(h,\eta) \frac{dR^{(4)}_{m,\,m+n}(h,\xi_0)}{d\eta} \right] \right.$$

(3.8b)

$$\left. - \frac{m}{h} \beta_{m,\,m+n} \left[\frac{R^{(4)}_{m,\,m+n}(h,\xi_0)}{(\xi_o^2-1)} \frac{d}{d\eta}[\eta S_{m,\,m+n}(h,\eta)] + \frac{S_{m,\,m+n}(h,\eta)}{(1-\eta^2)} \frac{d}{d\xi}[\xi_o R^{(4)}_{m,\,m+n}(h,\xi_o)] \right] \right\} = 0\ .$$

Obviously, in both (3.8a) and (3.8b), the individual terms in the series can not be matched term by term. To set up a system of equations for the unknown coefficients $\alpha_{m,\,m+n}$ and $\beta_{m,\,m+n}$, the following technique is used: equation (3.8a) is multiplied by the factor $(\xi_0^2-\eta^2)^{5/2} S_{m,\,m+N+1}$, and equation (3.8b) by $(\xi_0^2-\eta^2)/(\xi_0^2-1)^{1/2} S_{m,\,m+N+1}$, and the results are integrated over η. The resulting system of equations can be written in the form:

$$\sum_{n=0}^{\infty}[\alpha_{m,\,m+n}A^{(4)}_{m,\,N,\,n}(h,\xi_0)+\beta_{m,\,m+n}B^{(4)}_{m,\,N,\,n}(h,\ \xi_0)]=F_{m,\,m+N} \qquad (3.9a)$$

$$\sum_{n=0}^{\infty}[\alpha_{m,\,m+n}C^{(4)}_{m,\,N,\,n}(h,\xi_0)+\beta_{m,\,m+n}D^{(4)}_{m,\,N,\,n}(h,\ \xi_0)]=0 \qquad (3.9b)$$

where $m,N=0,\ 1,\ 2,\ .....\ \infty$. The known matrices $A,\ B,\ C,\ D$ and F are given by

$$A^{(4)}_{m,\,N,\,n}(h,\xi_0)=-m\xi_0R^{(4)}_{m,\,m+n}(h,\ \xi_0)\Big[(\xi_0^2-1)^2I_{1\,m\,N\,n}(\ h\ ,h)+$$

$$+2(\xi_0^2-1)+I_{2\,m\,N\,n}(\ h\ ,h)+I_{3\,m\,N\,n}(\ h\ ,h)\Big]\ , \qquad (3.10a)$$

$$B^{(4)}_{m,\,N,\,n}(h,\xi_0)=\frac{1}{h}\Big\{[(3\xi_0^2-1)R^{(4)}_{m,\,m+n}(h,\ \xi_0)+\xi_0(\xi_0^2-1)\frac{d}{d\xi}R^{(4)}_{m,\,m+n}(h,\ \xi_0)]\times$$

$$\times[(\xi_0^2-1)I_{4\,m\,N\,n}(\ h\ ,h)+I_{5\,m\,N\,n}(\ h\ ,h)]-2\xi_0{}^2(\xi_0^2-1)R^{(4)}_{m,\,m+n}(h,\ \xi_0)I_{4\,m\,N\,n}(\ h\ ,h)+$$

$$+\Big[[(\lambda_{m,\,m+n}(h)-h^2\xi_0^2)(\xi_0^2-1)+m^2]R^{(4)}_{m,\,m+n}(h,\ \xi_0)-$$

$$-2\xi_0(\xi_0^2-1)\frac{d}{d\xi}R^{(4)}_{m,\,m+n}(h,\ \xi_0)\Big]\times I_{6\,m\,N\,n}(\ h\ ,h)+$$

$$+[\lambda_{m,\,m+n}(h)-h^2\xi_0^2+\frac{m^2}{(\xi_0^2-1)}]\ I_{7\,m\,N\,n}(\ h\ ,h)R^{(4)}_{m,\,m+n}(h,\ \xi_0)+$$

$$+m^2R^{(4)}_{m,\,m+n}(h,\ \xi_0)\Big[(\xi_0^2-1)I_{8\,m\,N\,n}(\ h\ ,h)+2I_{6\,m\,N\,n}(\ h\ ,h)+\frac{I_{7\,m\,N\,n}(\ h\ ,h)}{(\xi_0^2-1)}\Big]\Big\}, \qquad (3.10b)$$

$$C^{(4)}_{m,N,n}(h,\xi_0) = \xi_0 R^{(4)}_{m,m+n}(h,\ \xi_0) I_{4\,m\,N\,n}\ (\ h\ ,h) - \frac{d}{d\xi} R^{(4)}_{m,m+n}(h,\ \xi_0) I_{6\,m\,N\,n}\ (\ h\ ,h)\ \ ,$$

(3.10c)

$$D^{(4)}_{m,N,n}(h,\xi_0) = -\frac{m}{h}\left\{[\xi_0 \frac{d}{d\xi} R^{(4)}_{m,m+n}(h,\ \xi_0) + R^{(4)}_{m,m+n}(h,\ \xi_0)]\ I_{1\,m\,N\,n}\ (\ h\ ,h) + \right.$$

$$\left. + \frac{R^{(4)}_{m,m+n}(h,\ \xi_0)}{(\xi_0^2 - 1)}\ [I_{9\,m\,N\,n}\ (\ h\ ,h) + I_{2\,m\,N\,n}\ (\ h\ ,h)]\right\}$$

(3.10d)

and

$$F_{m,m+N} = -\frac{V_0 k_o E_m}{h 2\Delta\eta} \int_{\eta_0 - \Delta\eta}^{\eta_o + \Delta\eta} \sqrt{(1-\eta^2)}\,(\xi_0^2 - \eta^2)^2 S_{m,m+N+1}(h,\eta\ )d\eta$$

(3.10e)

In the case of the narrow slot ($\Delta\eta \rightarrow 0$), (3.10e) becomes

$$F_{m,m+N} = -\frac{V_0 k_0}{h} E_m \sqrt{(1-\eta_0^2)}\,(\xi_0^2 - \eta_0^2)^2 S_{m,m+N+1}(h,\eta_0)$$

(3.10f)

Where $\lambda_{m,m+n}(h)$ is the spheroidal eignvalue [8]. In the present case $h = k_o F$, where, as usual, F is the semifocal distance for the spheroid. The integrals $I_{p\,m\,N\,n}$ ($p = 1,\ 2,\ \ldots\ldots\ 9$) are given and evaluated in Appendix **B** .

In order to solve (3.9) for α and β , the infinite series in (3.9) must be truncated by setting a suitable number N_0 for *m, n or N.* It can theoretically and practically be shown that the amplitude of radiated field should dampen down quite rapidly when

m, n *or* $N > N_0$. Sinha and MacPhie [21] have shown that for the perfectly conducting spheroid, the number N_0 depends on the electrical size $k_o a$ of the spheroid, and is approximately equal to the integer part of $k_o a + 4$. In this case, to determine the value of N_0 for the slotted spheroidal antenna, calculations are repeated for consecutive incremental value of n, commencing with the value stated by Sinha and MacPhie [20]. This evaluation is executed until a reasonable degree of accuracy is achieved.

3.4 Radiation Conductance

Once the coefficients $\alpha_{m,\,m+n}$ and $\beta_{m,\,m+n}$ are determined, the far–zone radiated electric field can be obtained from (3.6). Using (3.6), the total time –average power P_o radiated from the slotted spheroidal antenna can be calculated by integrating the poynting vector over an infinitely large spherical surface, and may be written in the following form:

$$P_o = \frac{1}{2Z_0 k_0^2} \sum_{m=0}^{\infty} \sum_{n=0}^{\infty} \sum_{N=0}^{\infty} (1+\delta_{m\,0})[\alpha_{m,\,m+n}\alpha^*_{m,\,m+N} + \beta_{m,\,m+n}\,\beta^*_{m,\,m+N}] \times$$
$$\times [\lambda_{m,\,m+n} I_{10\,m\,n\,N}(h\,,h) - h^2 I_{11\,m\,n\,N}(h\,,h)] \qquad (3.11)$$

where $Z_0 = \sqrt{\mu_0 / \epsilon_0}$, the symbol $*$ denotes the complex conjugation, and the two integrations $I_{10\,m\,n\,N}$ and $I_{11\,m\,n\,N}$ are given and evaluated in Appendix **B**.

The external slot conductance G_a is then given by

$$G_a = P_o / |V_0|^2 \qquad (3.12)$$

where V_0 is the slot voltage (see (3.1)).

An alternative approach to calculate the radiation conductance and slot susceptance is given in [23], Following Mushiake [23], the amplitude of the slot voltage of the *mth* mode along the narrow slot can be defined as:

$$V_m^{ex} = \int_{\eta_o-\Delta\eta}^{\eta_o+\Delta\eta} E_{\eta\, m}^{ex}\, h_\eta\, d\eta \tag{3.13}$$

where $E_{\eta\, m}^{ex}(m = 0\ ,1\ ,2\ ,\ldots\ldots)$ are the expansion coefficients of the excitation and given in (3.3). For the present case of narrow slot, (3.13) can be approximated as:

$$V_m^{ex} \approx 2E_{\eta\, m}^{ex}\, h_\eta\, \Delta\eta \tag{3.14}$$

The *mth* mode radiation admittance Y_m^e is defined as

$$Y_m^e = G_m^e + jB_m^e = \frac{I_m}{V_m^{ex}} \tag{3.15}$$

where G_m^e and B_m^e are the radiation conductance and susceptance of the slot, respectively and the current I_m is given by

$$I_m \approx -b' \int_{-\phi_o}^{\phi_o} \overline{H}_{m\,\phi}^R(\xi_o\ ,\eta\ ,\phi)\ d\phi \tag{3.16}$$

The radiated magnetic field distribution $H_{m\ ,\phi}^R$ on the narrow slot is approximated by its mean value $\overline{H}_{m,\phi}^R(\xi_o\ ,\eta_o\ ,\phi\ )$, *i.e* .

$$\overline{H}_{m\ ,\phi}^R = \frac{1}{2}[H_{m\,\phi}^R(\xi_o\ ,\eta_o + \Delta\eta\ ,\phi) + H_{m\,\phi}^R(\xi_o\ ,\eta_o - \Delta\eta\ ,\phi)] \tag{3.17}$$

where $H^R_{m,\phi}$ is given by

$$H_{m\phi}{}^{R} = \frac{j}{Z_o} \sum_{n=m}^{\infty} [\alpha_{mn} N^{r(4)}_{o\phi_{mn}} + \beta_{mn} M^{r(4)}_{e\phi_{mn}}] \tag{3.18}$$

For narrow slots, numerical results show that the external slot conductance G_a, based on (3.11), is in good agreement with $\sum_{m=0}^{\infty} G^e_m$. Extensions of the present formulation to the radiation by wide slot antennas and the scattering by the slotted spheroids are currently under investigation.

3.5 Numerical computations and results

In this investigation, the scheme developed by Sinha and MacPhie [20] is used to generate the eignvalues $\lambda_{m,n}$ and the expansion coefficients $d_r{}^{mn}(h)$ of the angular and radial functions, with at least six figures of accuracy. The infinite series in the linear system of equations (3.9) are also truncated to finite ones with the first N_0 terms. This evaluation for suitable values of N_0 is chosen to impose a convergence condition that provides the solution accuracy better than three digit accuracy.

To examine the accuracy of the solution over the boundary region, the tangential component of the radiated electric field E^R_η has been calculated using (3.5) with $\eta_o = 0.0$. For some examples, computed results for certain design parameters are shown in Figs. 3.2–3.4. Obviously, these figures confirm that the tangential electric field satisfies the boundary val-

ue stated in (3.7).

3.5.1 Radiation Pattern

The relative radiation patterns calculated for a center–driven slot which is near a half –wavelength long ($2L = \lambda/2$) and located on the equator ($\eta_0 = 0$ *or* $\theta_0 = \pi/2$) of the spheroid as illustrated in Fig. 3.1 are shown in Figs. 3.5 –3.7. As a further test of the validity and accuracy of the solution, the radiation patterns for an extreme case, *i.e.*, a spherical antenna (a/b $\approx$ 1), are calculated and shown in Fig. 3.5 with $ka = 1, 2, 3$ and 5. Also shown are the corresponding spherical results calculated by Mushiake [23] based on the spherical wave functions. It can be noted that our results are in perfect agreement with Mushiake's results. To examine the effects of the axial ratio a/b on the magnitude of the radiated field, E–plane ($\phi = 0.0^o$) and H–plane ($\theta = 90.0^o$) patterns (in dB) for the slot antenna with some different values of a/b are calculated and shown in Figs. 3.6–3.7. From these figures, one notes that (i) when the slot length $2L$ is fixed, increasing a/b increases the total radiation power; (ii) for a given $k_o a$, the main beam (on the direction $\theta = 90^o$ and $\phi = 0^o$) becomes wider for H–plane and narrower for E–plane, as the ratio a/b increases; (iii) as the electrical size of the spheroid $k_o a$ increases, the side lobes is increasing.

3.5.2 Aperture Conductance

Numerical results for the aperture conductance G_a calculated for different design parameters are shown in Figs. 3.7–3.10. In all cases, the conductance G_a is plotted as a func-

tion of L/λ_o, the ratio of the slot length to the wavelength in free–space. As the third check on the accuracy of the solution, the extreme case, *i.e* the axial ratio $a/b \approx 1$, is considered again. The calculated results for a sphere with electrical size $k_o a = 1.0, 2.0$ and 6.0 are shown in Fig. 3.7 and compared with the known spherical results calculated from a formula given by Mushiake [23]. Once again, there is a perfect agreement between our solution and Mushiake's results. The corresponding results for spheroidal cases are shown in Figs. 3.8–3.10 with three different values of $k_o a$ and a/b. The results given in Figs. 3.8–3.10 show that for a given $k_o a$ the aperture conductance is increasing with the ratio a/b. For thinner spheroids, *i.e*, with larger values of a/b (≥ 2), the aperture conductance increases with $k_o a$. This is contrary to the results for spherical cases shown in Fig. 3.7.

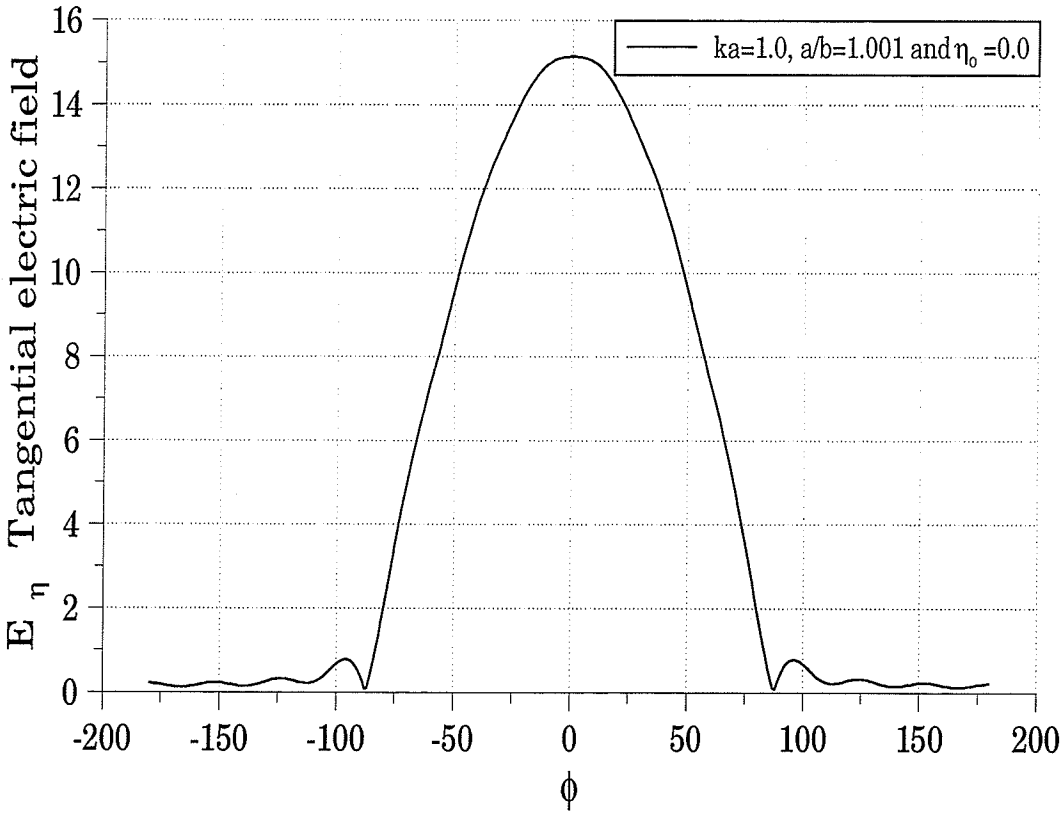

Fig. 3.2 Tangential electric field with $k_o a$=1.0, a/b=1.0 and η_o=0.0 on the surface ξ_o and $|\phi_o| \leq |\phi_{o\,max}| = L/b' = \pi/2$.

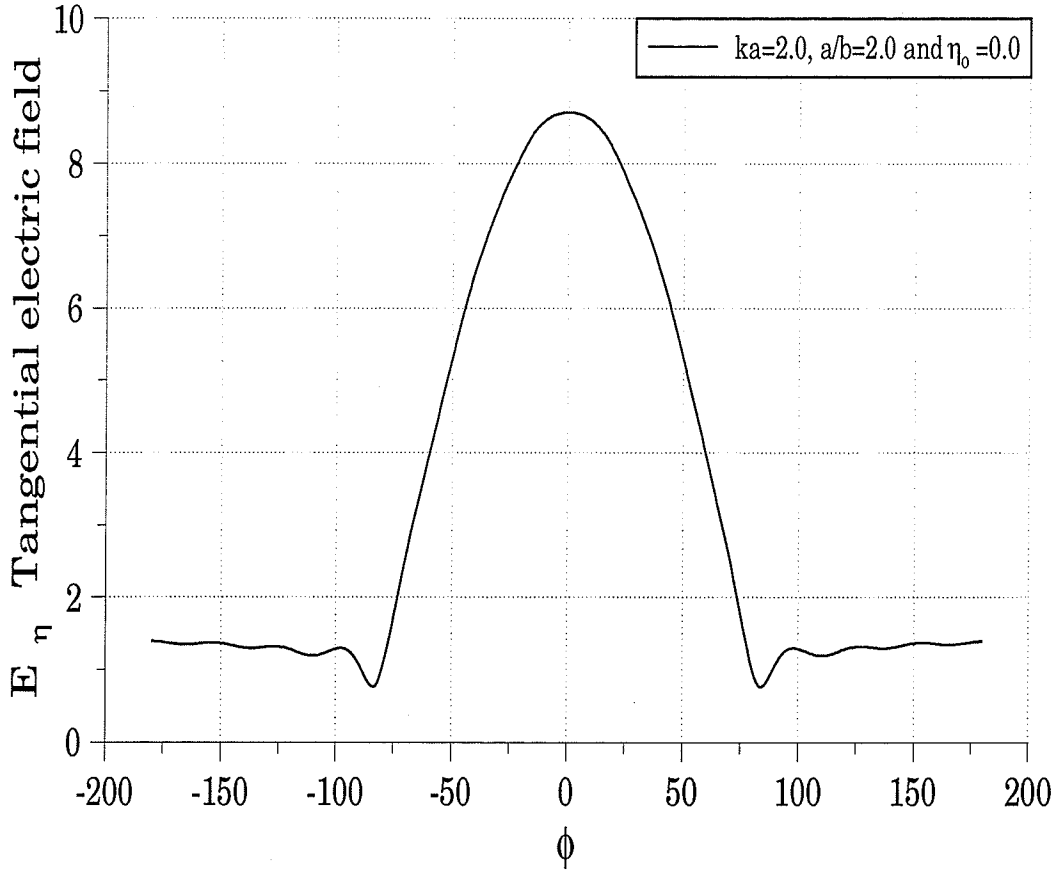

Fig. 3.3 Tangential electric field with $k_o a$=2.0, a/b=2.0 and η_o=0.0 on the surface ξ_o and $|\phi_o| \leq |\phi_{o\,max}| = L/b' = \pi/2$.

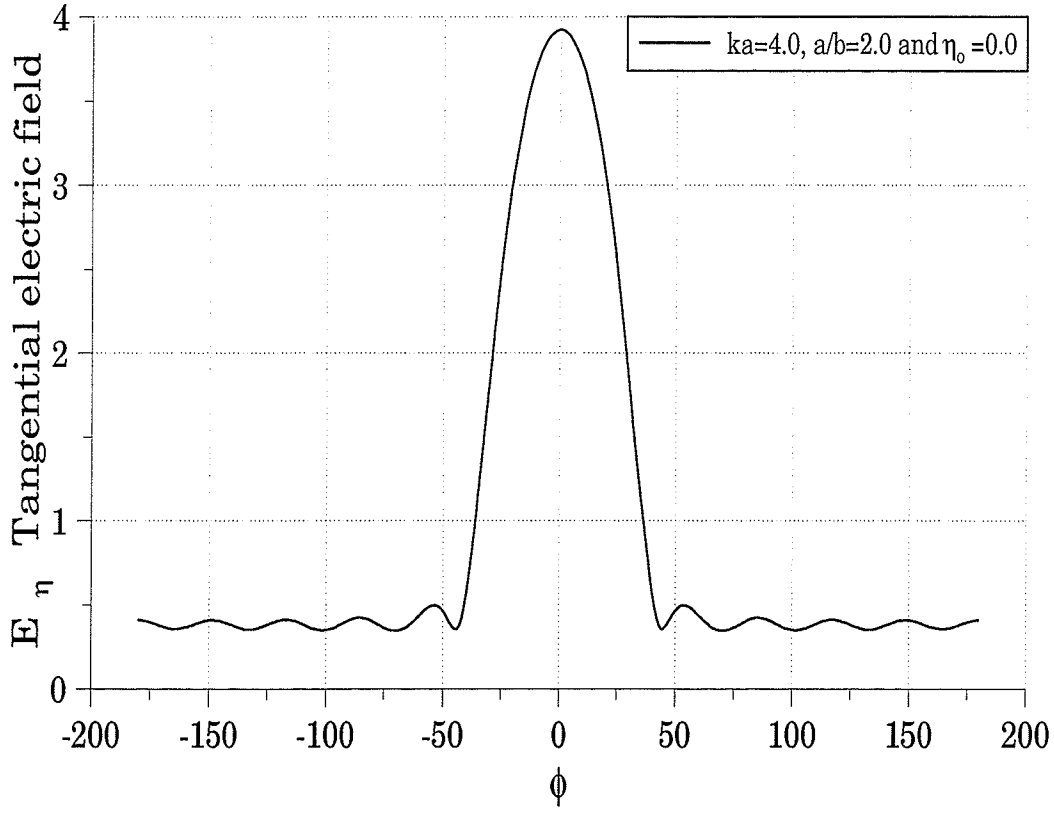

Fig. 3.4 Tangential electric field with $k_o a$=4.0, a/b=2.0 and η_o=0.0 on the surface ξ_o and $|\phi_o| \leq |\phi_{o\,max}| = L/b' = \pi/4$.

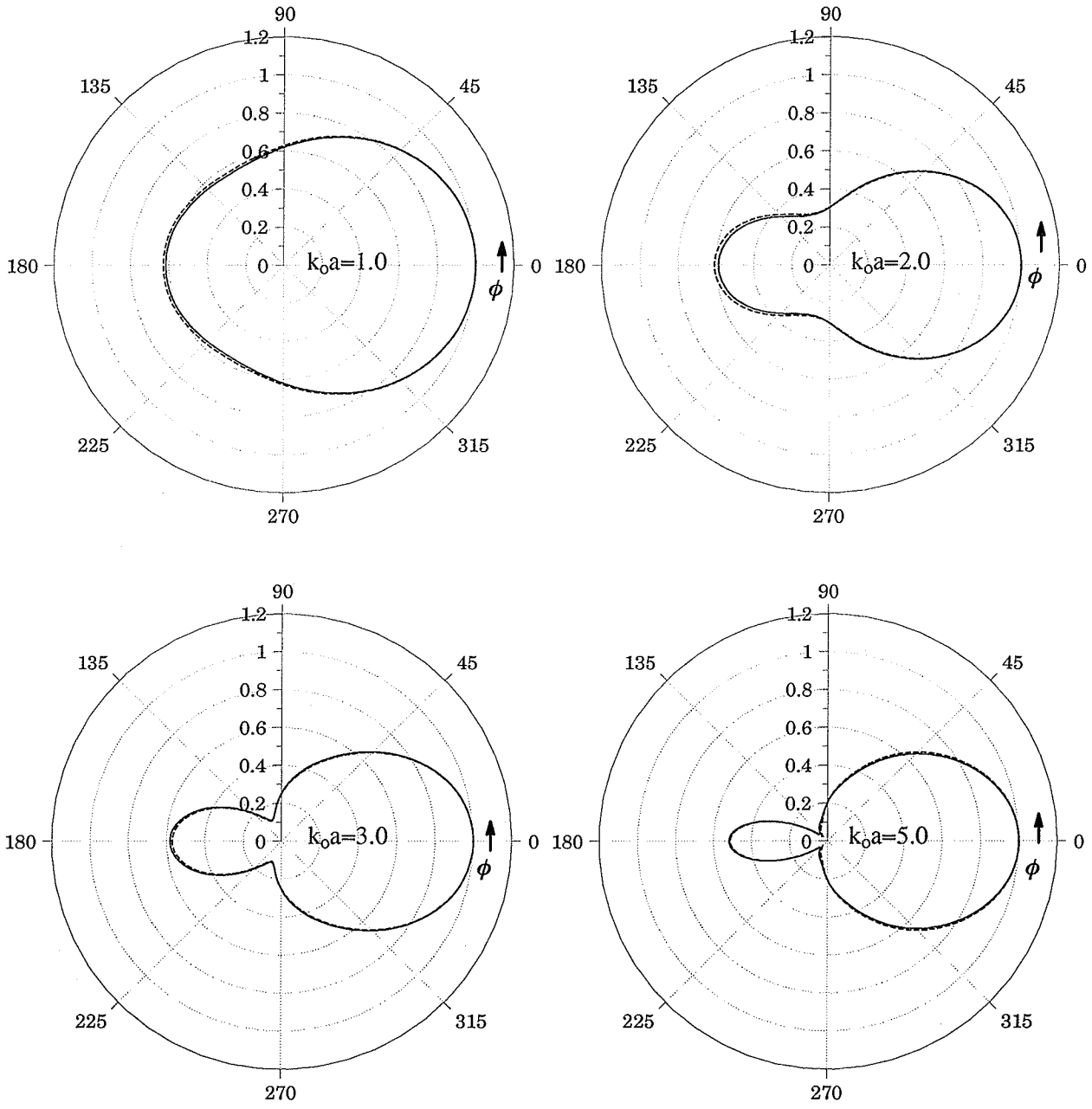

—— this work (a/b=1.0001) - - - - - - results by Y.Mushiake *et al.* [23] at $\eta_0 = 0.0$

Fig. 3.5 Calculated relative radiation pattern (H–Plane) of a half–wave slot on a perfectly conducting sphere

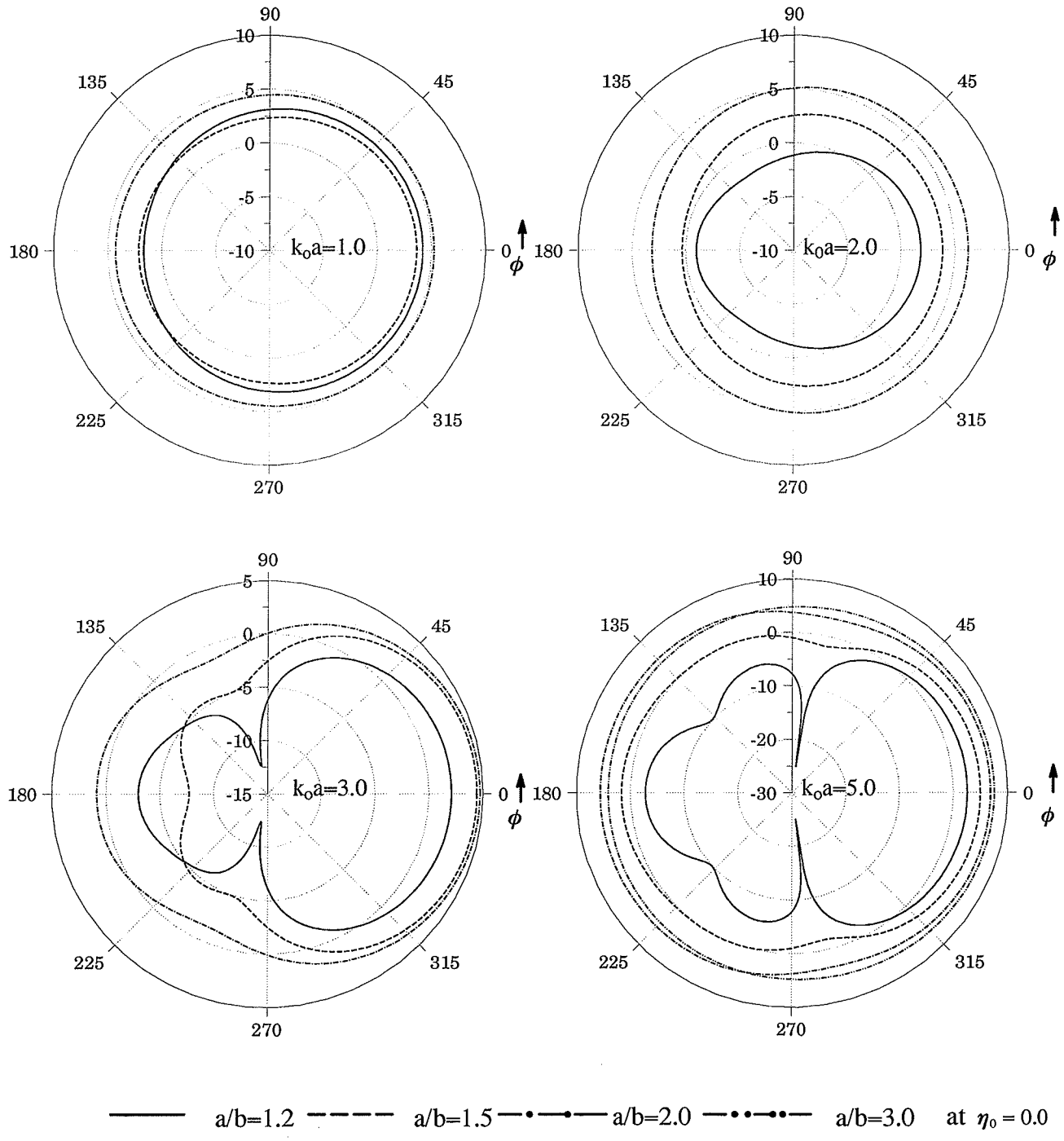

Fig. 3.6 Calculated radiation pattern (H–Plane in dB) of a half–wave narrow slot on a perfectly conducting spheroid.

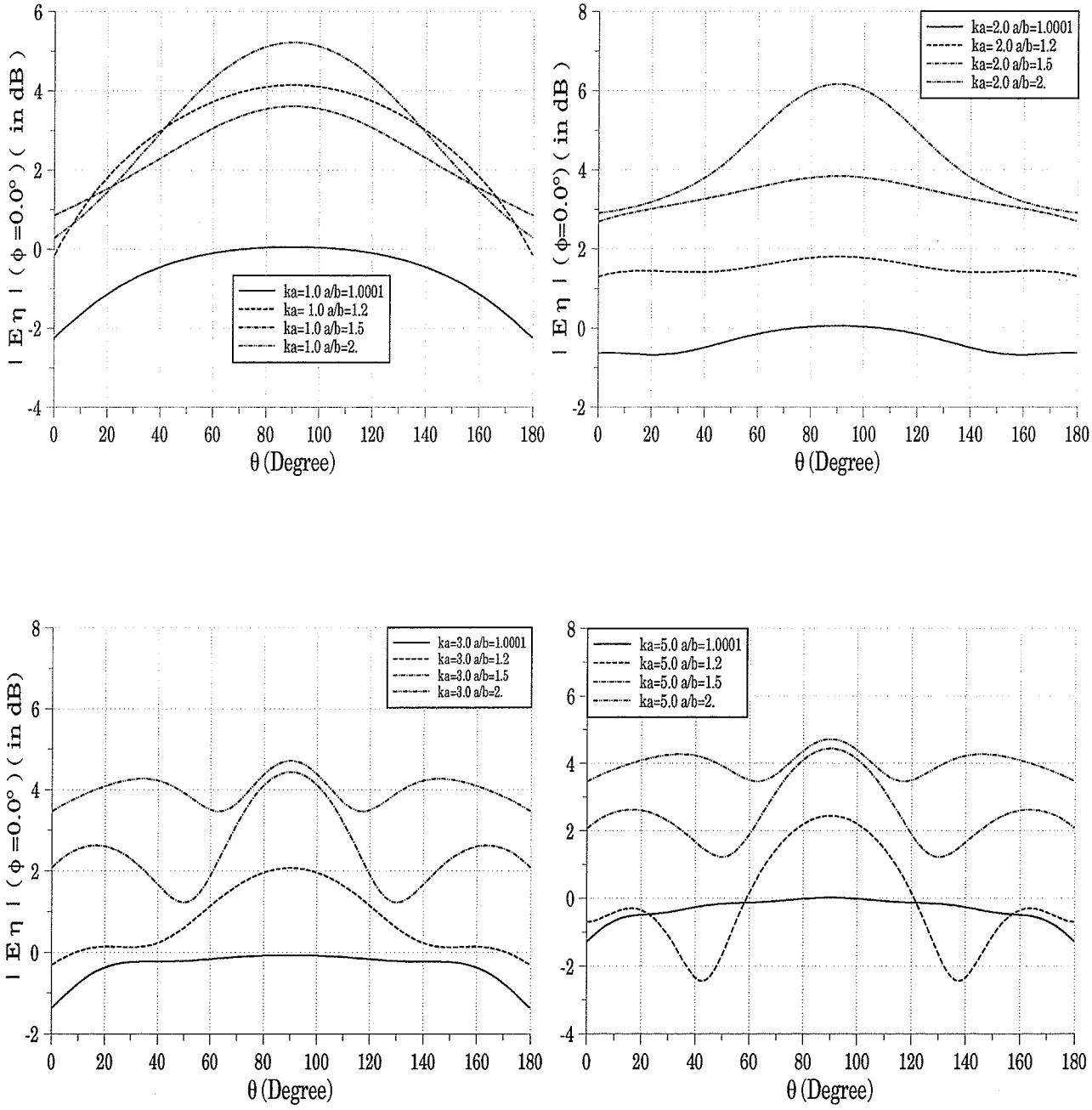

Fig. 3.7 Calculated radiation pattern (E–Plane in dB) of a half–wave narrow slot on a perfectly conducting spheroid.

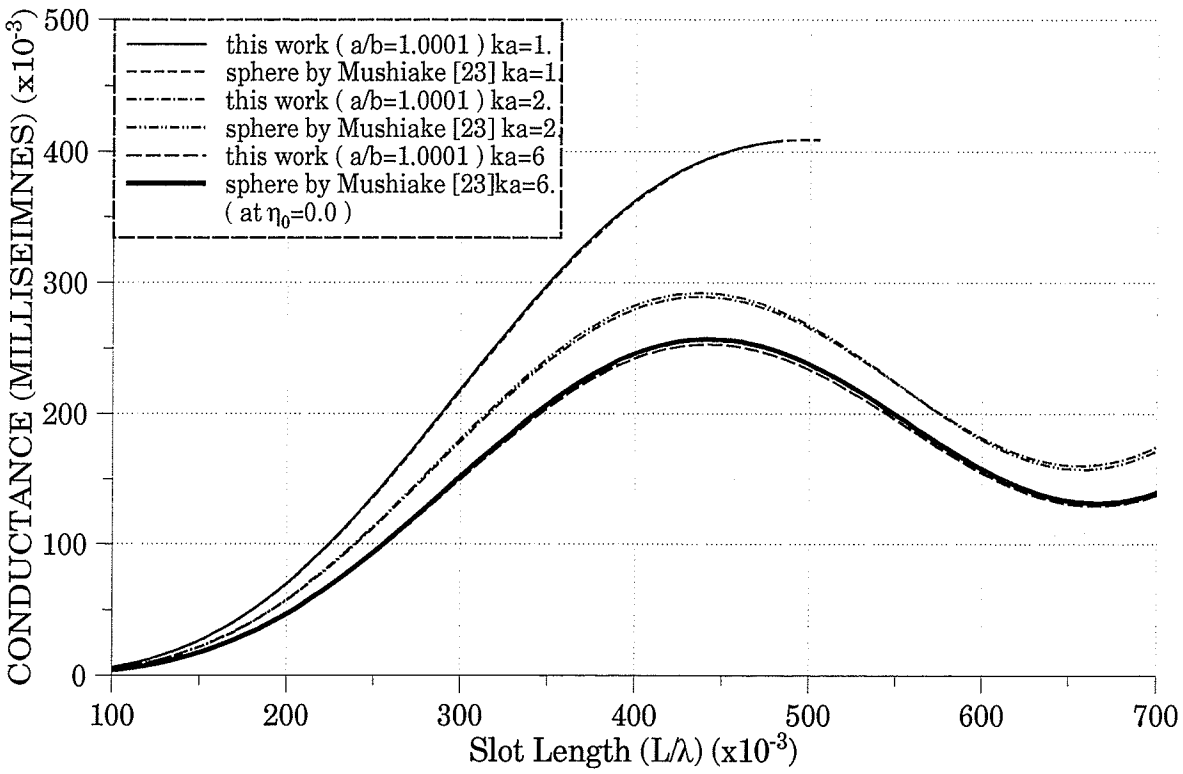

Fig. 3.8 Aperture conductance G_a versus L/λ for a half–wave narrow slot on a perfectly conducting sphere.

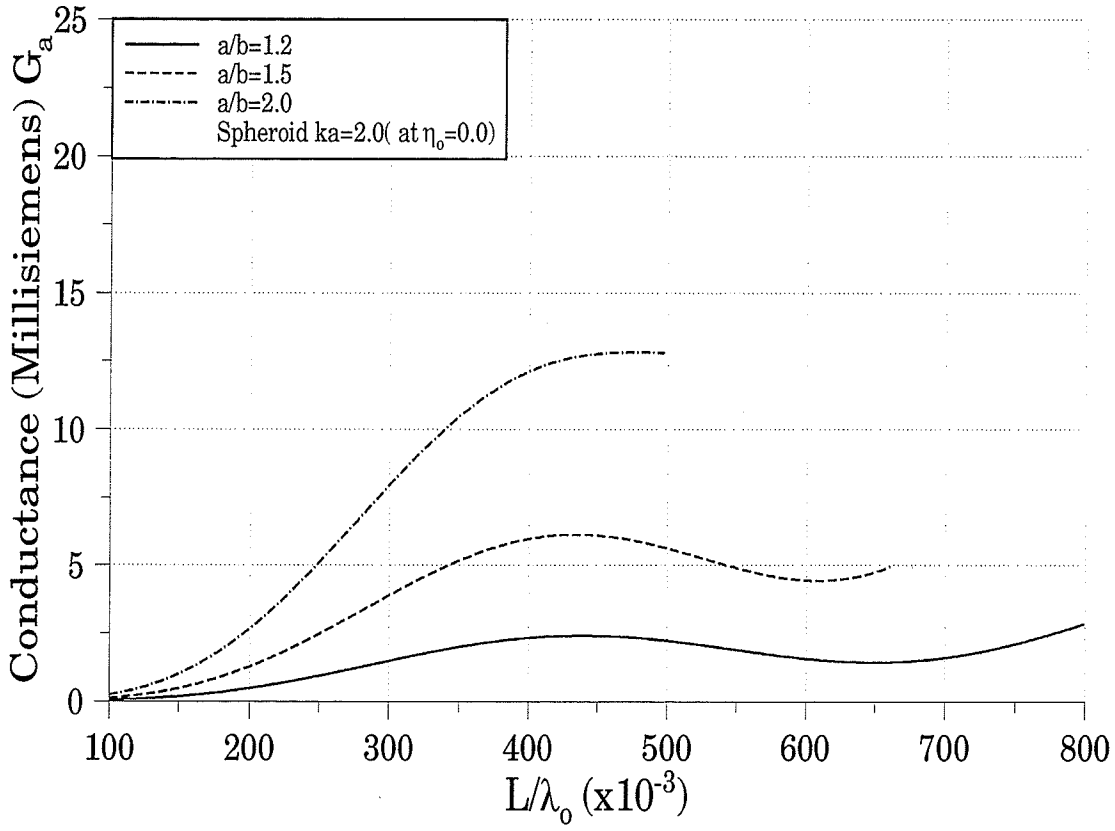

Fig. 3.9 Aperture conductance G_a versus L/λ for a narrow slot on a perfectly conducting spheroid for $k_o a$=2.0 and η_0 = 0.0 .

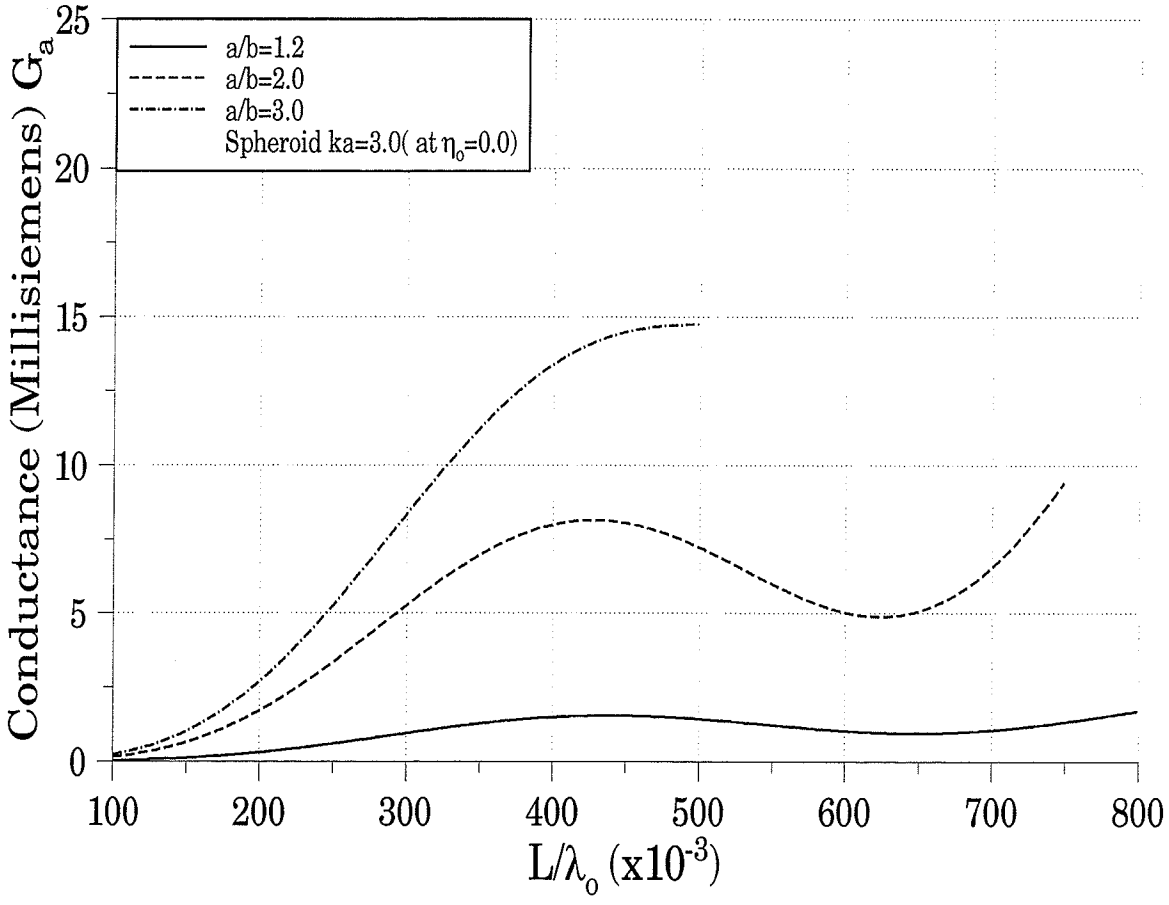

Fig. 3.10 Aperture conductance G_a versus L/λ for a narrow slot on a perfectly conducting spheroid for $k_o a$=3.0 and $\eta_0 = 0.0$.

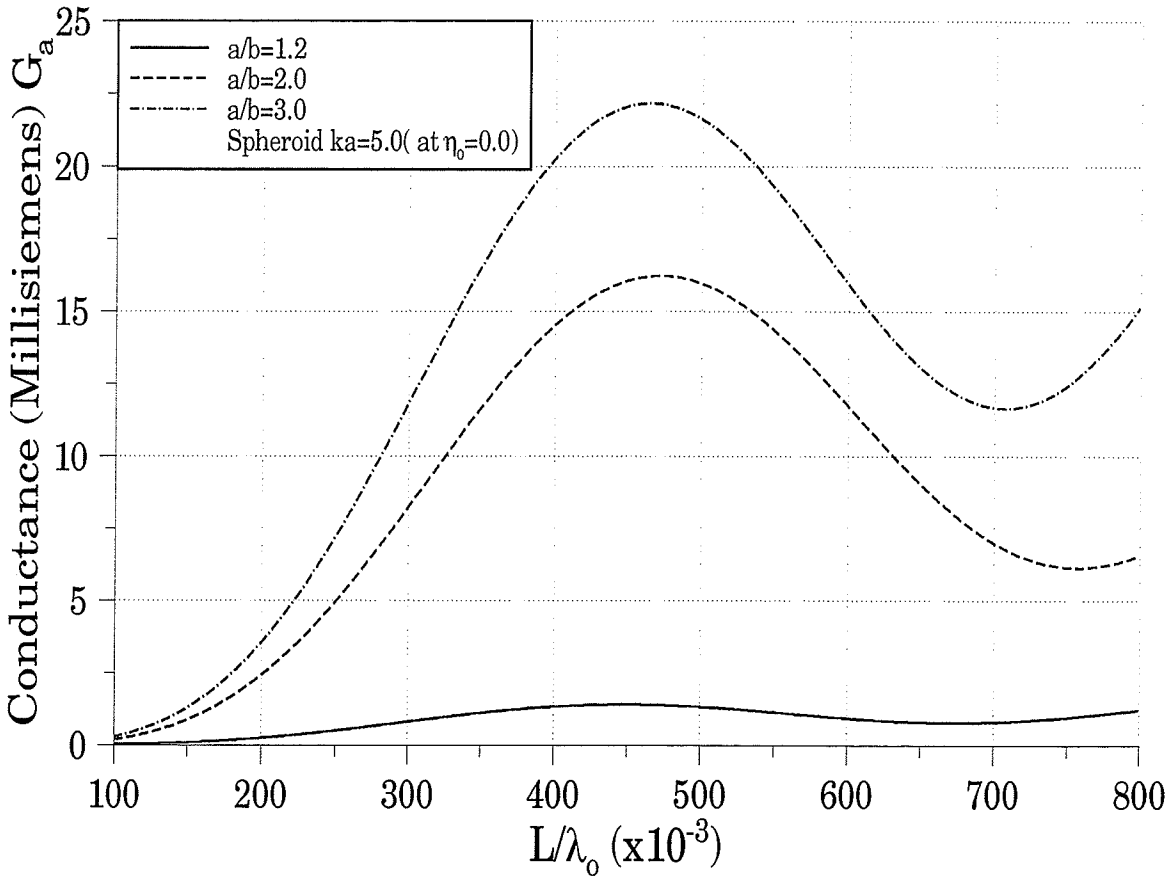

Fig. 3.11 Aperture conductance G_a versus L/λ for a narrow slot on a perfectly conducting spheroid for $k_o a$=5.0 and $\eta_0 = 0.0$.

3.6. Conclusion

In this chapter, an analytical solution for an asymmetrically rotationally slotted antenna on a perfectly conducting prolate spheroid has been presented. Explicit expressions for the radiated fields and aperture conductance were derived in spheroidal coordinates system. The radiated field was first expanded in terms of spheroidal vector wave functions, then the expansion coefficients were determined by imposing the boundary conditions.

Numerical results for the radiation patterns and aperture conductance for the slotted antenna were obtained for different parameters. The effect of the slot length and the shape of the slotted spheroid on both the radiation pattern and aperture conductance were considered. In addition, when the slotted spheroid approaches the spherical shape, our results are in a perfect agreement with the known results for a slotted sphere.

CHAPTER 4

RADIATION CHARACTERISTICS OF SLOTTED ANTENNAS COATED WITH HOMOGENEOUS MATERIALS

4.1 Introduction

In this chapter, the radiation characteristics of a coated spheroidal antenna excited by a symmetric or asymmetric narrow slot is analyzed. This is an extension of the analysis developed in Chapter 3 of a slot antenna on a conducting prolate spheroid. In this case, however slotted antennas are coated with homogeneous materials. Similar to the analysis used in Chapter 3, the solution of the wave equations is expanded in terms of the spheroidal vector wave functions, and the unknown coefficients for the fields are determined by employing proper boundary conditions. But, since the slotted prolate spheroidal antennas are coated with homogeneous materials, the transmitted fields must be considered, the solution is more complicated due to the dependence of the angular function on the material properties of the coating. Numerical results are presented for the far–field radiation patterns and radiation power. Furthermore, the influence of various design parameters on the radiated power, and the resonance effects in the coating materials are discussed. In order to check the validity and accuracy of the solution, computed data for spherical cases (*i.e* when the axial ratio

approaches one) are compared to known results of coated slotted spherical cases.

4.2. FORMULATION OF THE PROBLEM

4.2.1 Geometry of the spheroidal antenna

Figures 4.1 and 4.2 illustrate two cases of perfectly conducting prolate spheroidal antennas which are coated with a confocal homogeneous layer of relative permittivity ϵ_r and permeability μ_r, respectively. In these two cases, the semimajor and semiminor axes are denoted by a and b for the conducting spheroids, and c and d for the outer surface of the coating layer. It is assumed that both of the spheroids have identical foci which are located at $z = \pm F$ on the z axis. Designating the surface of the conducting spheroid by $\xi = \xi_1$ and the outer surface of the coating layer by $\xi = \xi_0$, it then follows that

$$\xi_1 = \frac{a}{F} = a(a^2 - b^2)^{-1/2} \tag{4.1}$$

and

$$\xi_o = \frac{c}{F} = c(c^2 - d^2)^{-1/2} \quad . \tag{4.2}$$

Two types of structure of slot antennas will be considered. As shown in Fig. 4.1, the first is a so–called rotationally symmetric slot. It is a circumferential slot located at $\eta = \eta_o$ going all the way around the spheroid and is uniformly excited. The other is a rotationally asymmetric slot with an arbitrary length $2L$, and at an arbitrary angular location $\eta = \eta_o$, as indicated in Fig. 4.2. Obviously the first type is just a special case of the second one.

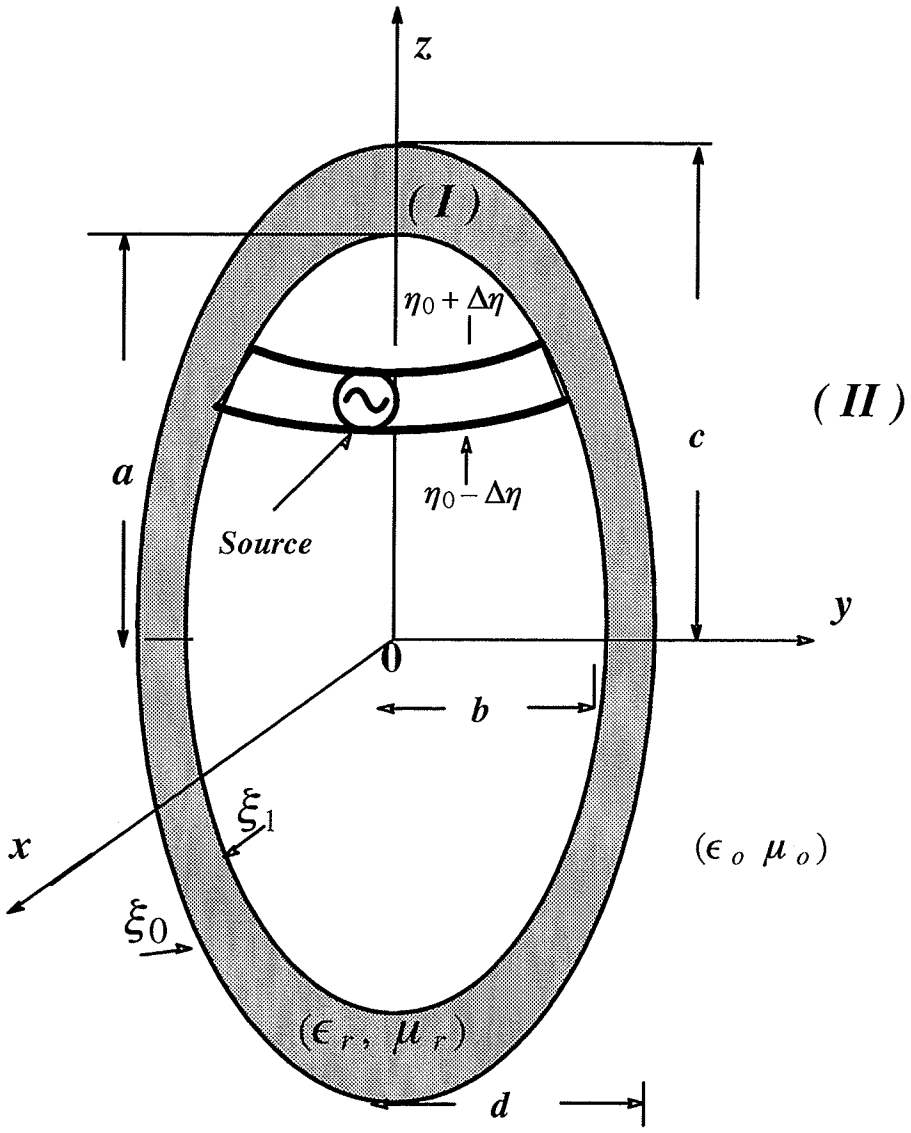

Fig. 4.1 Geometry of the slotted coated prolate spheroid excited by a rotationally symmetric slot

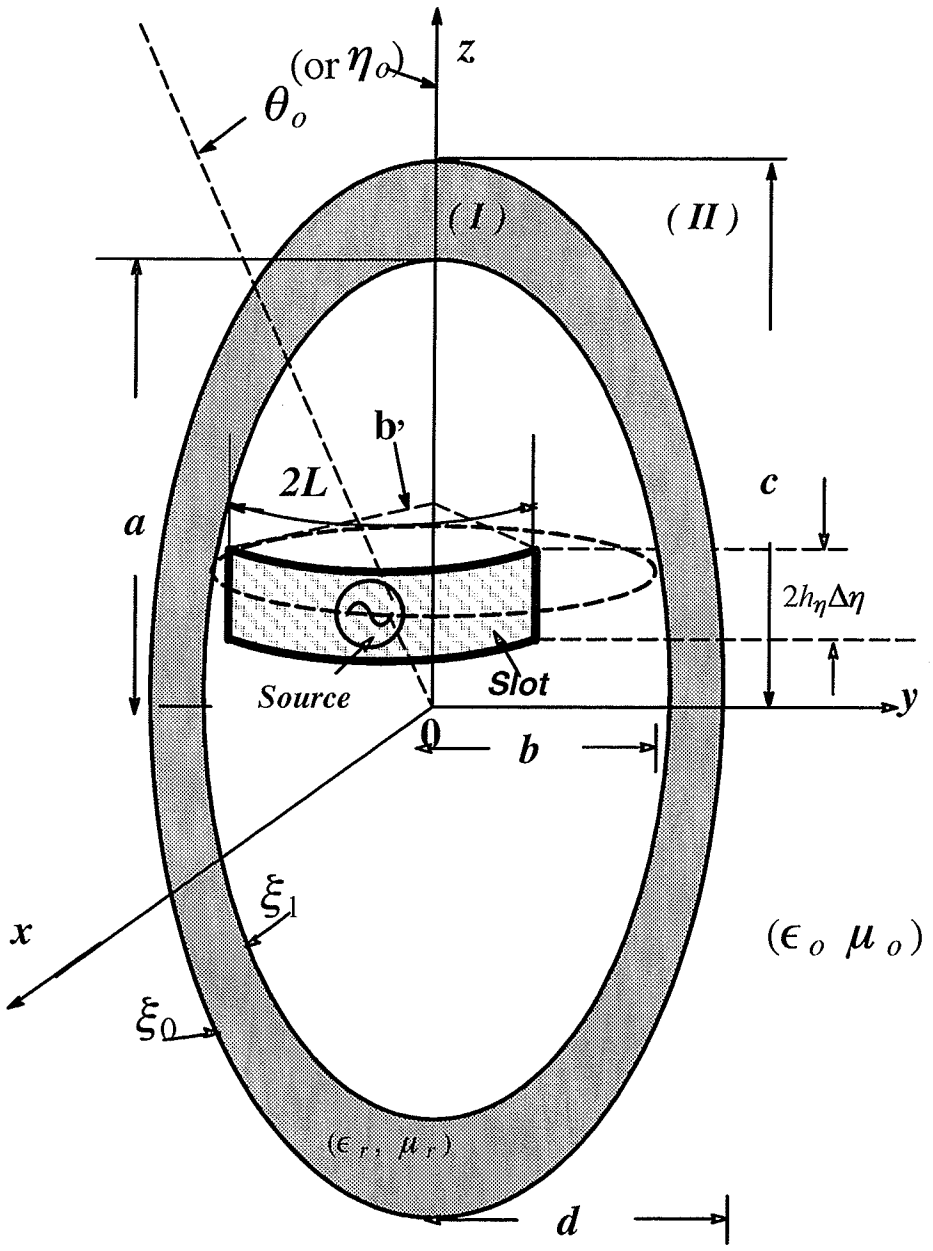

Fig. 4.2 Geometry of the slotted coated prolate spheroid excited by a rotationally asymmetric slot.

4.2.2 Excitation Field

To place our analysis in a more general context, we consider the asymmetrical configuration illustrated in Fig. 4.2 and assume that the exciting electric field over the aperture is ϕ –dependent and polarized in the η –direction, and is given by the following form:

$$E_{\eta}^{ex} = \begin{cases} \sum_{m=0}^{\infty} E_m^{ex} \cos m\phi & at\ \xi = \xi_1\ ,\eta_0 - \Delta\eta \le \eta \le \eta_0 + \Delta\eta \text{ and } -\phi_0 \le \phi \le \phi_0 \\ 0 \quad \text{otherwise} \end{cases} \tag{4.3}$$

and $$E_{\phi}^{ex} = 0 \tag{4.4}$$

where E_m^{ex} (m=0,1,2 ..... ∞) are expansion coefficients which depend on the virtual excitation field distribution and will be determined later.

4.2.3 Radiated Field

The radiated field outside the coating may be expanded in terms of spheroidal vector wave functions $\vec{M}$ and $\vec{N}$ as described in the proceeding chapter. According to (2.43) through (2.36), the fourth kind vectors $\vec{M}_{m,n}^{r(4)}$ and $\vec{N}_{m,n}^{r(4)}$ must be used here, since the physical nature of the problem requires that only outgoing waves will be present for $h\xi \to \infty$. Furthermore, the components of the radiated field must have the same ϕ – dependence as the corresponding components of the excitation field. Thus the radiated electric and magnetic fields are set up in the following forms:

$$\vec{E}^{R} = \sum_{m=0}^{\infty}\sum_{n=m}^{\infty}[\gamma_{mn}\vec{M}^{r(4)}_{o\,mn}(h_0,\xi,\eta,\phi) + \delta_{mn}\vec{N}^{r(4)}_{e\,mn}(h_0,\xi,\eta,\phi)] \tag{4.5}$$

and $$\vec{H}^{R} = j/Z_o \sum_{m=0}^{\infty}\sum_{n=m}^{\infty}[\gamma_{mn}\vec{N}^{r(4)}_{o\,mn}(h_0,\xi,\eta,\phi) + \delta_{mn}\vec{M}^{r(4)}_{e\,mn}(h_0,\xi,\eta,\phi)] \tag{4.6}$$

The coefficients γ_{mn} and δ_{mn} are to be determined by employing the boundary matching technique, and $h_0 = Fk_o$.

It is easy to show that if the asymptotic forms of $\vec{M}^{r(4)}_{m,n}$ and $\vec{N}^{r(4)}_{m,n}$ are applied to (4.5) and (4.6), the far–zone fields may be written in the forms

$$H^{R}_{\eta} = -E_{\phi}{}^{R}/Z_0 = -\frac{e^{-jk_0 r}}{k_o Z_o r}\sum_{m=0}^{\infty}\sum_{n=m}^{\infty} j^n(\sin\theta\; j\frac{dS_{mn}(h_o,\cos\theta)}{d(\cos\theta)}\gamma_{mn} - \\ -\frac{m\; S_{mn}(h_o,\cos\theta)}{\sin\theta}\delta_{mn})\sin(m\phi) \tag{4.7}$$

and

$$H^{R}_{\phi} = E_{\eta}{}^{R}/Z_o = \frac{e^{-jk_o r}}{k_o Z_o\; r}\sum_{m=0}^{\infty}\sum_{n=m}^{\infty} j^n(-\frac{m\; jS_{mn}(h_o,\cos\theta)}{\sin\theta}\gamma_{mn} + \\ +\sin\theta\frac{dS_{mn}(h_o,\cos\theta)}{d(\cos\theta)}\delta_{mn})cos(m\phi) \tag{4.8}$$

Where Z_o is the intrinsic impedance of free space.

4.2.4 Transmitted Field

In the coating region $\xi_1 < \xi < \xi_0$, the expressions for the transmitted fields must include "ingoing" and "outgoing" radial waves due to the fact that both the first and second spheroidal radial function are finite. Thus the expressions for the transmitted fields are

given by:

$$\vec{E}^{T} = \sum_{m=0}^{\infty}\sum_{n=m}^{\infty}[\alpha^{(1)}_{mn}\vec{M}^{r(1)}_{omn}(h_1,\xi,\eta,\phi) + \beta^{(1)}_{mn}\vec{N}^{r(1)}_{emn}(h_1,\xi,\eta,\phi) +$$

$$+\alpha^{(2)}_{mn}\vec{M}^{r(2)}_{omn}(h_1,\xi,\eta,\phi) + \beta^{(2)}_{mn}\vec{N}^{r(2)}_{emn}(h_1,\xi,\eta,\phi)] \qquad (4.9)$$

$$\vec{H}^{T} = j/Z_1\sum_{m=0}^{\infty}\sum_{n=m}^{\infty}[\alpha^{(1)}_{mn}\vec{N}^{r(1)}_{omn}(h_1,\xi,\eta,\phi) + \beta^{(1)}_{mn}\vec{M}^{r(1)}_{emn}(h_1,\xi,\eta,\phi) +$$

$$+\alpha^{(2)}_{mn}\vec{N}^{r(2)}_{omn}(h_1,\xi,\eta,\phi) + \beta^{(2)}_{mn}\vec{M}^{r(2)}_{emn}(h_1,\xi,\eta,\phi)] \qquad (4.10)$$

Where $h_1 = k_1 F$ and $\alpha^{(1)}_{mn}$, $\beta^{(1)}_{mn}$, $\alpha^{(2)}_{mn}$ and $\beta^{(2)}_{mn}$ are unknown expansion coefficients. Z_1 is the intrinsic impedance of the coating layer.

4.3 BOUNDARY CONDITION

The expansion coefficients given in (4.5), (4.6), (4.9) and (4.10) can be evaluated by imposing boundary conditions which require that the tangential components of the electric and magnetic fields be continuous across the interface $\xi = \xi_o$, and that the tangential components of the electric field vanish at $\xi = \xi_1$, except at the slot. The boundary conditions may be explicitly stated in the following forms

$$E_\eta{}^{T} = E_\eta{}^{R} \quad \text{and} \quad E_\phi{}^{T} = E_\phi{}^{R}, \quad \xi = \xi_o \qquad (4.11)$$

$$H_\eta{}^{T} = H_\eta{}^{R} \quad \text{and} \quad H_\phi{}^{T} = H_\phi{}^{R}, \quad \xi = \xi_o \qquad (4.12)$$

$$E_\eta{}^T = \begin{cases} E_\eta{}^{ex} & \text{at the slot,i.e. } \xi = \xi_1 \ , \ \eta_0 - \Delta\eta < \eta < \eta_0 + \Delta\eta \text{ and } \phi \le |\phi_o| \\ 0 & \text{otherwise} \end{cases} \tag{4.13}$$

$$\text{and} \qquad E_\phi{}^T = 0 \qquad \text{at} \quad \xi = \xi_1 \tag{4.14}$$

The substitution of the field expressions (4.5), (4.6), (4.9) and (4.10) into (4.11) to (4.14) leads to a system of equations for the unknown coefficients. Obviously, in the summation over m in each expression for these conditions, it is not difficult to match term by term due to the orthogonality of the functions $\cos m\phi$ and $\sin m\phi$. However, for the summation over n, the individual terms in the series can not be matched term by term because of the dependence of the spheroidal angular functions on the property of the medium. To overcome this problem, a method of handling the boundary–value problem of the coated spheroid, similar to Yeh's approach [18] mentioned in Chapter 1, is used here. Explicitly stated, the equations that stand for the continuity of η – components are multiplied by $(\xi_1^2-\eta^2)^{5/2}S_{m+1,\,m+1+N}\,(h_1,\eta)$ at $\xi = \xi_1$ and by $(\xi_o^2-\eta^2)^{5/2}S_{m+1,\,m+1+N}\,(h_1,\eta)$ at $\xi = \xi_o$. The equations for the continuity of ϕ – components are multiplied by $(\xi_1^2-\eta^2)(\xi_1^2-1)^{-1/2}S_{m+1,\,m+1+N}\,(h_1,\eta)$ at $\xi = \xi_1$ and by $(\xi_o^2-\eta^2)(\xi_o^2-1)^{-1/2}S_{m+1,\,m+1+N}\,(h_1,\eta)$ at $\xi = \xi_o$. Then the resulting expressions are integrated over the region $(-1 \le \eta \le +1)$. By the quasi–orthogonality of the spheroidal angular function indicated in(2.27) and the orthogonality of Legendre functions, an infinite system of equations in an infinite set of unknown coefficients $\alpha_{mn}^{(1)}, \beta_{mn}^{(1)}, \alpha_{mn}^{(2)}, \beta_{mn}^{(2)}, \gamma_{mn}$ and δ_{mn} can be set up, and can be written in the form

$$\sum_{n=0}^{\infty}[\alpha^{(1)}_{m,\,m+n}A^{(1)}_{m,\,N,\,n}(h_1,\ h_1,\xi_1)+\beta^{(1)}_{m,\,m+n}B^{(1)}_{m,\,N,\,n}(h_1,\ h_1,\ \xi_1)+$$

$$+\alpha^{(2)}_{m,\,m+n}A^{(2)}_{m,\,N,\,n}(h_1,\ h_1,\ \xi_1)+\beta^{(2)}_{m,\,m+n}B^{(2)}_{m,\,N,\,n}(h_1,\ h_1,\ \xi_1)]=F_{m+1,\,m+N+1}(h_1,\ h_1,\ \xi_1) \qquad (4.15)$$

$$\sum_{n=0}^{\infty}[\alpha^{(1)}_{m,\,m+n}C^{(1)}_{m,\,N,\,n}(h_1,\ h_1,\ \xi_1)+\beta^{(1)}_{m,\,m+n}D^{(1)}_{m,\,N,\,n}(h_1,\ h_1,\ \xi_1)+$$

$$+\alpha^{(2)}_{m,\,m+n}C^{(2)}_{m,\,N,\,n}(h_1,\ h_1,\ \xi_1)+\beta^{(2)}_{m,\,m+n}D^{(2)}_{m,\,N,\,n}(h_1,\ h_1,\ \xi_1)]=0 \qquad (4.16)$$

$$\sum_{n=0}^{\infty}[\alpha^{(1)}_{m,\,m+n}A^{(1)}_{m,\,N,\,n}(h_1,\ h_1,\ \xi_o)+\beta^{(1)}_{m,\,m+n}B^{(1)}_{m,\,N,\,n}(h_1,\ h_1,\ \xi_o)+$$

$$+\alpha^{(2)}_{m,\,m+n}A^{(2)}_{m,\,N,\,n}(h_1,\ h_1,\ \xi_o)+\beta^{(2)}_{m,\,m+n}B^{(2)}_{m,\,N,\,n}(h_1,\ h_1,\ \xi_o)]$$

$$=\sum_{n=0}^{\infty}[\gamma_{m,\,m+n}A^{(4)}_{m,\,N,\,n}(h_o,\ h_1\ ,\xi_o)+\delta_{m,\,m+n}B^{(4)}_{m,\,N,\,n}(h_o,\ h_1,\ \xi_o)] \qquad (4.17)$$

$$\sum_{n=0}^{\infty}[\alpha^{(1)}_{m,\,m+n}C^{(1)}_{m,\,N,\,n}(h_1,\ h_1,\ \xi_o)+\beta^{(1)}_{m,\,m+n}D^{(1)}_{m,\,N,\,n}(h_1,\ h_1,\ \xi_o)+$$

$$+\alpha^{(2)}_{m,\,m+n}C^{(2)}_{m,\,N,\,n}(h_1,\ h_1,\ \xi_o)+\beta^{(2)}_{m,\,m+n}D^{(2)}_{m,\,N,\,n}(h_1,\ h_1,\ \xi_o)]$$

$$=\sum_{n=0}^{\infty}[\gamma_{m,\,m+n}C^{(4)}_{m,\,N,\,n}(h_o,\ h_1\ ,\xi_o)+\delta_{m,\,m+n}D^{(4)}_{m,\,N,\,n}(h_o,\ h_1,\ \xi_o)] \qquad (4.18)$$

$$Z_r \sum_{n=0}^{\infty} [\alpha^{(1)}_{m,\,m+n} B^{(1)}_{m,\,N,\,n}(h_1,\ h_1,\ \xi_o) - \beta^{(1)}_{m,\,m+n} A^{(1)}_{m,\,N,\,n}(h_1,\ h_1,\ \xi_o) +$$

$$+ \alpha^{(2)}_{m,\,m+n} B^{(2)}_{m,\,N,\,n}(h_1,\ h_1, \xi_o) - \beta^{(2)}_{m,\,m+n} A^{(2)}_{m,\,N,\,n}(h_1,\ h_1,\ \xi_o)]$$

$$= \sum_{n=0}^{\infty} [\gamma_{m,\,m+n} B^{(4)}_{m,\,N,\,n}(h_o,\ h_1\ , \xi_o) - \delta_{m,\,m+n} A^{(4)}_{m,\,N,\,n}(h_o,\ h_1,\ \xi_o)] \qquad (4.19)$$

$$Z_r \sum_{n=0}^{\infty} [-\alpha^{(1)}_{m,\,m+n} D^{(1)}_{m,\,N,\,n}(h_1,\ h_1,\ \xi_o) + \beta^{(1)}_{m,\,m+n} C^{(1)}_{m,\,N,\,n}(h_1,\ h_1,\ \xi_o) -$$

$$- \alpha^{(2)}_{m,\,m+n} D^{(2)}_{m,\,N,\,n}(h_1,\ h_1, \xi_o) + \beta^{(2)}_{m,\,m+n} C^{(2)}_{m,\,N,\,n}(h_1,\ h_1,\ \xi_o)]$$

$$= \sum_{n=0}^{\infty} [-\gamma_{m,\,m+n} D^{(4)}_{m,\,N,\,n}(h_o,\ h_1\ , \xi_o) + \delta_{m,\,m+n} C^{(4)}_{m,\,N,\,n}(h_o,\ h_1,\ \xi_o)] \qquad (4.20)$$

Where m, N=0, 1, 2, ... ∞. These matrix elements A, B, C, D and F of above expressions are evaluated by

$$A^{(j)}_{m,\,N,\,n}(x,\ y,\ \xi) = -m\xi\ R^{(j)}_{m,\,m+n}(x,\ \xi)\Big[\,(\xi^2-1)^2 I_{1\,m\,N\,n}\ (x,\ y) +$$

$$+ 2(\xi^2-1) I_{2\,m\,N\,n}\ (x,\ y) + I_{3\,m\,N\,n}\ (x,\ y)\Big] \qquad (4.21)$$

$$B^{(j)}_{m,\,N,\,n}(x,\ y,\ \xi) = \frac{1}{x}\Big\{\,[(3\xi^2-1) R^{(j)}_{m,\,m+n}(x,\ \xi) + \xi(\xi^2-1)\frac{d}{d\xi} R^{(j)}_{m,\,m+n}(x,\ \xi)] \times$$

$$\times\ [(\xi^2-1) I_{4\,m\,N\,n}\ (\ x,\ y) + I_{5\,m\,N\,n}\ (x,\ y)] - 2\xi^{\,2}(\xi^2-1) R^{(j)}_{m,\,m+n}(x,\ \xi) I_{4\,m\,N\,n}\ (\ x,\ y)$$

$$+\Big[[(\lambda_{m,\,m+n}(x)-x^2\xi^2)(\xi^2-1)+m^2]R^{(j)}_{m,\,m+n}(x,\ \xi)-$$

$$-2\xi(\xi^2-1)\frac{d}{d\xi}R^{(j)}_{m,\,m+n}(x,\ \xi)\Big]\times I_{6\,m\,N\,n}\ (x,\ \xi)+$$

$$+[\lambda_{m,\,m+n}(x)-x^2\xi^2+\frac{m^2}{(\xi^2-1)}]\ I_{7\,m\,N\,n}\ (x,\ y)R^{(j)}_{m,\,m+n}(x,\ \xi)+$$

$$+[\lambda_{m,\,m+n}(x)-x^2\xi^2+\frac{m^2}{(\xi^2-1)}]\ I_{7\,m\,N\,n}\ (x,\ y)R^{(j)}_{m,\,m+n}(x,\ \xi)+$$

$$+m^2R^{(j)}_{m,\,m+n}(x,\ \xi)\Big[(\xi^2-1)I_{8\,m\,N\,n}\ (x,\ y)+2I_{6\,m\,N\,n}\ (x,\ y)+\frac{I_{7\,m\,N\,n}\ (x,\ y)}{(\xi^2-1)}\quad\Big]\Big\} \tag{4.22}$$

$$C^{(j)}_{m,\,N,\,n}(x,\ y,\ \xi)=\xi\ R^{(j)}_{m,\,m+n}(x,\ \xi)I_{4\,m\,N\,n}\ (x,\ y)-\frac{d}{d\xi}R^{(j)}_{m,\,m+n}(x,\ \xi)I_{6\,m\,N\,n}\ (x,\ y) \tag{4.23}$$

$$D^{(j)}_{m,\,N,\,n}(x,\ y,\ \xi)=-\frac{m}{x}\Big\{[\xi\frac{d}{d\xi}R^{(j)}_{m,\,m+n}(x,\ \xi)+R^{(j)}_{m,\,m+n}(x,\ \xi)]\ I_{1\,m\,N\,n}\ (x,\ y)+$$

$$+\frac{R^{(j)}_{m,\,m+n}(x,\ \xi)}{(\xi^2-1)}\ [I_{9\,m\,N\,n}\ (x,\ y)+I_{2\,m\,N\,n}\ (x,\ y)]\Big\} \tag{4.24}$$

$$F_{m+1,\,m+1+N}(x,\ \xi)=-\int_{\eta_o-\Delta\eta}^{\eta_o+\Delta\eta}E^{ex}_m(\xi^2-\eta^2)^{5/2}S_{m+1\,,\,m+N+1}(x,\eta)d\eta$$

$$=-\int_{\eta_o-\Delta\eta}^{\eta_o+\Delta\eta}\frac{V_0k_1E_m}{x2\Delta\eta}\sqrt{(1-\eta^2)}\,(\xi^2-\eta^2)^2S_{m+1\,,\,m+N+1}(x,\eta)d\eta \tag{4.25}$$

In the case of the narrow slot($\Delta\eta \rightarrow 0$), (4.25) becomes

$$F_{m+1,\, m+1+N}(x,\ \xi) = -\frac{V_0 k_1 E_m}{x}\sqrt{(1-\eta_0^2)}\,(\xi^2-\eta_0^2)^2 S_{m+1\,,\, m+N+1}(x,\eta_0) \qquad (4.26)$$

Where $x,\ y = h_1$ *or* h_o and $\lambda_{m,\, m+n}(x)$ is the spheroid eignvalue [8] and, as usual, the index j indicates the kind of the spheroidal prolate radial functions. E_m $(m = 0\ ,1\ ,2\ \ldots\ldots)$ are expansion coefficients of the excitation field function on the slot. The integrals $I_{p,\, m,\, N,\, n}(x,\ y)$ $(p = 1, 2\ldots 9)$ are given and evaluated in Appendix **B**.

Once the coefficients $\gamma_{m,\, n}$ and $\delta_{m,\, n}$ are obtained, the far–zone radiation field (that is, $\xi \rightarrow \infty$) may be calculated from expressions (4.7) and (4.8). Then the time–average radial component of the poynting vector in the radiation zone is given by

$$p = \frac{1}{2}(\vec{E}^R \times \vec{H}^{R*}) \cdot \hat{e}_r = \frac{1}{2Z_o}(|E_\eta\ |^2 + |E_\phi\ |^2) \qquad (4.27)$$

where $\hat{e}_r$ is a unit vector in the radial direction. An integration of the expression (4.27) over an infinitely large spherical surface gives the total radiation power, and it can be readily shown that

$$P = \frac{1}{2Z_0 k_0^2}\sum_{m=0}^{\infty}\sum_{n=0}^{\infty}\sum_{N=0}^{\infty}(1+e_{m\,0})[\gamma_{m,\, m+n}\gamma^*_{m,\, m+N} + \delta_{m,\, m+n}\ \delta^*_{m,\, m+N}] \times$$

$$\times\ [\lambda_{m,\, m+n}(h_o) I_{10\, m\, n\, N}(h_o,\ h_o) - h_o^2 I_{11\, m\, n\, N}(h_o,\ h_o)] \qquad (4.28)$$

where the symbol * denotes the complex conjugation. The two integrations $I_{10\, m\, n\, N}$ and $I_{11\, m\, n\, N}$ are also given and evaluated in Appendix **B**.

It is worth noticing that the analysis developed above is based only on a general bound-

ary value problem. No assumption of an aperture field distribution along the slot is being made. In the next section, these formulas will be applied to two cases of narrow slot antennas on the conducting spheroid with coating.

4.4 NUMERICAL COMPUTATION AND RESULTS

The convergence properties of the linear system of equations (4.15) through (4.20) are similar to those of the scattering problem of conducting spheroid with dielectric coating which has been discused by Sebak and Sinha [24]. To solve these equations, the infinite series can be truncated to finite ones with the first N_o terms. Analogous to the approaches pointed out by Sinha and MacPhie [20], the value of N_o for the coated slotted spheroidal antenna is chosen by repeating computations for successively larger values of N_0 until the desired figure of accuracy is achieved, *i.e.*, at least three digit accuracy.

In the following two subsections, the above analysis will be applied to two cases of the coated conducting spheroidal antennas.

4.4.1 Rotationally symmetric circumferential slot

As the first application of the above analysis, let us consider a so–called rotationally symmetric slotted spheroid antenna coated with a confocal homogeneous layer whose electric property is described by ϵ_r and μ_r as illustrated in Fig. 4.1. The field distribution across the slot is taken to be independent of ϕ, that is,

$$E_\eta^{ex} = \frac{V_o}{2h_\eta \Delta\eta}\delta(\eta - \eta_o) \qquad (4.29)$$

where $h_\eta = F\dfrac{(\xi_1^2-\eta^2)^{1/2}}{(1-\eta^2)^{1/2}}$ and V_o is the applied voltage across the slot. Although this type of slot has been discussed by authors such as Week [17] and Yeh [18], the effect of coating thickness and other physical parameters on the radiation power has not been given. In this case, the term E_m^{ex} in the expression (4.3) is obtained as follows

$$E_m^{ex} = e_{m\,0} \tag{4.30}$$

Thus, in equation (4.15) only the term of $m=0$ does not vanish and equals

$$F_{1,\,1+N}(x,\xi) = -\frac{V_0 k_1}{x}\sqrt{(1-\eta_0^2)}\,(\xi^2-\eta_0^2)^2 S_{1\,,\,N+1}(x,\eta_0) \tag{4.31}$$

where $e_{m\,0}=1$ for $m=0$ and $e_{m\,0}=0$ for $m \neq 0$. This in effect means that the field components, whose ϕ – dependance is of the form $\sin m\phi$, are zero, and the summations over m in all equations given in the proceeding section are reduced to only $m=0$ term. It follows that, from expression (4.28), the total radiated power is given by

$$P = \frac{1}{Z_0 k_0^2}\sum_{n=0}^{\infty}\sum_{N=0}^{\infty}\delta_{1,\,1+n}\;\delta^*_{1,\,1+N}\;\left[\lambda_{1,\,1+n}(h_o)I_{10\,,1\,n\,N}(h_o,h_o) - h_o^2 I_{11\,,1\,n\,N}(h_o,h_o)\right] \tag{4.32}$$

Equation (4.32) shows the dependance of the radiated power on the geometric and coating parameters. Clearly the dependence on the slot geometry, the angular location η_0 and the coating is relatively complex. It is nearly impossible to express the dependence with close explicit formulas due to the complexity of the mathematical expressions. However, in order to study the dependence, the treatment used by Shafai [13] is introduced here. Nu-

merically, the radiated powers are computed for certain parameters and shown in Figs. 4.3–4.7. In all cases, the power ratio P/P_o , *i.e.* the ratio of the radiated powers with and without coating, is plotted as a function of ratio d/λ_r , the ratio of the coating thickness to the wavelength in the coating, with the electrical size $k_o a = 2.0$ and the slot location $\eta_0 = 90^o$ and 60^o.

To test the validity and accuracy of our solutions, an extreme case $a/b \approx 1$ (*i.e.*spherical case) is considered. Figure 4.3 shows the computed P/P_o for $\epsilon_r = 4$ and 9 , whereas, Figure 4.4 shows the results for the magnetic type coatings $\mu_r = 4.0$ and 9.0. It can be seen that these results are identical to those of spherical cases given by Shafai [13]. In his very interesting work, Shafai has shown how some modes becomes resonant for certain coating parameters.

The corresponding results for the spheroidal cases with $a/b = 2.0$ and the slot location $\eta_o = 0$. are shown in Figs. 4.5–4.6. Figure 4.5 is for the electric type materials, and Figure 4.6 for the magnetic type materials. From the results given in these two figures, it is clear that there are still significant resonant peaks, but the locations and magnitude of the peaks are different from the spherical cases. Specifically, the number of the peaks is less.

In Fig. 4.7, the effect of the shape factor a/b of the spheroid on the radiation power is considered with the parameters $k_o a = 2.0$, $\eta_r = 1/2(\theta_o = 60^o)$, $\mu_r = 4.0$, $\epsilon_r = 4.0$ and a/b =2.0, 3.0 and 5.0. One notes that as the ratio a/b increases, the resonance becomes small and the curve shifts backwards successively.

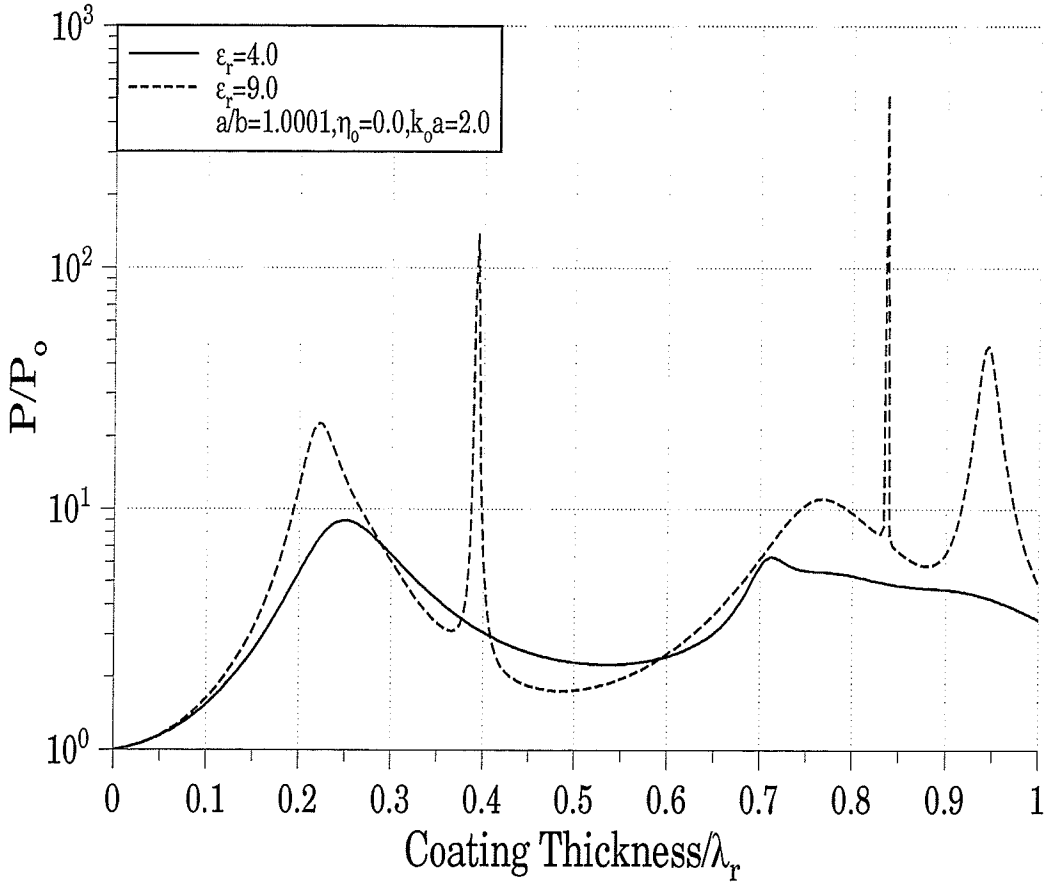

Fig. 4.3 Radiation power of a coated sphere (a/b=1.001)

for $k_o a = 2.0, \eta_o = 0.0$ and $\mu_r = 1.0$.

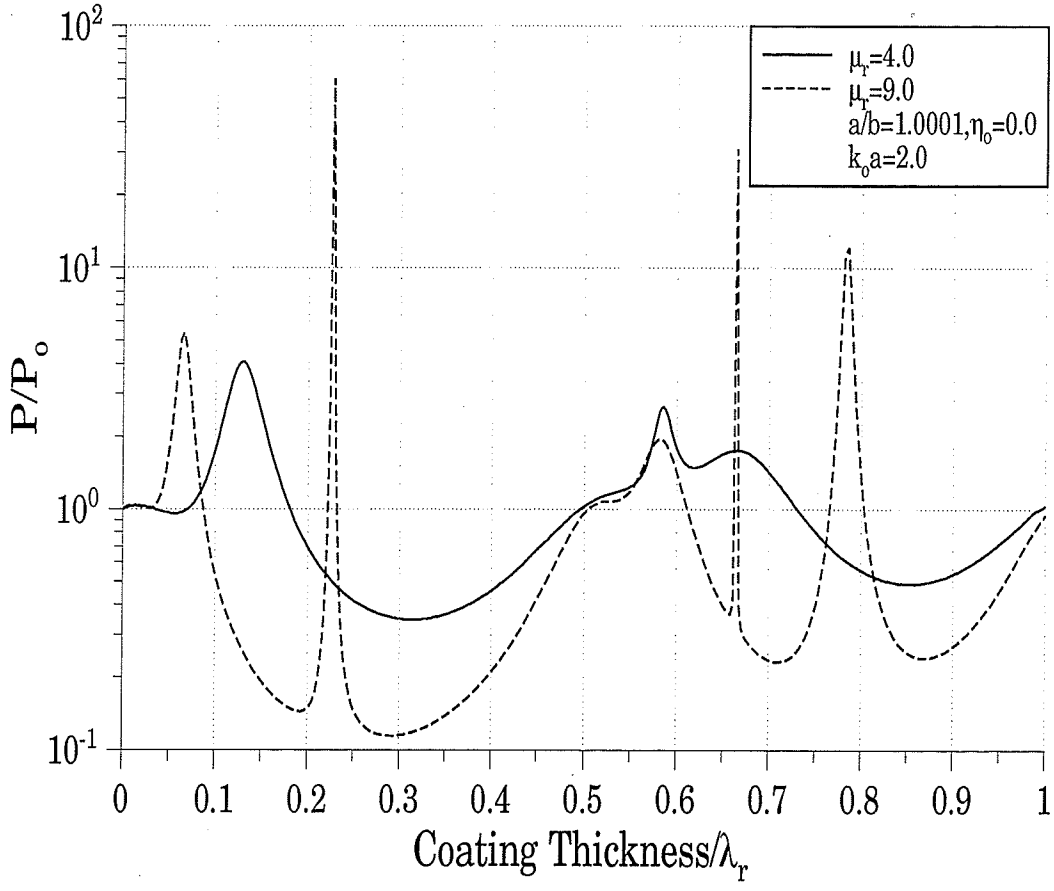

Fig. 4.4 Radiation power of a coated sphere (a/b=1.001) for $k_o a = 2.0, \eta_o = 0.0$ and $\epsilon_r = 1.0$.

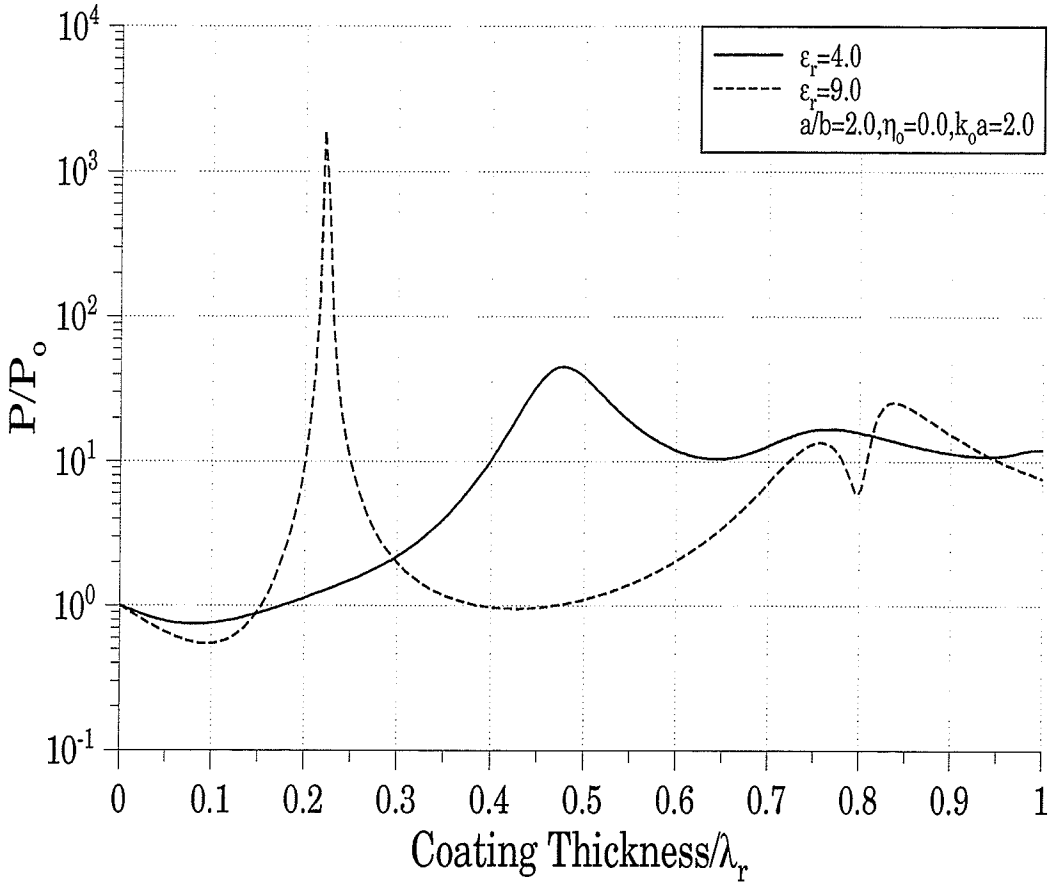

Fig. 4.5 Radiation power of a coated spheroid (a/b=2.0) for $k_o a = 2.0, \eta_o = 0.0$ and $\mu_r = 1.0$.

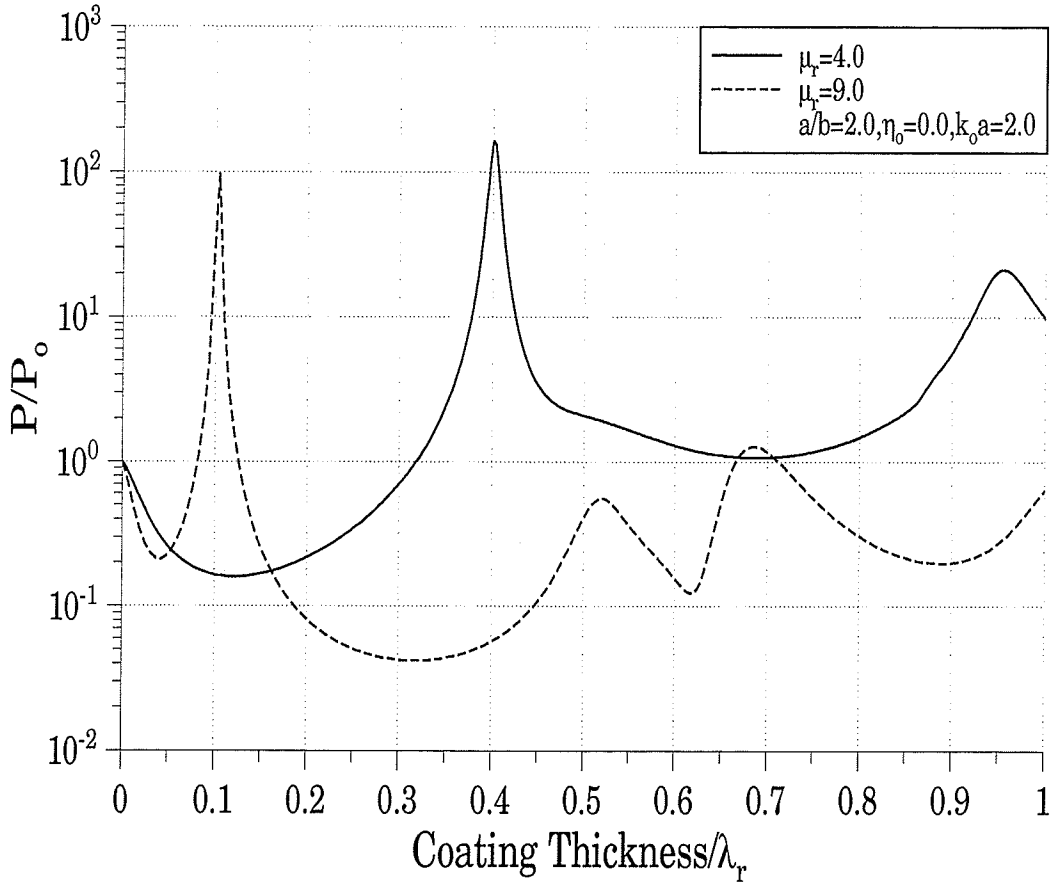

Fig. 4.6 Radiation power of a coated spheroid (a/b=2.0) for $k_o a = 2.0, \eta_o = 0.0$ and $\epsilon_r = 1.0$.

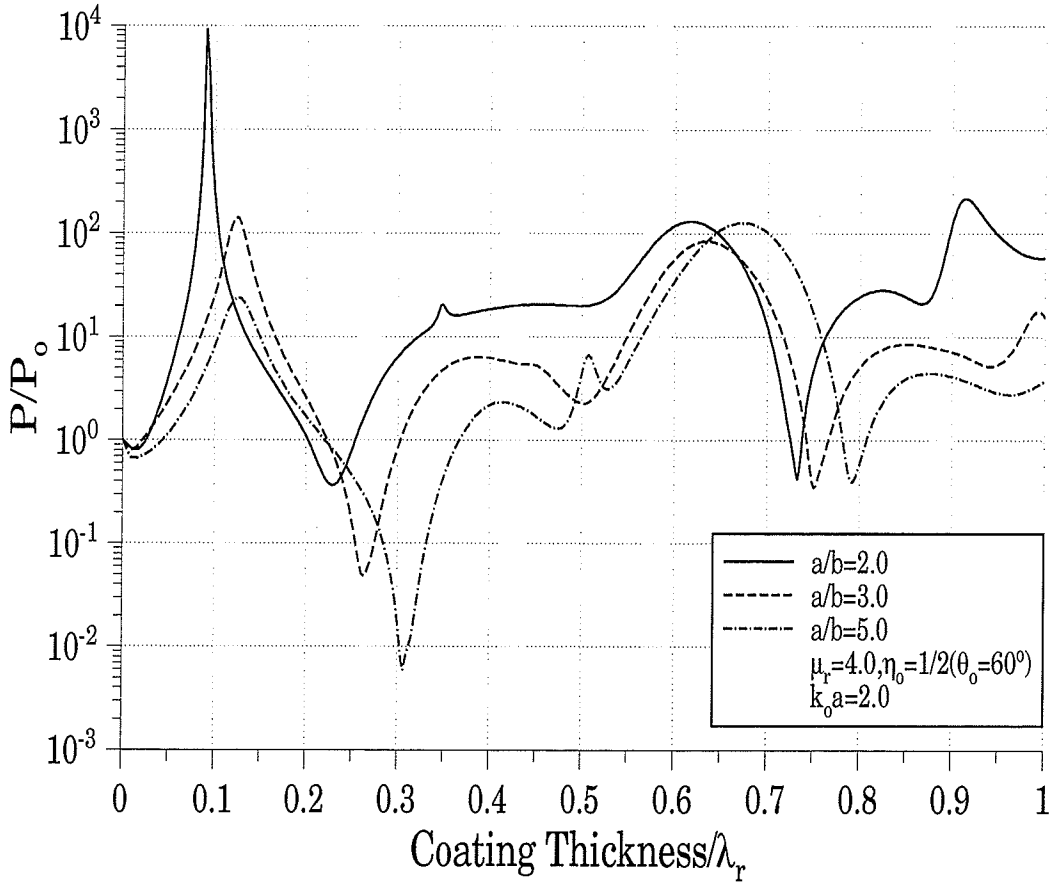

Fig. 4.7 Radiation power of a coated spheroid (a/b=2.0,3.0 and 5.0) for $k_o a = 2.0, \eta_o = 1/2(\theta_o = 60^o)$, $\mu_r = 4.0$ and $\epsilon_r = 1.0$.

4.4.2 Rotationally asymmetric slot

The second application of our solution is one of rotationally asymmetric circumferential slots. As illustrated in Fig. 4.2, the narrow slot with length $2L = \lambda_o/2$ and angular width $2\Delta\eta$ is located at $\eta = \eta_0$ on the spheroidal surface defined by $\xi = \xi_1$. For the purpose of comparison with the known data, the electric field distribution on the slot is assumed to be sinusoidal, *i.e.*,

$$E_\eta^{ex} = \begin{cases} \dfrac{V_o}{2h_\eta(\Delta\eta)} \sin[k_1\ (L - b'|\phi\ |)]\ ,\ \phi \le |\phi_o| = L/b'\ ,\eta_0 - \Delta\eta \le \eta\ \le \eta_0 + \Delta\eta \\ 0 \qquad\qquad\qquad\qquad \text{otherwise} \end{cases} \tag{4.33}$$

$$\text{and} \qquad E_\phi{}^{ex} = 0 \qquad\qquad \text{at} \qquad\qquad \xi = \xi_1 \tag{4.34}$$

where $b' = F[(\xi_1^2 - 1)(1 - \eta_o^2)\ ]^{1/2}$. In the same manner, we expand the expression (4.33) in a Fourier series, namely,

$$E_\eta^{ex}(\phi) = \sum_{m=0}^{\infty} E_m^{ex} \cos m\phi. \tag{4.35}$$

It follows that

$$\begin{aligned} E_m^{ex} &= \frac{V_o}{(1+\delta_m)\pi\ h_\eta(\Delta\eta)} \times \int_0^{\phi_o} \sin[k_1\ (L - b'\phi)] \cos m\phi\, d\phi \\ &= \frac{V_0}{\pi\ h_\eta(\Delta\eta)} E_m \qquad \text{(m=0, 1, 2 .....)} \end{aligned} \tag{4.36}$$

Accordingly, by integration, the coefficients E_m can readily be found as

$$E_m = \begin{cases} \dfrac{1}{k_1 b'}(1-\cos(k_1 L)) & m = 0 \\ \dfrac{2k_1 b'}{\pi\,[(k_1 b)^2 - m^2]}[\cos(m\dfrac{L}{b'}) - cos(k_1 L)] & m \neq 0 \ or \ \neq k_1 b' \\ \dfrac{L}{b'}\sin(k_1 L) & m = k_1 b' \end{cases} \qquad (4.37)$$

Substituting these values of E_m into the system of linear equations (4.15)–(4.20) and (4.25) and solving them for the unknown expansion coefficients $\alpha^{(1)}_{m,n}, \beta^{(1)}_{m,n}, \alpha^{(2)}_{m,n}$, $\beta^{(2)}_{m,n}$, $\delta_{m,n}$ and $\gamma_{m,n}$ give the solution of the far–zone fields. Consequently, the radiated power can be calculated by (4.28).

Again, to examine the accuracy of the solution over the boundary region, the tangential component of the radiated electric field E^T_η has been calculated using (4.9) with $\eta_o = 0.0$ and $1/2$. Some of the computed results for certain design parameters are shown in Figs. 4.8–4.9. Obviously, these figures show that the tangential electric field component satisfies the boundary conditions stated in (4.13) and (4.14).

Some numerical results for the radiation patterns of both E– and H–plane with certain parameters are obtained and presented in Figs. 4.10–4.12. As a further check, Figure 4.10 shows the radiation H– plane patterns for an extreme case in which the ratio of a/b is approximately taken to be one, and the coating is assumed to become transparent(*i.e.* $\epsilon_r \approx 1$ and $\mu_r \approx 1$). Thus this spheroidal slot antenna with a coating layer degenerates as a spherical slot antenna without coating. This has been investigated by Mushiake

and Webster [23]. In comparison, the results calculated by the formulas given in [23] are also shown in Fig. 4.10. It is evident that our data are in close agreement with those reported by [23].

In Fig. 4.11 and Fig. 4.12, the $E-$ and $H-$plane patterns are shown for the spheroidal antennas with slot length $2L = \lambda_o/2$, $\epsilon_r = 2.0$ and 4.0, $\mu_r = 1.0$ and the electric size $k_o a = 1$ and 3, for different values of a/b. It is observed that from the results shown in Figs. 4.11 and 4.14, for given $k_o a$ and $k_o c$, increasing a/b may leads to the increment of radiated power. On the other hand, if fixed a/b, the bigger value of $k_o a$ and $k_o c$ will lead to more side lobes to occur.

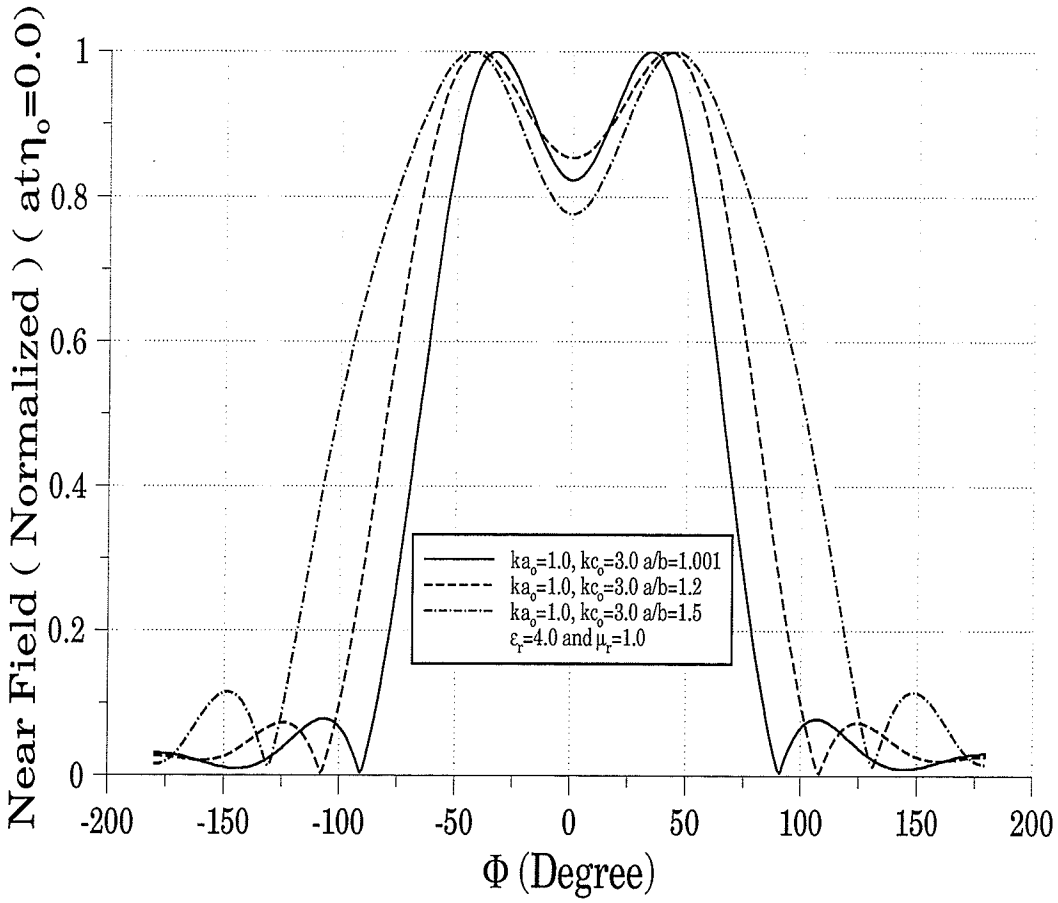

Fig. 4.8 Tangential electric field with $k_o a$=1.0, $k_o c$=3.0 and $\epsilon_r = 4.0$ on the surface ξ_1 and $|\phi_o| \leq |\phi_{o\,\max}| = L/b' = \pi/2, 3\pi/5$ and $3\pi/4$.

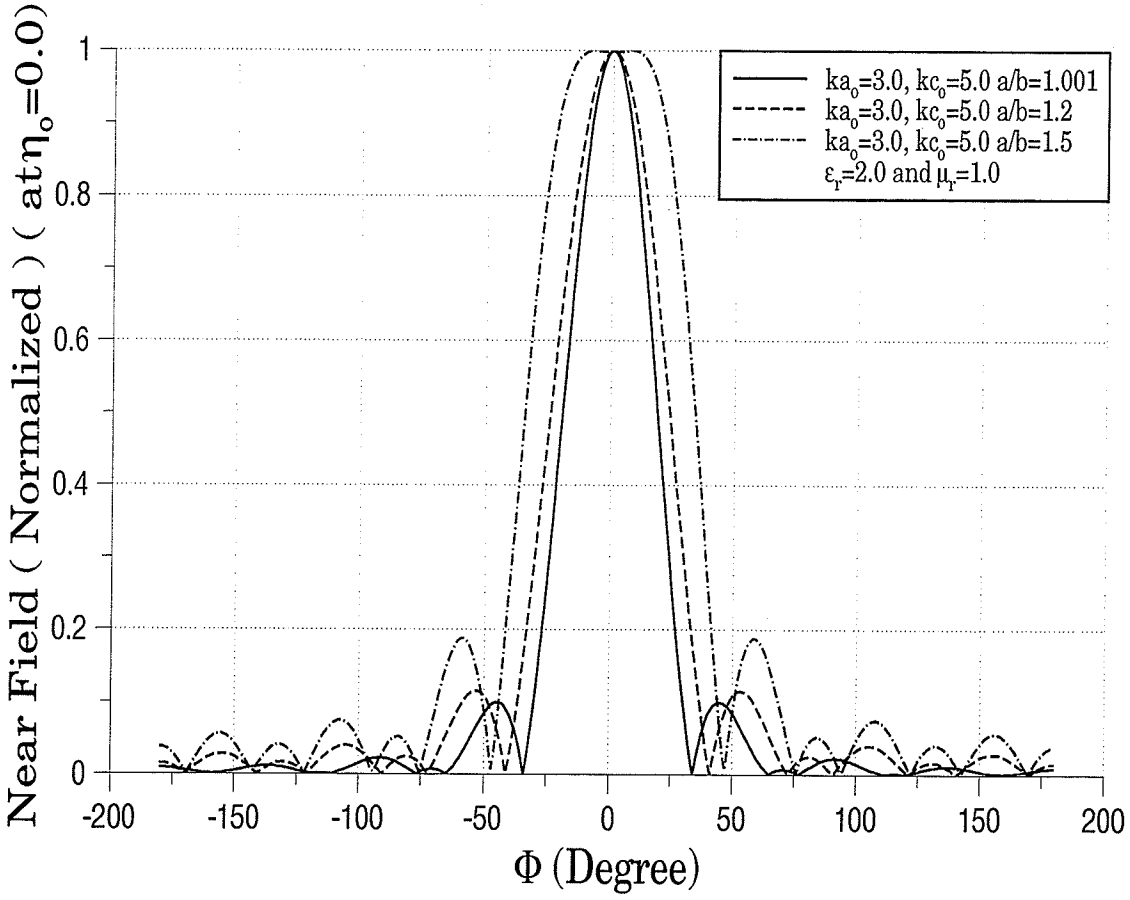

Fig. 4.9 Tangential electric field with k_0a=3.0, k_0c=5.0 and $\epsilon_r = 2.0$ on the surface ξ_1 and $|\phi_o| \leq |\phi_{o\,max}| = L/b' = \pi/6, \pi/5$ and $\pi/4$.

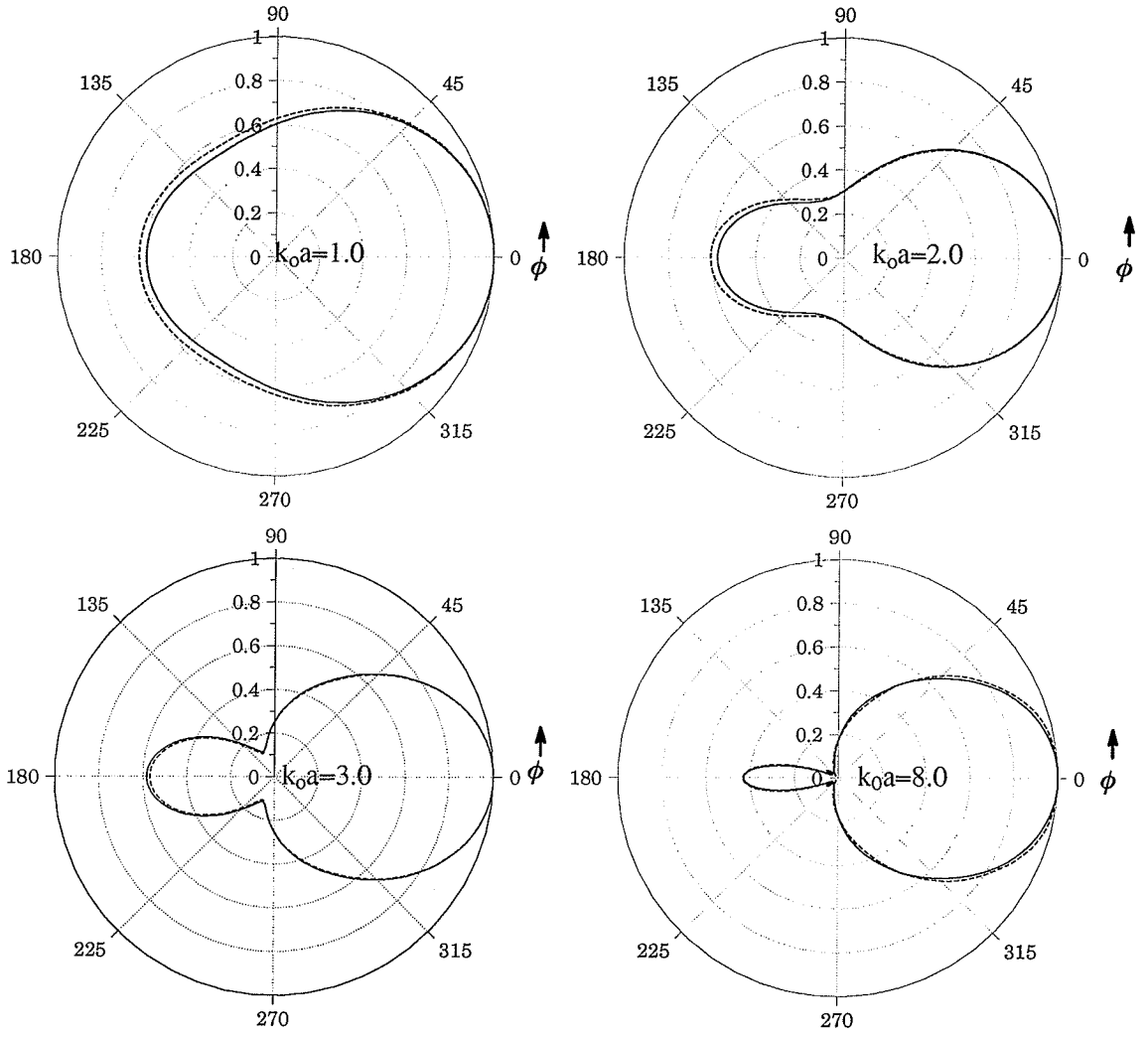

—— this work (a/b=1.0001) - - - - - results by Y.Mushiake *et al.* [23] at $\eta_0 = 0.0$

Fig. 4.10 Calculated radiation patterns (*H*–plane)of a half–wavelength narrow slot on perfectly onducting sphere (a/b=1.0001) without coating ($\epsilon_r = 1.001$ and $\mu_r = 1.0$).

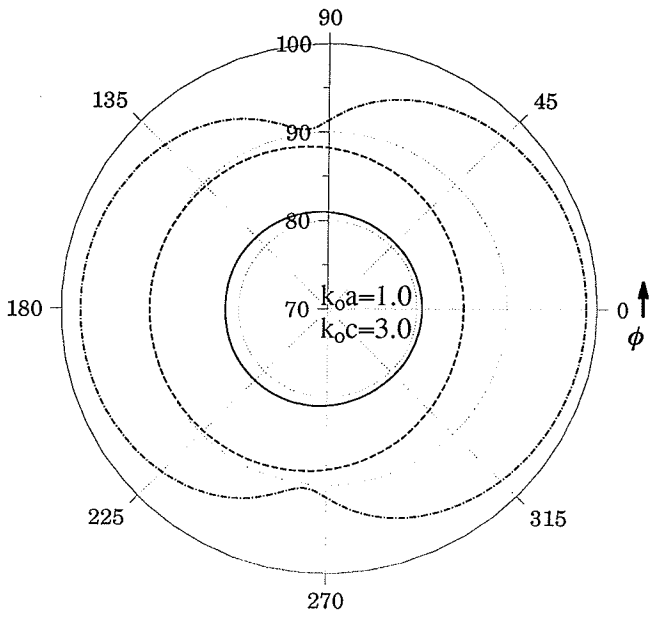

(*a*) : ($\epsilon_r = 2.0$, $\mu_r = 1.0$ and $\eta_o = 0.0(\theta_o = 90^o)$)

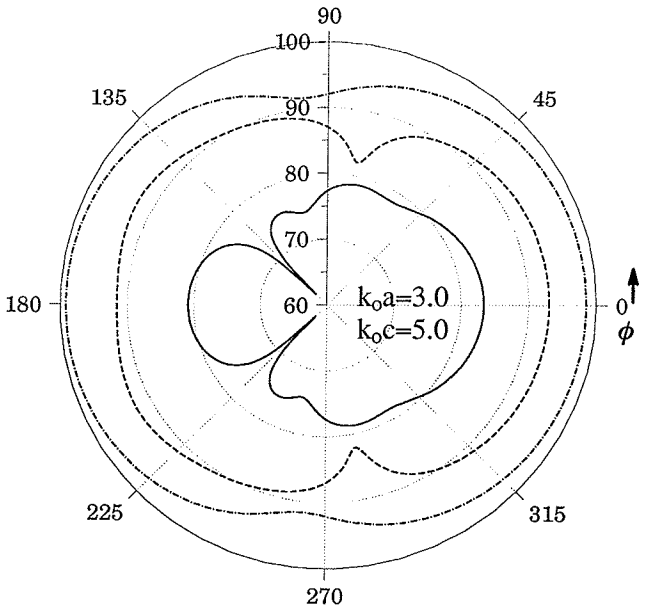

(*b*) : ($\epsilon_r = 4.0$, $\mu_r = 1.0$ and $\eta_o = 0.0(\theta_0 = 90^o)$)

——— a/b=1.2 — — — a/b=1.5 —·— a/b=2.0

Fig. 4.11 Calculated radiation patterns (*H*–plane in dB) of a half–wavelength narrow slot on a perfectly conducting spheroid with coating.

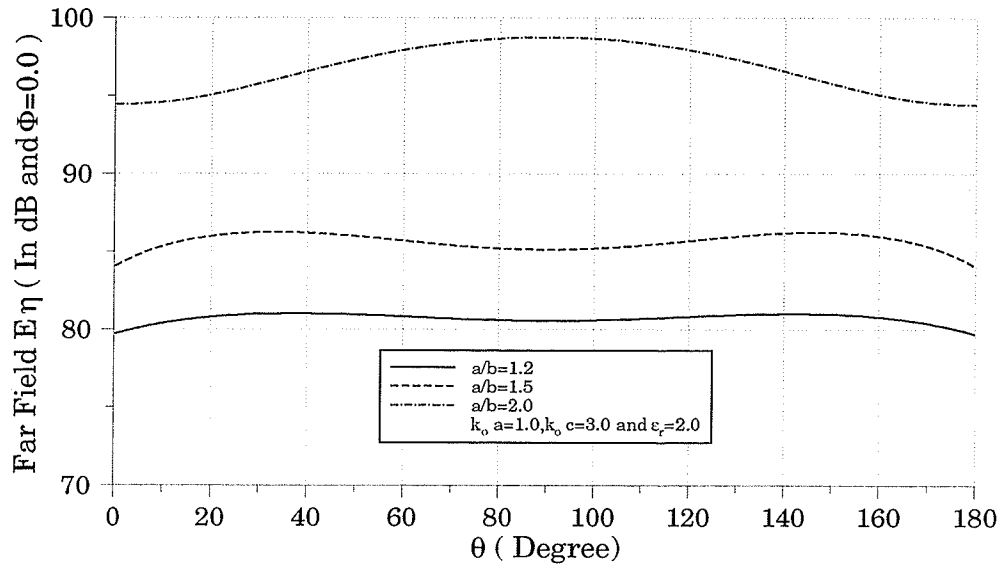

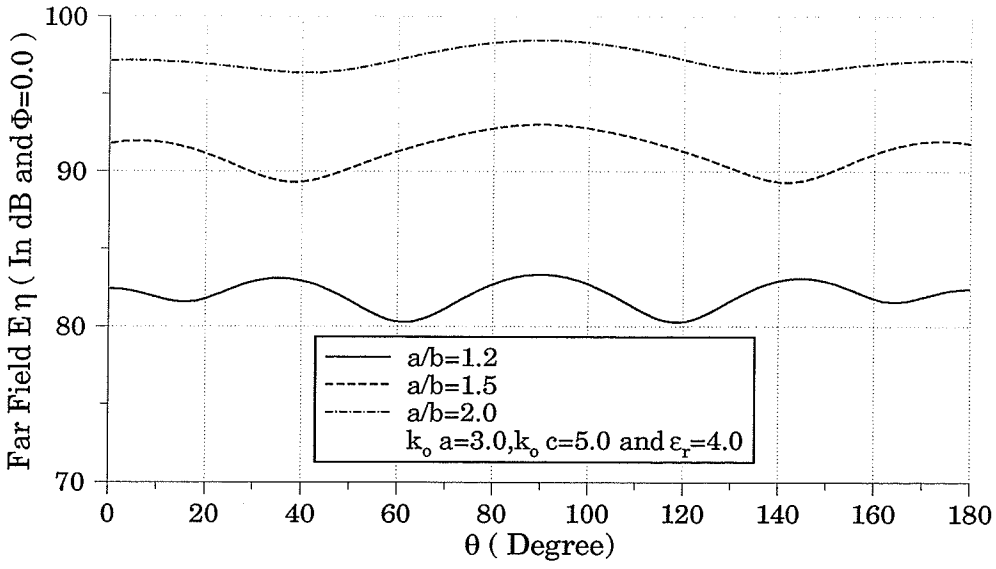

Fig. 4.12 Calculated radiation pattern (E–Plane in dB) of a half–wave narrow slot on a perfectly conducting spheroid with coating.

The effect of coating thickness and some physical parameters on the radiated power are shown in Figs. 4.13–17, where P_0 is the radiated power from uncoated slot antenna . In these cases, P/P_o is plotted as a function of thickness $/\lambda_r$, the ratio of the thickness of the coating to the wavelength in the coating.

From the results shown in Figs. 4.13–4.17, it is noticed that (1) for certain coating thickness and design parameters ($k_o a, a/b, \eta_o$ and ϵ_r), radiated power is enhanced and becomes resonant; (2) Figures 4.13 and 4.15 illustrate the results for the spheroid with the ratio of $a/b = 1.5$. For such a smaller value of a/b, the coating thickness is near uniform, and the resonance peaks are higher and narrower. In contrast, those results for $a/b = 2.0$, *i.e.* for these cases of higher non–uniform coating thickness, are shown in Figs. 4.14 and 4.16 where the resonances are highly damped. This situation is similar to that of the slot antenna on a coated elliptic cylinder investigated by Richmond [7]; (3) Figure 4.17 shows the results for $k_o a = 2.0$, $a/b = 2.0$ and $\theta_o = 60^o$. For this location of the slot, both even and odd modes of the excitation field in the expression (4.26)contribute to the radiated power and enhance the resonance effect. In this case there are still significant resonance peaks, even though higher nonuniformity $a/b = 2.0$ may lead to damping of the resonance, as shown in Fig. 4.16.

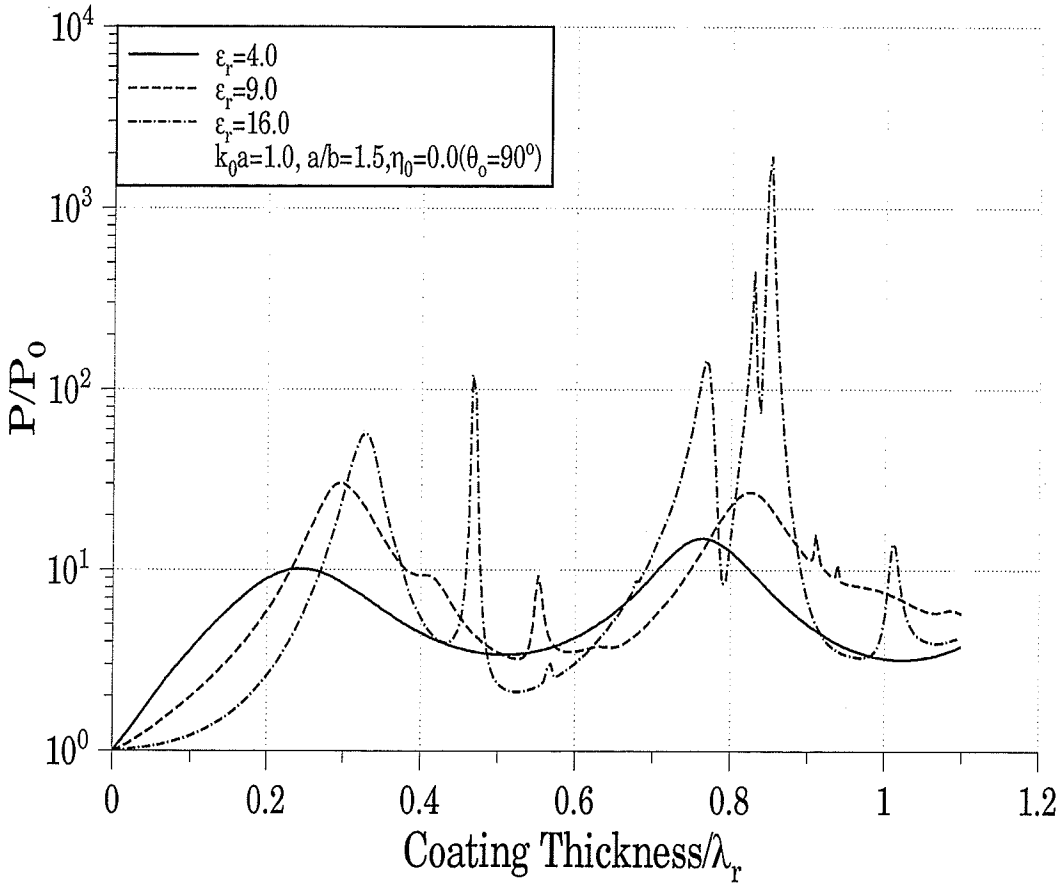

Fig. 4.13 Radiated power of asymmetrically slotted spheroid versus coating thickness for k_oa=1.0, a/b=1.5,μ_r=1.0 and η_o=0.0 (θ_o=90°).

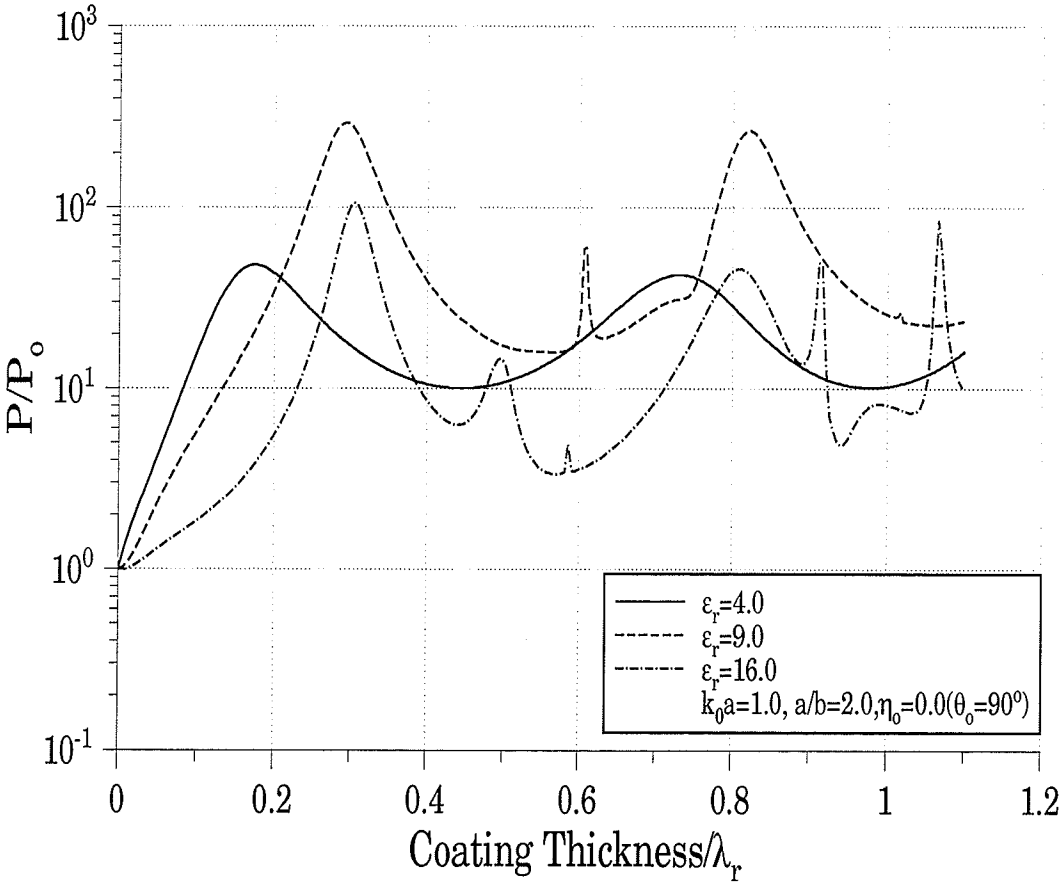

Fig. 4.14 Radiated power of asymmetrically slotted spheroid versus coating thickness for k_oa=1.0, a/b=2.0,μ_r=1.0 and η_o=0.0 (θ_o=90°).

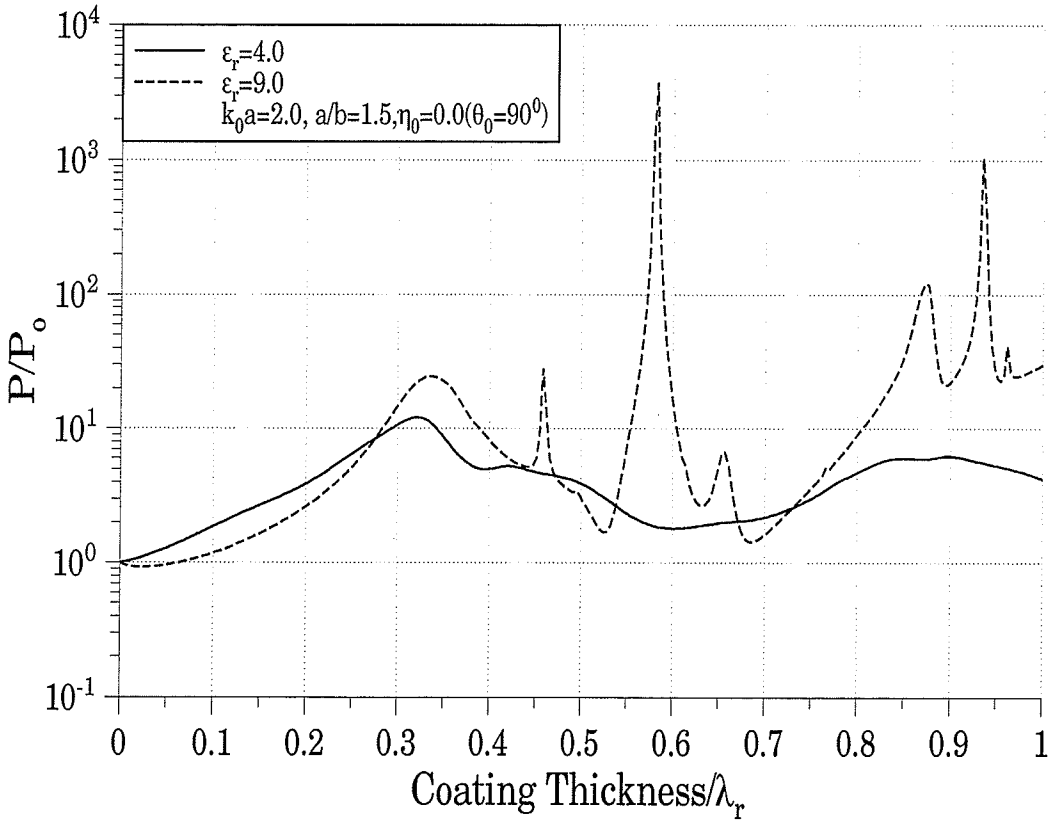

Fig. 4.15 Radiated power of asymmetrically slotted spheroid versus coating thickness for k_oa=2.0, a/b=1.5,μ_r=1.0 and η_o=0.0 (θ_o=90°).

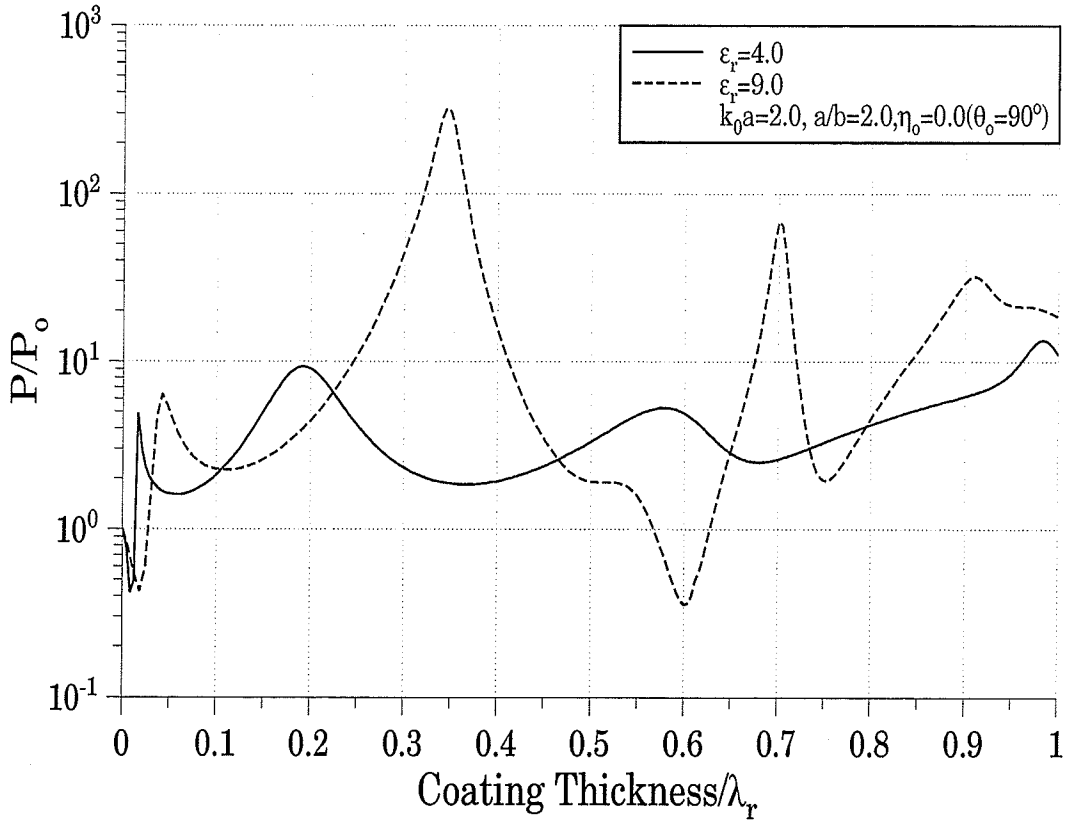

Fig. 4.16 Radiated power of asymmetrically slotted spheroid versus coating thickness for k_oa=2.0, a/b=2.0,μ_r=1.0 and η_o=0.0 (θ_o=90°).

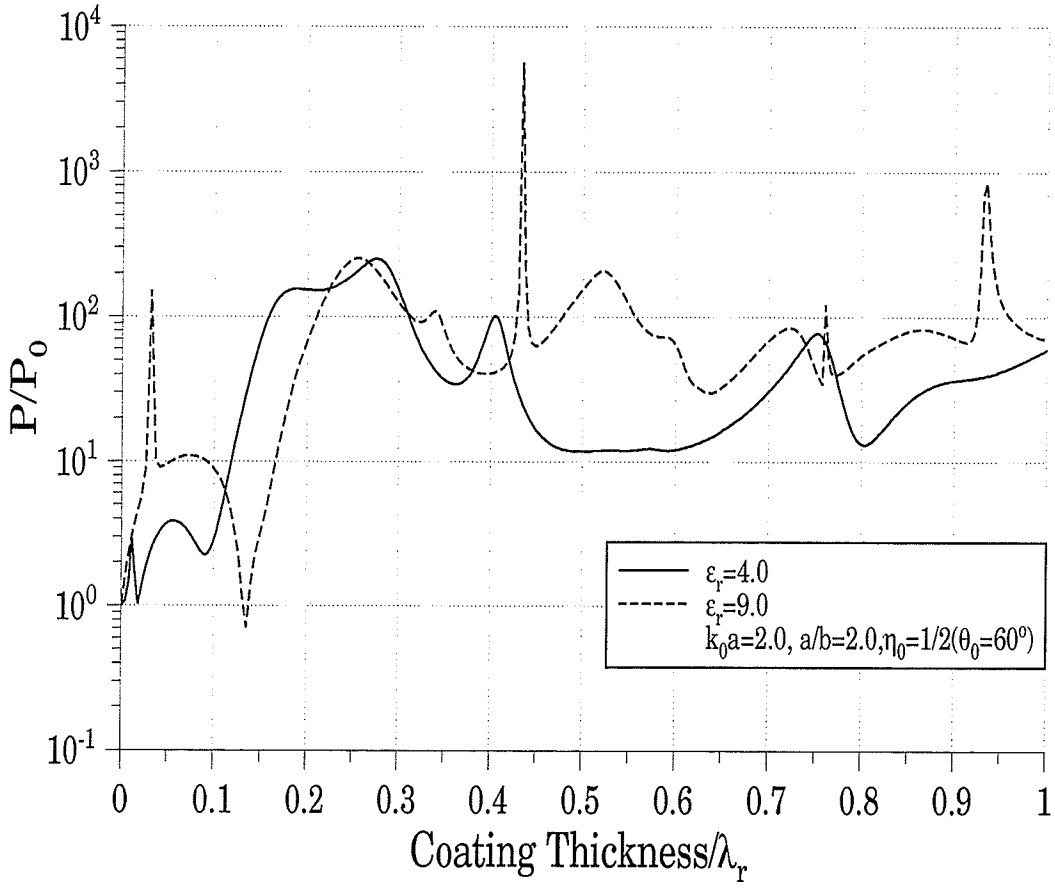

Fig. 4.17 Radiated power of asymmetrically slotted spheroid versus coating thickness for k_oa=2.0, a/b=2.0,μ_r=1.0 and η_o=1/2 (θ_o=60°).

4.5 CONCLUSION

An analytical solution to the radiation problem of asymmetrically excited narrow slots on dielectric–coated perfectly conducting prolate spheroid has been presented in this chapter. The problem was treated using the technique of separating the wave equation and the boundary conditions for given aperture field distributions along the slot. The radiated field and transmitted fields were first expanded in terms of spheroidal vector wave functions and the expansion coefficients were then determined by imposing boundary conditions. After evaluation of the expansion coefficients, the far–zone fields and radiation power were obtained.

The solution was firstly applied to analyze the radiation characteristics of a rotationally symmetric narrow circumferential slot on a perfectly conducting spheroid coated with a homogeneous material. The effect of coating thickness and other physical parameters on the radiated power was investigated. Further application was given for rotationally asymmetric circumferential narrow slots on spheroids with dielectric coating. Numerical results were obtained for electric field over boundary region, radiation patterns and radiated power, and the effect of some physical parameters on the radiation power was discussed.

The accuracy of the solution is evident from the numerical calculations. When the coated spheroid approaches the spherical shape excited by either a asymmetric or symmetric slot, the calculations agree well with the known results for a coated sphere. When the coating material tends to become transparent, our calculated results came into agreement with the known results for an uncoated spheroid. Our calculated results also showed that, for cer-

tain coating thickness, some modes become resonant. This greatly enhances the radiated power and affects the radiation field.

In addition, it was observed that the radiation patterns and power were modified by the shape factor a/b of the spheroid, the magnitude of the dielectric constant of the coating and other physical parameters.

CHAPTER 5

SUMMARY AND RECOMMENDATIONS

The problem of radiation from a perfectly conducting slotted spheroidal antenna has been investigated in this thesis. In Chapter 3, discussion focused on an asymmetrically slotted antenna on a perfectly conducting prolate spheroid without coating. The analysis was carried out by separating the wave equation and enforcing the boundary conditions in the spheroidal coordinates. The radiated field was first expanded in terms of spheroidal vector wave functions, then the expansion coefficients were determined by imposing boundary conditions.

Numerical results for the radiation patterns and aperture conductance for the slotted antenna were obtained for different parameters. The effect of the slot length and the shape of the slotted spheroid on both the radiation pattern and aperture conductance were considered. The accuracy and validity of the solution was obtained by examining the solution over the boundary region. The tangential electric field on the conducting spheroid was calculated, and the results confirmed that the tangential electric field satisfies the boundary conditions. The solution was also examined for the case where the slotted spheroid approaches the spherical shape ($a/b \approx 1$). The results were in a perfect agreement with the known results for a slotted sphere. Calculated results also show that the radiation characteristics of the antenna are apparently modified by the design parameters of the electric size *ka*, the

slot length L and the shape factor a/b.

In Chapter 4, slotted spheroidal antennas coated with homogeneous were considered. Methods of analysis used were almost the same as those used in Chapter 3. An analytical solution to the radiation problem of the asymmetrically excited narrow slots on dielectric–coated perfectly conducting prolate spheroid was obtained. The solution was firstly applied to analyze the radiation characteristics of a rotationally symmetric narrow circumferential slot. The effect of coating thickness and other physical parameters on the radiation power was investigated. Further application was shown for rotationally asymmetric circumferential narrow slots on spheroids with dielectric coating. Numerical results were obtained for the far–zone fields, radiation patterns and radiated power. The effect of some physical parameters on the radiation power was also considered.

Good validity and accuracy of the solution is contested from our calculations. As in the case of no coating, boundary tests were carried out and results showed that the boundary conditions were well satisfied on intersections. Furthermore, when the coated spheroid approaches the spherical shape, the calculations agree well with the known results for a coated sphere. Also, when the coating material tends to become transparent, our calculated results came into agreement with the results for an uncoated spheroid. Our calculated results also show that, for certain coating thickness, some modes become resonant. This greatly enhances the radiated power and affects the radiation field.

Although specifically the solution for radiating from prolate slotted spheroidal antennas has been discussed, the solution for radiating by oblate spheroidal antennas can be obtained from that of the prolate one by replacing the prolate spheroidal wave functions with the oblate ones. Also, it is naturally of interest to extend the effort from narrow slots to finite

width slots and from the circumferential slots to axial slots. Another potential study is the investigation of optimum designs for the slotted spheroidal antennas, taking into account the shape of the spheroid, the location and length of the slot, the electric property, and the thickness of the coating. Finally, the analytic method could be extended to obtain the solution to the scattering problem from a perfectly conducting slotted spheroid with or without coating.

REFERENCES

[1] R. A. Hurd, " Radiation patterns of a dielectric coated axially–slotted cylinder ", *Canadian J. Phys.*, vol. 34, *pp.* 638–642,July 1956.

[2] J. R. Wait, *Electromagnetic Radiation from cylindrical Structures.* Elmsford, NY: Pergamon, 1959.

[3] L . Shafai, " Radiation from an axial slot on a dielectric coated metal cylinder ", *Canadian J. Phys.*, vol. 50, no. 23,1972.

[4] L . Shafai, " Resonance effects in slotted spherical antennas coated with homogeneous materials ", *Canadian J. Phys.*, vol. 51, no. 22,1973.

[5] C.C. Lin and K. M. Chen, " Improved radiation from a spherical antenna by over dense plasma coating ", *IEEE Trans. Antennas Propagt.*, vol.Ap–17,*pp.* 675–678, 1969.

[6] S. J. Towaij and M. A. K. Hamid, " Diffraction by a mutiplayered dielectric–coated sphere with an azimuthal slot ", *Proc. IEE*, vol. 118, *pp.* 1209–1213, 1971.

[7] J. H. Richmond, " Axial slot antenna on dielectric–coated elliptic cylinder ", *IEEE Trans. Antennas Propagt.*, vol. Ap–37, *pp.*1235–1241, Oct. 1989.

[8] C. Flammer. *Spheroidal wave functions*,Stanford Univ.Press, Stanford, California,1957.

[9] J. A. Stratton. *Electromagnetic theory.* McGraw–Hill Book Co., New York .1941.

[10] C. Flammer. *The Prolate Spheroidal Monopole Antenna, Tech. Report No.22,* Stanford Research Institute, 1954.

[11] J. R. Wait, " Theories of Prolate Spheroidal Antennas ", *Radio Sci.*, Vol.1,no.**4**, April, 1966.

[12] B. P. Sinha and R H. Macphie," Electromagnetic scattering by prolate spheroids for plane waves with arbitrary polarization and angle ", *Radio Sci*. vol.**12**,*pp*. 171–184, 1977.

[13] B. P. Sinha and R. H MacPhie. " Mutual Admittance Characteristic for Two–Element Parallel Prolate Spheroidal Antenna Systems ", *IEEE Trans. Antennas Propag*. Vol.**33**, *pp*.1255–1263,1985.

[14] B. P. Sinha and R. H MacPhie." Translation Addition Theorems for Spheroidal Scalar and Vector Wave Functions ", *Quart.Appl. Math.*, Vol.**38,** *pp*.143–158,1980.

[15] I.R.Ciric and M.F.R. Cooray. " Admittance Characteristics and Far–Field Patterns for Coupled Spheroidal Dipole Antennas in Arbitrary Configuration ", *IEE Proceeding*, vol.**137**, *pp*.337–342,1990.

[16] T.Do–Nhat and R. H MacPhie." the Input Admittance of the Thin prolate Spheroidal Dipole Antennas with Finite Gap Widths ", *URSI IEEE Proceeding*, Seattle, Washington, Jun.1994.

[17] W.L. Weeks, " Electromagnetic Theory for Engineering Applications ", John Wily&Sons, Inc.New York,1964.

[18] C.W.H. Yeh. " On the Dielectric–Coated Prolate Spheroidal Antenna ", *J.Math. Phys.*, Vol.**42** *pp*.68–77, 1963.

[19] S. Asano and G. Yamamoto. " Light Scattering by a Spheroidal Particle ", *Appl. Optics*, Vol.**14,** *pp*.29–49,1975.

[20] B. P. Sinha, " Electromagnetic Scattering from Conducting Prolate Spheroids in the

Resonance Region ", *Ph.D.Dissertation*, Uni. of Waterloo, Waterloo, Ontario, Canada, March 1974.

[21] P.M. Morse and H.Feshbach, *Methods of Mathematical Physics*, Mc–Graw Hill Book Co., New York,1953.

[22] B. P. Sinha and R. H MacPhie," On the computation of the Prolate Spheroidal Radial Functions of the Second Kind ", *J. Math. Phys.*, Vol. **16**, no.12, *pp*.2378–2381,1975.

[23] Y. Mushiake and R. E.Webster. " Radiation Characteristics with Power Gain for Slots on a Sphere ", *IRE Trans. Antennas Propag*.**5**,*pp*.47–55,1957.

[24] A. Sebak and B. P. Sinha, " Scattering by a conducting spheroidal object with dielectric coatingat axial incidence ", *IEEE Trans. Antennas Propagt*., Vol.Ap–**40**, *pp*.268–274,1992.

APPENDIX A

In accordance with the notation of Flammer [1], The prolate spheroidal vector wave functions $\vec{M}^{r(j)}_{\substack{e\\o}m,\,n}(h;\eta,\xi,\phi)$ and $\vec{N}^{r(j)}_{\substack{e\\o}m,\,n}(h;\eta,\xi,\phi)$ are as follows

$$\underline{\vec{M}^{r(j)}_{\substack{e\\o}m,\,n}(h;\eta,\xi,\phi)}$$

$$M^{r(j)}_{\substack{e\\o}m,\,n,\eta}(h;\eta,\xi,\phi)=\frac{m\xi}{(\xi^2-\eta^2)^{1/2}(1-\eta^2)^{1/2}}S_{m,\,n}(h;\eta)R^{(j)}_{m,\,n}(h;\xi)\begin{matrix}\sin\\(-)\cos\end{matrix}m\phi \tag{A.1}$$

$$M^{r(j)}_{\substack{e\\o}m,\,n,\xi}(h;\eta,\xi,\phi)=\frac{-m\xi}{(\xi^2-\eta^2)^{1/2}(1-\eta^2)^{1/2}}S_{m,\,n}(h;\eta)R^{(j)}_{m,\,n}(h;\xi)\begin{matrix}\sin\\(-)\cos\end{matrix}m\phi \tag{A.2}$$

$$M^{r(j)}_{\substack{e\\o}m,\,n,\phi}(h;\eta,\xi,\phi)=\frac{(\xi^2-\eta^2)^{1/2}(1-\eta^2)^{1/2}}{\xi^2-\eta^2}[\xi\frac{d}{d\eta}S_{m,\,n}(h;\eta)R^{(j)}_{m,\,n}(h;\xi)-$$

$$-\eta S_{m,\,n}(h;\eta)\frac{d}{d\xi}R^{(j)}_{m,\,n}(h;\xi)]\begin{matrix}\cos\\\sin\end{matrix}m\phi \tag{A.3}$$

$$\underline{\vec{N}^{r(j)}_{\substack{e\\o}m,\,n}(h;\eta,\xi,\phi)}$$

$$N_{e\,o\,m,n,\eta}^{r(j)}(h;\eta,\xi,\phi)=\frac{(1-\eta^2)^{1/2}}{h(\xi^2-\eta^2)^{1/2}}\left[\frac{d}{d\eta}S_{m,n}(h;\eta)\frac{\partial}{\partial\xi}\left[\frac{\xi(\xi^2-1)}{\xi^2-\eta^2}R_{m,n}^{(j)}(h;\xi)\right]\right.$$

$$-\eta S_{m,n}(h;\eta)\frac{\partial}{\partial\xi}\left[\frac{(\xi^2-1}{\xi^2-\eta^2}\frac{d}{d\xi}R_{m,n}^{(j)}(h;\xi)\right]+$$

$$\left.+\frac{m\eta^2}{(1-\eta^2)(\xi^2-1)}S_{m,n}(h;\eta)R_{m,n}^{(j)}(h;\xi)\right]\begin{matrix}\cos\\ \sin\end{matrix} m\phi \qquad \text{(A.4)}$$

$$N_{e\,o\,m,n,\xi}^{r(j)}(h;\eta,\xi,\phi)=\frac{-(\xi^2-1)^{1/2}}{h(\xi^2-\eta^2)^{1/2}}\left[-\frac{\partial}{\partial\eta}\left[\frac{\eta(1-\eta^2)}{\xi^2-\eta^2}S_{m,n}(h;\eta)\right]\frac{d}{d\xi}R_{m,n}^{(j)}(h;\xi)\right.$$

$$+\xi\frac{\partial}{\partial\eta}\left[\frac{(1-\eta^2)}{\xi^2-\eta^2}\frac{d}{d\eta}S_{m,n}(h;\eta)\right]R_{m,n}^{(j)}(h;\xi)-$$

$$\left.-\frac{m^2\xi}{(1-\eta^2)(\xi^2-1)}S_{m,n}(h;\eta)R_{m,n}^{(j)}(h;\xi)\right]\begin{matrix}\cos\\ \sin\end{matrix} m\phi \qquad \text{(A.5)}$$

$$N_{e\,o\,m,n,\phi}^{r(j)}(h;\eta,\xi,\phi)=\frac{m(\xi^2-\eta^2)^{1/2}(1-\eta^2)^{1/2}}{h(\xi^2-\eta^2)}\left[-\frac{1}{(\xi^2-1)}\frac{d}{d\eta}\left[\ \eta S_{m,n}(h;\eta)\ \right]R_{m,n}^{(j)}(h;\xi)-\right.$$

$$\left.-\frac{1}{1-\eta^2}S_{m,n}(h;\eta)\frac{d}{d\xi}\left[\ \xi R_{m,n}^{(j)}(h;\xi)\ \right]\right]\begin{matrix}\sin\\ -cos\end{matrix} m\phi$$

(A.6)

Where $h=kd/2$, and $d=2F$.

APPENDIX B

Definition and Evaluation of Integrals

The integrals $I_{p\,m\,N\,n}$, $p = 1, 2, \ldots 11$ in Chapter 3 and 4, which are defined later in this appendix, are evaluated by employing the recurrence relations of associated Lengdre functions and the following integrals

$$\int_{-1}^{1} P_\mu{}^m(\eta) P_\nu{}^m(\eta) d\eta = \frac{2}{(2\mu+1)} \frac{(\mu+m)!}{(\mu-m)!} \delta_{\mu\nu} \tag{B.1}$$

and

$$\int_{-1}^{1} P_\mu{}^{m+2}(\eta) P_\nu{}^m(\eta) d\eta = 0 \ , \quad \nu > \mu$$

$$= -\frac{2}{(2\nu+1)} \frac{(\nu+m)!}{(\nu-m-2)!} \qquad \nu = \mu$$

$$= 2(m+1) \frac{(\nu+m)!}{(\nu-m)!} [1 + (-1)^{\mu+\nu}], \qquad \nu < \mu \tag{B.2}$$

$$I_{1\,m\,N\,n}(x,y) = \int_{-1}^{+1} \frac{S_{m+1,\,m+N+1}(x) S_{m,\,m+n}(y)}{\sqrt{1-\eta^2}} d\eta$$

$$= 2 \sum_{k=0,1}^{\infty}{}' \frac{(2m+k)!}{k!} d_k^{m,\,m+n}(y) \sum_{r=k}^{\infty}{}' d_r{}^{m+1,\,m+N+1}(x)$$

(for (n+N)=even);

=0, for (n+N)=odd (B.3)

$$I_{2\,m\,N\,n}(x,y) = \int_{-1}^{+1} \sqrt{1-\eta^2}\, S_{m,\,m+n}(\,y,\eta\,)S_{m+1,\,m+N+1}(\,x,\eta\,)d\eta$$

$$= 2\sum_{k=0,1}^{\infty}{}' \frac{(2m+k+2)!}{(2m+2k+3)k!}\left[\frac{d_k^{m,\,m+n}(y)}{(2m+2k+1)} - \frac{d_{k+2}^{m,\,m+n}(y)}{(2m+2k+3)}\right] d_k{}^{m+1,\,m+N+1}(x)$$

(for (n+N)=even);

=0, for (n+N)=odd

(B.4)

$$I_{3\,m\,N\,n}(x,y) = \int_{-1}^{+1} (1-\eta^2)^{3/2} S_{m,\,m+n}(\,y,\eta\,)S_{m+1,\,m+N+1}(\,x,\eta\,)d\eta$$

$$= 2\sum_{k=0,1}^{\infty}{}' \frac{1}{(2m+2k+3)} \frac{(k+2m+2)!}{k!} d_k{}^{m+1,\,m+N+1}(x)\{ \frac{(k+2m+3)(k+2m+4)}{(2m+2k+5)} \times$$

$$\times \left[\frac{d_{k+4}^{m,\,m+n}(y)}{(2m+2k+7)(2m+2k+9)} + \frac{d_k^{m,\,m+n}(y)}{(2m+2k+1)(2m+2k+3)} - \frac{2d_{k+2}^{m,\,m+n}(y)}{(2m+2k+3)(2m+2k+7)}\right] -$$

$$- \frac{k(k-1)}{(2m+2k+1)}\left[\frac{d_{k+2}^{m,\,m+n}(y)}{(2m+2k+3)(2m+2k+5)} - \frac{2d_k^{m,\,m+n}(y)}{(2m+2k-1)(2m+2k+3)} +\right.$$

$$\left. + \frac{d_{k-2}^{m,\,m+n}(y)}{(2m+2k-3)(2m+2k-1)}\right]\}$$ (for (n+N)=even);

=0, for (n+N)=odd

(B.5)

$$I_{4\,m\,N\,n}(x,y)=\int_{-1}^{+1}\sqrt{1-\eta^2}\,\frac{dS_{m,\,m+n}(\,y,\eta\,)}{d\eta}S_{m+1,\,m+N+1}(\,x,\eta\,)d\eta$$

$$=2\sum_{k=0,1}^{\infty}{}'\,\frac{(k+m+2)(2m+k+1)!}{(2m+2k+3)k!}d_k^{\,m+1,\,m+N+1}(x)d_{k+1}^{m,\,m+n}(y)-$$

$$-2\sum_{r=0,1}^{\infty}{}'\,m\frac{(r+2m)!}{r!}d_r^{m,\,m+n}(y)\sum_{k=r+1}^{\infty}{}'\,d_k^{\,m+1,\,m+N+1}(x)$$

(for (n+N)=odd);

=0, for (n+N)=even (B.6)

$$I_{5\,m\,N\,n}(x,y)=\int_{-1}^{+1}(1-\eta^2)^{3/2}\frac{dS_{m,\,m+n}(\,y,\eta\,)}{d\eta}S_{m+1,\,m+N+1}(\,x,\eta\,)d\eta$$

$$=2\sum_{k=0,1}^{\infty}{}'\,\frac{(2m+k+2)!}{(2m+2k+3)k!}\{\,\frac{d_{k+1}^{m,\,m+n}(y)}{(2m+2k+3}\times[\frac{(2m+k+1)(k+m+2)}{(2m+2k+1)}+\frac{(k+m+1)(k+2)}{(2m+2k+5)}]$$

$$-\frac{k(m+k-1)}{(2k+2m-1)(2k+2m+1)}d_{k-1}^{m,\,m+n}(y)-\frac{(m+k+4)(k+2m+3)}{(2m+2k+5)(2m+2k+7)}d_{k+3}^{m,\,m+n}(y)\,\}d_k^{\,m+1,\,m+N+1}(x)$$

(for (n+N)=odd);

=0, for (n+N)=even (B.7)

$$I_{6\,m\,N\,n}(x,y)=\int_{-1}^{+1}\eta\sqrt{1-\eta^2}\,S_{m,\,m+n}(\,y,\eta\,)S_{m+1,\,m+N+1}(\,x,\eta\,)d\eta$$

$$=2\sum_{k=0,1}^{\infty}{}'\frac{(2m+k+2)!}{(2m+2k+3)k!}\left\{\frac{kd_{k-1}^{m,\,m+n}(y)}{(2m+2k-1)(2m+2k+1)}+\frac{d_{k+1}^{m,\,m+n}(y)}{(2m+2k+3)}\left[\frac{(k+2m+3)}{(2m+2k+5)}-\right.\right.$$

$$\left.\left.-\frac{k}{(2m+2k+1)}\right]-\frac{(k+2m+3)}{(2m+2k+5)(2m+2k+7)}d_{k+3}^{m,\,m+n}(y)\right\}d_k{}^{m+1,\,m+N+1}(x)$$

(for (n+N)=odd);

=0, for (n+N)=even (B.8)

$$I_{7\,m\,N\,n}(x,y)=\int_{-1}^{+1}\eta(1-\eta^2)^{3/2}S_{m,\,m+n}(\,y,\eta\,)S_{m+1,\,m+N+1}(\,x,\eta\,)d\eta=2\sum_{k=0,1}^{\infty}{}'\frac{1}{(2m+2k+3)}\times$$

$$\times\frac{(k+2m+2)!}{k!}d_k{}^{m+1,\,m+N+1}(x)\left\{-\frac{k(k-1)(k-2)d_{k-3}^{m,\,m+n}(y)}{(2m+2k-5)(2m+2k-3)(2m+2k-1)(2m+2k+1)}\right.$$

$$+\frac{kd_{k-1}^{m,\,m+n}(y)}{(2m+2k-1)(2m+2k+1)}\left\{\frac{1}{(2m+2k+1)}\left[\frac{2k(k-1)}{(2m+2k-3)}+\frac{(2m+k+2)(2m+k+3)}{(2m+2k+3)}\right]-\right.$$

$$\left.-\frac{(k+1)(2m+k+3)}{(2m+2k+3)(2m+2k+5)}\right\}+$$

$$+\frac{d_{k+1}^{m,\,m+n}(y)}{(2m+2k+3)}\left\{\frac{(2m+k+3)}{(2m+2k+5)^2}\left[\frac{2(k+1)(k+2)}{(2m+2k+1)}+\frac{(2m+k+5)(2m+k+4)}{(2m+2k+7)}\right]-\right.$$

$$-\frac{k}{(2m+2k+1)^2}\left[\frac{2(2m+k+2)(2m+k+3)}{(2m+2k+5)}+\frac{(k-1)(k-2)}{(2m+2k-1}\right]\}$$

$$+\frac{(2m+k+3)d_{k+3}^{m,\,m+n}(y)}{(2m+2k+5)(2m+2k+7)}\left\{-\frac{1}{(2m+2k+5)}\left[\frac{2(2m+k+5)(2m+k+4)}{(2m+2k+9)}+\frac{k(k+1)}{(2m+2k+3)}\right]\right.$$

$$\left.+\frac{k(2m+k+2)}{(2m+2k+3)(2m+2k+1)}\right\}+\frac{(2m+k+5)(2m+k+4)(2m+k+3)d_{k+5}^{m,\,m+n}(y)}{(2m+2k+11)(2m+2k+9)(2m+2k+7)(2m+2k+5)}\Bigg\}$$

(for (n+N)=odd);

=0, for (n+N)=even (B.9)

$$I_{8\,m\,N\,n}(x,y)=\int_{-1}^{+1}\frac{\eta}{\sqrt{1-\eta^2}}S_{m,\,m+n}(\,y,\eta\,)S_{m+1,\,m+N+1}(\,x,\eta\,)d\eta$$

$$=2\sum_{k=0,1}^{\infty}{}'\frac{(2m+k+1)!}{(2m+2k+3)k!}d_k{}^{m+1,\,m+N+1}(x)d_{k+1}^{m,\,m+n}(y)+$$

$$+2\sum_{r=0,1}^{\infty}{}'\frac{(r+2m)!}{r!}d_r^{m,\,m+n}(y)\sum_{k=r+1}^{\infty}{}'d_k{}^{m+1,\,m+N+1}(x)$$

(for (n+N)=odd);

=0, for (n+N)=even (B.10)

$$I_{9\,m\,N\,n}(x,y)=\int_{-1}^{+1}\eta\sqrt{(1-\eta^2)}\frac{dS_{m,\,m+n}(\,y,\eta\,)}{d\eta}S_{m+1,\,m+N+1}(\,x,\eta\,)d\eta$$

$$=-2\sum_{k=0,1}^{\infty}{}'\frac{(k+1)(k+m+1)}{(2m+2k+3)}[\frac{(2m+k+1)!d_k^{m,\,m+n}(y)}{(2m+2k+1)k!}+\frac{(2m+k+2)!d_{k+2}^{m,\,m+n}(y)}{(2m+2k+5)(k+1)!}]d_k{}^{m+1,\,m+N+1}(x)$$

$$+2\sum_{k=0,1}^{\infty}{}'\frac{(m+1)}{(2m+2k+1)}\frac{(2m+k)!}{(k-1)!}d_k{}^{m+1,\,m+N+1}(x)d_k^{m,\,m+n}(y)+$$

$$+2\sum_{r=0,1}^{\infty}{}'(m+1)\frac{(r+2m)!}{r!}d_r^{m,\,m+n}(y)\sum_{k=r+2}^{\infty}{}'d_k{}^{m+1,\,m+N+1}(x)\qquad(\text{for (n+N)=even});$$

$$=0,\ \text{for (n+N)=odd}\qquad\text{(B.11)}$$

$$I_{10\,m\,N\,n}(x,y)=\int_{-1}^{+1}S_{m,\,m+n}(\,y,\eta\,)S_{m,\,m+N}(\,x,\eta\,)d\eta$$

$$=2\delta_{N\,n}\sum_{k=0,1}^{\infty}{}'\frac{(2m+k)!}{(2m+2k+1)k!}d_k^{m,\,m+n}(\,x)d_k^{m,\,m+n}(y)\qquad\text{(B.12)}$$

$$I_{11\,m\,N\,n}(x,y)=\int_{-1}^{+1}\eta^2S_{m,\,m+n}(\,y,\eta\,)S_{m,\,m+N}(\,x,\eta\,)d\eta$$

$$=2\sum_{k=0,1}^{\infty}{}'\frac{1}{(2m+2k+1)}\frac{(2m+k)!}{k!}d_k{}^{m,\,m+N}(x)\{\frac{(2m+k+2)(2m+k+1)}{(2m+2k+5)(2m+2k+3)}d_{k+2}^{m,\,m+n}(y)+$$

$$+\frac{d_k^{m,\,m+n}(y)}{(2m+2k+1)}\left[\frac{k(k+2m)}{(2m+2k-1)}+\frac{(k+1)(k+2m+1)}{(2m+2k+3)}\right]+\frac{k(k-1)}{(2m+2k-3)(2m+2k-1)}d_{k-2}^{m,\,m+n}(y)\Big\}$$

(for (n+N)=even);

=0, for (n+N)=odd (B.13)